EFFECTS OF LIGHT ON THE ELECTRON SPIN RESONANCE OF DIAMOND

By

JOHN PAUL KING

Bachelor of Science

Central State College

Edmond, Oklahoma

1961

Submitted to the faculty of the Graduate College
of the Oklahoma State University
in partial fulfillment of the requirements
for the degree of
DOCTOR OF PHILOSOPHY
July, 1966

EFFECTS OF LIGHT ON THE

ELECTRON SPIN RESONANCE OF DIAMOND

Thesis Approved:

William J. Lewis
Thesis Adviser

Herbert L. Jones

Paul Arthur

Leon W. Schmeder

Jeanne Agnew

Dean of the Graduate College

ACKNOWLEDGMENTS

The author would like to express his sincere gratitude to Dr. W. J. Leivo for his help, guidance, and constant encouragement during the course of this investigation. Special thanks are extended to Dr. M. D. Bell for his many enlightening discussions and suggestions regarding ESR in solids.

Particular thanks are also extended to Dr. J. Agnew, Dr. P. Arthur, Dr. H. Jones, and Dr. L. Schroeder for their aid and encouragement.

The cooperative atmosphere among those associated with the research on diamonds is deeply appreciated. The help by members of the Physics-Chemistry shop and glass shop in the design and construction of various equipment used in the study is appreciated.

Semiconducting diamonds used in preliminary phases of the study were kindly made available by Dr. J. F. H. Custers, Research Consultant, Industrial Distributers (1946) Limited, South Africa, Dr. H. B. Dyer, Director, Diamond Research Laboratory, South Africa, and Dr. G. Switzer of the U. S. National Museum. The author would like to thank Dr. Custers and Dr. Dyer for their continued interest and assistance in the diamond research at Oklahoma State University.

The financial support administered through the Research Foundation and made available by the National Science Foundation and the personal assistance of an NDEA Fellowship are gratefully acknowledged.

TABLE OF CONTENTS

Chapter		Page
I.	INTRODUCTION	1
	Preliminary Remarks	1
	Properties of Diamond	2
II.	ELECTRON SPIN RESONANCE	24
	Simple Theory	24
	Bloch Equations	29
III.	INSTRUMENTATION	36
	General ESR Spectrometer	36
	Description of the ESR Spectrometer Used in the Study	39
IV.	RESULTS AND DISCUSSION OF THE STUDY	70
	General Remarks	70
	Optical Illumination Effects on the ESR Spectra	71
	Discussion	98
	Summary	102
BIBLIOGRAPHY		104

LIST OF TABLES

Table		Page
I.	SUMMARY OF SOME OPTICAL PROPERTIES OF GROUP 2 DIAMONDS . .	78
II.	SUMMARY OF SOME OPTICAL PROPERTIES OF GROUP 3 AND GROUP 4 DIAMONDS	91
III.	SUMMARY OF SOME OPTICAL PROPERTIES OF GROUP 5 DIAMONDS . .	95

LIST OF FIGURES

Figure		Page
2-1.	Separation of the energy levels of an unpaired electron by a static magnetic field H_o	25
2-2.	Typical electron spin resonance from an electron associated with a nucleus of spin I = 1	26
2-3.	(a) Rotating coordinate system. (b) Effective magnetic field in rotating system	28
2-4.	Transverse magnetization	32
2-5.	Separation of an alternating field into two rotating components	33
3-1.	Basic components of an ESR bridge spectrometer	40
3-2.	Magnetic field plot of Varian Model V4007-1 electromagnet	41
3-3.	Modification of the Triconix stabilizer	44
3-4.	Modified Pound frequency stabilizer	45
3-5.	Klystron reflector voltage supply	47
3-6.	Cylindrical reference cavity	48
3-7.	Cylindrical reference cavity frequency calibration	49
3-8.	Electron spin resonance spectrometer used in the study	51
3-9.	100 kc/sec modulation field calibration	53
3-10.	Sample cavities showing microwave magnetic field and location of sample	55
3-11.	Aluminum mandrel and potting shell	58
3-12.	Cylindrical sample cavity	60
3-13.	(a) Cavity with sample mount. (b) Oriented and mounted sample	62

Figure		Page
3-14.	Dielectric coupling system	63
3-15.	Suprasil light pipe mounting arrangement	66
3-16.	X-ray illumination dewar	68
4-1.	Electron spin resonance spectrum of D-22. (a) Normal or deactivated state. (b) Activated state produced by uv excitation	74
4-2.	ESR spectrum of D-37. (a) Normal or deactivated state. (b) Activated state produced by uv excitation	76
4-3.	ESR spectrum of D-3. (a) In-phase, low power. (b) Out-of-phase, high power	80
4-4.	ESR spectrum of D-53B. (a) In-phase, high power. (b) In-phase, low power	81
4-5.	ESR spectrum of D-3. (a) Normal signal. (b) Signal obtained during illumination with 313 mμ light	82
4-6.	ESR spectrum of D-53B. (a) Normal signal. (b) Signal during 313 mμ illumination	83
4-7.	ESR spectrum of D-59. (a) Normal signal. (b) Signal during 313 mμ illumination	84
4-8.	ESR spectrum of D-59. (a) Fast scan. (b) Slow scan . . .	86
4-9.	ESR spectrum of D-61. (a) Normal spectrum. (b) After 366 mμ illumination. (c) Inequivalent $\langle 111 \rangle \parallel \vec{H}_o$ orientation	88
4-10.	ESR spectrum of D-61, out-of-phase. (a) Normal spectrum. (b) Spectrum during 366 mμ illumination	90
4-11.	ESR of D-51B	93
4-12.	ESR of D-58	94
4-13.	Energy level diagram for diamonds D-22 and D-37	98
4-14.	Energy level diagram for blue luminescing Type I diamonds	100

CHAPTER I

INTRODUCTION

Preliminary Remarks

Although the properties of diamond have been studied for many years, the detailed nature of various energy levels in diamond has not been determined. The calculations of the band structure assuming a perfect crystal agree with the experiments that diamond should be a very good insulator with a band gap of approximately 5.5 eV. However, imperfections in the lattice give rise to allowed energy states within the forbidden gap. The types and concentrations of these states depend on the impurities present, the conditions of crystal growth, and the subsequent damaging conditions. Even though diamonds have recently been grown synthetically, the conditions of growth have prohibited control of the impurities. Therefore, in order to obtain a reasonable knowledge of the energy levels in diamond, it is necessary to make an analysis of several properties of each sample in a variety of samples. Attempts are then made to correlate the properties and ultimately identify the centers responsible.

A sensitive method for observing paramagnetic defects in solids is the use of electron spin resonance (ESR)[1] techniques. ESR absorp-

---

[1]Electron spin resonance is usually referred to as ESR for brevity. This notation will be adopted and used where appropriate.

tion is detected only in defects with an unpaired spin, thus allowing small amounts of paramagnetic impurities to be examined in the presence of other non-paramagnetic defects. The impurity nucleus associated with the defect may sometimes be identified by hyperfine interactions.

Electrons or holes may be excited to higher allowed energy levels by optical illumination with proper wavelength light. Thus the relative populations of certain levels may be temporarily changed. The magnitude of the change will depend upon the number of states available, the lifetime of the states, the temperature, and the intensity of the light.

The purpose of the present research is to obtain further information on the energy level distribution in diamond and to identify the defect centers responsible for the levels by the use of ESR spectra obtained during simultaneous illumination of the sample with monochromatic light. The study will also include a review of the pertinent properties of diamond and the theory of ESR and a discussion of the equipment and techniques used in the investigation.

Properties of Diamond

Optical Studies

Luminescence studies were conducted and reported for diamond as early as 1859 by E. Becquerel and 1879 by W. Crookes. In 1891, Walter observed a dark band at 4155 Å in the absorption spectrum of diamond (1). Other optical properties of diamonds including ultraviolet absorption, infrared absorption, and photoconductivity were studied by other early writers (2). A systematic study of the properties of

diamond was conducted by Robertson, Fox, and Martin and reported in 1934 and 1936 (3,4). They classified diamonds into two types: Type I opaque to ultraviolet radiation of wavelengths shorter than 3000 Å and Type II transparent to 2250 Å. Many diamonds show characteristics between these extremes. Correlations were also made between the absorption at 3000 Å and other properties such as 7.8 μ absorption, birefringence, and photoconductivity.

In 1952 Custers (5) proposed a further division of the Type II diamonds. Normal Type II he classified IIa, and Type II specimens showing unusual phosphorescence and electrical conductivity were classified IIb. The conductivity was subsequently shown to be typical of impurity activated conduction in semiconductors by Leivo and Smoluchowski (6).

An intensive study of luminescence and related properties was conducted by several Indian investigators and reported from 1941 to 1946. Nayer (7,8) found a band structure in the luminescence spectra associated with the 4156 Å line at liquid nitrogen temperature. He demonstrated that the peaks in the absorption spectrum for wavelengths shorter than 4156 Å were the mirror image of the luminescence peaks with respect to frequency about the 4156 Å line. Mani (1) showed that there was also a mirror image of the absorption bands and luminescence bands about 5032 Å. She identified many more lines in the absorption band related to the 4156 Å system and further correlated them with the luminescence band. In no specimen did she find the green luminescence system without the blue luminescence also being present. The green was sometimes much stronger than the blue, however. In a later paper she also examined the intensity of the blue and green systems versus the ex-

citing light in the excitation region 3700 Å to 6500 Å (9). She noted that no blue luminescence was excited by wavelengths longer than 440 mμ. The peaks in the intensity of blue luminescence corresponded to the peaks in the absorption spectra for the 4156 Å system. The same general behavior was obtained for the green absorption system and exciting fluorescence peaks for the green. However, the green was not excited noticeably by the 4156 Å absorption system, and she concluded that the two systems were independent.

In 1956, Clark, Ditchburn, and Dyer (10) reported the existence of eight absorption systems in natural Type I diamonds. These systems were labeled N_1, N_2, ... N_8. Subsequently, Raal (11) observed another system in very thin slabs of Type I diamond. This system, which occurs at 2290 - 2310 Å and 2350 - 2370 Å, was labeled N_9. This band had previously been observed in intermediate diamonds by Robertson, Fox, and Martin (3) and others.

Dyer and Matthews (12) reported in 1957 a comparison of the luminescence of Type I, IIa, and IIb diamonds using the 3650 Å Hg group as the excitation source. The luminescence is strongest in Type I diamonds. The 4150 Å emission system was found in all Type I specimens tested, although the intensity varied considerably. The 5032 Å system was found in only about one third of the Type I crystals. The luminescence of the Type IIa crystals was fairly weak, but the intensity of the 5032 Å system was nearly equal to that of the 4150 Å system. One Type IIa crystal having several properties characteristic of Type IIb crystals did not have detectable luminescence. There was no detectable luminescence in any of the semiconducting (Type IIb)

diamonds using this exciting light. However, using light with energy greater than the band gap, they did obtain the phosphorescence reported earlier by Custers (5). In a few Type I crystals, a 6195 Å luminescence system was detected. It appeared to be related to the blue luminescence since it was detected only from the blue luminescing region of the specimens. Nayer (7) had previously mentioned a luminescence band with concentration near 6200 Å, and Gomon (13) mentioned a luminescence band in the region 6095 - 6445 Å.

A study of long lifetime luminescence was conducted by Chandrasekharan (14, 15). The diamonds studied included strongly blue luminescing samples, greenish-yellow luminescing samples, and samples with patches of blue and/or yellow luminescence. The yellow luminescing samples had little afterglow, but the blue luminescing samples had a weak, short lifetime blue afterglow and a strong, longer lifetime, yellow glow. Photographs obtained by placing the glowing sample directly on the film showed that the blue luminescing regions were responsible for the afterglow of diamonds with yellow and blue luminescing regions. The afterglow of the blue diamonds contains a blue component which decays in approximately 20 sec, and a strong yellow afterglow that lasts about 30 minutes. Blue luminescing diamonds were illuminated with uv and subsequently with red light (above 6800 Å). The red light induced a blue flash which lasted about 4 minutes. The blue flash was observed through a filter complementary to the red light used for illumination. The blue flash also contained a small component of green which could be observed by the use of appropriate filters. Illumination with green light after ultraviolet activation gave a violet flash and a

persistent red luminescence. The activated state lasted for at least a few days, giving rise to flashes from red or green light. The flash could be stopped by cutting off the red (or green) illumination. When the red (or green) illumination was resumed, the flash resumed near the cutoff intensity. However, there was no flash observed by illumination with red light after deactivation by green, and likewise for green after red. Illumination with blue light after uv activation did not appear to cause a flash but gave persistent green and red luminescence. One of the green luminescing samples behaved similarly to the blue samples, except the flash was green rather than blue. The blue flash induced by red light was split by a three prism spectrograph and photographed. The 4152 Å line and its system of bands was faintly detected. Unpublished work by Mani on one of the samples showed that the 4152 Å and 5032 Å luminescence systems were present in the long lifetime luminescence.

The temperature dependence of the luminescence of Type IIb diamonds, observed by Krumme and Leivo (16, 17, 18), indicates that the luminescence in semiconducting diamond is a phosphorescence rather than a slow fluorescence. They observed a blue system with a decay lifetime of 0.7 ± 0.1 sec at room temperature and a much weaker red system with longer decay lifetime. The red system could be detected only by eye. The luminescence could be observed through an interference filter centered at 680 mμ. This wavelength is not included in the red system in Type I diamonds (7). The luminescence appeared to be a bulk effect rather than a surface effect. Because of the very weak luminescence of the samples, it was suggested that non-radiative

recombination processes must be dominant.

Wayland and Leivo (19) obtained a carrier lifetime of 9 μsec for photoexcited carriers in semiconducting diamond from the rise time of the photocurrent. This is believed to be independent of trapping. Lifetimes of 125 μsec, 800 μsec, 0.25 sec, 12 min, and 84 min, which include trapping, were obtained from the photoconductivity decay curves.

Male (20) studied the luminescence excited by wavelengths near the fundamental absorption edge. He found peaks corresponding to absorption bands at 5.250 eV, 5.363 eV, and 5.391 eV in all except the semiconducting diamond. Also, broad bands at 5.51 eV, 5.56 eV, and 5.73 eV occur in all but the semiconducting crystal. The luminescence in the semiconducting diamond increased sharply in the uv beginning near 5.25 eV. This is seen to be consistent with an acceptor level at approximately 0.35 eV above the valence band. Relative intensities of the 4156 Å and 5032 Å luminescence bands were observed by using a series of Wratten filters to observe emission in the wavelength ranges 3200 - 4700 Å, 4800 - 6000 Å, and 5500 Å up. No change in the relative intensity of these bands with exciting wavelength was observed.

Dean and Male (21) extended this study to the energy interval 5.0 to 7.5 eV. They also checked the temperature dependence in the range 30° to 350° K.

Work by Elliott, Matthews, and Mitchell (22) and by Clark, Maycraft, and Mitchell (23) utilizing polarized exciting light for examination of polarization of luminescence has indicated a ⟨110⟩ symmetry axis for the 5032 Å group and a ⟨111⟩ symmetry axis for the 4156 Å group. Attempts to examine the polarization of luminescence were begun as early as 1945 by Mani (24) who observed that the luminescence was only

partially polarized.

Several authors have studied the effects of irradiation on the absorption and luminescence of diamond (10, 12, 13, 25, 26, 27, 28). The samples were irradiated by various energy electrons, neutrons, or γ-rays. In Type I diamonds, a band referred to as the A-band (27) or GR1-band (28, 29) appears in absorption beginning at 1.7 eV and extending to 2.5 eV. Also there appears a uv-band beginning at 3.0 eV. Heating the sample above 600° C significantly decreases both of these absorption bands and produces a B-band from 2.5 to 3.0 eV. The B-band corresponds to the green luminescence band found in non-irradiated diamonds except for a line at 4960 Å which is always observed in irradiated and heat treated samples but only occasionally in natural samples (13). Type IIa samples exhibit very similar behavior if they are changed significantly, but at temperatures above 900° C all absorption lines disappear, and only continuous absorption remains. Clark, Ditchburn, and Dyer (26) suggest that the imperfections are anchored to the normally occurring crystal imperfections of Type I diamonds preventing complete annealing. In studying the luminescence of irradiated diamonds, Dyer and Matthews (12) reported a new system of emission for some Type I diamonds in the region between 5000 and 6000 Å. There was no correlation with observed absorption. Very little change occurred in the luminescence of most of the Type I specimens. All showed some decrease due to increased background absorption at 3650 Å, which was the exciting wavelength being used. Effects of heat treatment depended upon irradiation conditions for temperatures below 450° C. Heating at 580° C produced a 5032 Å system similar to that of

natural crystals in all specimens examined. Using different exciting wavelengths gave several new emission lines in these heated specimens, but similar tests prior to high temperature heating had not been made for comparison. Two of the three Type IIa samples did not show changes in their emission spectra due to irradiation or heating. In the third Type IIa specimen, lines were found at 4175 and 4700 Å at 80° K in the emission spectrum.

Ralph (30) examined the electron-excited (cathodoluminescence) luminescence spectra of natural and irradiated diamond. Features observed in natural diamonds included: (1) a broad emission band centered near 4400 Å and extending from 3800 Å to 5200 Å; (2) three overlapping broad bands at 5150 Å, 5750 Å, and 6300 Å; (3) sharp line systems with principal lines at 5030 Å, 5755 Å, and occasionally at 4150 Å; and (4) several additional sharp lines at 3940 Å, 4845 Å, and 4910 Å observed only in diamonds with the 5755 Å system and at 5390 Å observed only in diamonds with the 5030 Å system. The diamonds were irradiated with 500 keV electrons or neutrons and annealed in vacuo at temperatures between 600° and 800° C. Tests indicated that annealing began to occur near 580° C. In the electron irradiated diamonds having a natural 5755 Å system, a number of sharp lines referred to as the 3940 Å system appeared. Annealing produced no change in the 3940 Å system. However, the 5755 Å system was increased, and the 5030 Å system was induced, if not already present, by annealing. In crystals with no natural line emission, the 5030 Å and 5755 Å systems were observed only after annealing. No change in the spectra was observed from radiation alone. The 3940 Å system did not appear in any crystals

in which the 5755 Å system was completely artificially produced.

Dyer and Du Preez (28), working with Type I electron irradiated diamonds, checked the effects of heating at 500° C in the dark and subsequent illumination with intense light from a quartz envelope, high-pressure mercury lamp. Care was taken that the electrons from the radiation source had energy below that required for multiple-defect generation. They observed a band which they called the ND1 band, with absorption between 3.1 and 3.8 eV. The first line of the system corresponds with the third line in the 4150 Å band. The second corresponds with the fourth, and so on. However, it is pointed out that this is most likely coincidental due to the structure of the bands. The ND1 band is produced by heating to 500° C in darkness after irradiation. Intense light from a mercury lamp quenched the peak, but further heating in darkness brought it back. The heating and bleaching cycle could be repeated indefinitely.

In a study of electron-irradiated Type IIb diamonds, Dyer and Ferdinando (31) found evidence that the radiation induced GR1 (1.6-2.6 eV) and uv (2.8 eV to fundamental absorption edge) absorption centers are donor centers which do not absorb when ionized. Several Type IIb diamonds were irradiated with 0.6 MeV electrons. Also, Type IIa diamonds were irradiated simultaneously for comparison. The optical absorption of the IIb diamonds was unaffected except for a very weak reduction in absorption below 3.0 eV. Heating to 600° C after irradiation produced no additional effect. The infrared absorption decrease corresponds to further compensation of the acceptor states (32) in full accord with observation that irradiation reduces the conductivity of Type IIb diamonds (33). In one weakly Type IIb diamond, the GR1 and

uv bands appeared only after an irradiation dose greater than 3.0×10^{18} electrons/cm^2, and then both appeared weakly. The TH5 absorption band in the region 2.3 - 2.8 eV appears in the Type IIa specimens after heating, but as was mentioned above, no change occurred in the IIb samples after heating. It was suggested that the TH5 centers are also optically nonabsorbing when ionized.

Diffusion Effects

An analysis of the diffusion processes in diamond was conducted by Fratzke, et al (34, 35) of this laboratory. Impurities had previously been diffused into silicon and germanium which have the diamond type lattice. However, according to the calculations of Fratzke, et al, the activation energies for vacancy and impurity diffusion are so high for diamond that significant diffusion should not occur below 1000° C. Since the rate of change of diamond to graphite is significant above 1000° C at atmospheric pressure, diffusion experiments above this temperature would require high pressure techniques. The experimental results were in agreement with the calculations. The diamond sample was kept in contact with Al, Be, or B for times on the order of 100 hours at 900° C in a moderate vacuum. No change occurred in the surface or bulk resistivities or in the optical transmission. The possiblilty of nitrogen diffusion was considered, but no change in the 7.8 μ absorption was detected after 200 hours at 900° C in a moderate vacuum.

Later attempts by Wentorf and Bovenkerk (36) to diffuse B and Be into diamond at a high temperature and pressure were successful. The crystals which were heated to approximately 1600° C under 8.5 or 35

kbar pressure in contact with boron did not have reduced resistivities, but treatment at 1600° C and 60 kbar pressure for 12 min resulted in greatly reduced resistivities.

Optical Effects on Counting Diamonds

Crystal counting was first demonstrated in AgCl by Van Heerden (37). He also experimented with a gem quality diamond, but without success. Curtiss and Brown (38) found that two of 100 diamond specimens tested responded well to γ-rays. Type II diamonds were at first thought to be the best γ-ray counters (39), but later work by Williardson and Danielson (40) and Champion (41) has indicated that intermediate type crystals which are very nearly Type II are somewhat better than the true Type II samples. The indications were that the division into Type I and Type II was a helpful criterium but not a sufficient one for selecting counting diamonds.

The major problem in using diamonds as crystal counters was the decrease in counting rate with time. When a gamma-, beta-, or alpha-particle enters the sample, it may collide with an electron, giving the electron considerable energy which is imparted to other electrons by further collisions. For each electron which is raised from the valence band to the conduction band, two electrical carriers have been liberated, the electron and a positive hole. Thus the current due to an applied external electric field is a measure of the liberated carriers and therefore of the incident particles. However, the carriers may fall into intermediate traps before leaving the crystal. Since the electrons and holes move in opposite directions, the filling of these

traps forms an internal field that eventually cancells the effects of the external field. Prevention of this internal field build-up has been accomplished by using alternating fields, by heating the samples, and by optically bleaching the traps with light. It is this last method which is of interest in the present study.

Chynoweth (42) used a Nernst filament to illuminate the crystals used for alpha-particle counting. He obtained an increased counting rate with no noticeable decay when the light was left on. The counting rate decreased rapidly when the light was turned off. No photoconductivity was observed due to the Nernst filament alone. In later experiments counting β-particles, there was no improvement in the counting rate obtained by use of the Nernst filament (43). Rather, there was a transient increase, then a continuing decrease. In fact, the rate of decay increased with intensity of light. A tentative explanation of the effect was increased separation of trapped holes and electrons. He changed to light pulsing techniques using white light as well as infrared and red. The external field was temporarily disconnected during the light pulse. Measurements were between light pulses.

Effects of monochromatic light on the counting properties of diamond have been studied by Urlau, Logie, and Nabarro (44) and Elmgren and Hudson (45). Elmgren and Hudson obtained curves for variation in the photon-induced decay constant with photon energy for a few samples. They postulated levels 0.5 eV, 2.9 eV, and 4.8 eV above the valence band. The level at 2.9 eV and lower levels were assumed to be filled with electrons, while those above were assumed void of electrons. Urlau, et al plotted curves for the variation of the photoconductive

current per unit power of incident light as a function of the energy of the incident light for a few samples. Experiments were conducted to determine the charge of diamonds which had been bombarded with β-particles or irradiated with light. Since the penetration of the β-particles into the diamonds was small, the irradiation was sometimes conducted through the anode or cathode so that more electrons or holes would be trapped due to longer paths through the crystal. Effects of light would then give further information concerning which levels were hole traps and which were electron traps. Levels were postulated at 0.94 eV, 1.64 eV, and 3.3 eV above the valence band. The 3.3 eV level was assumed to be partly filled and give rise to either n- or p-type photoconductivity.

In addition to the levels assumed by the above groups, many levels had been postulated from earlier optical data including counting effects. These are summarized in a table in the report by Urlau, et al (44). The results are not at all consistent.

The Problem of Two Types of Diamond

Although the division of diamonds into Types I and II was generally accepted following the work of Robertson, Fox, and Martin (3), it was many years before a widely accepted explanation was presented; and there are many details which are still not fully explained. Type I diamonds exhibit an infrared absorption band in the 7 - 8 μ region in addition to the bands in the 3 - 5 μ region found in all diamonds. Type II diamonds are transparent to 2250 Å, while Type I diamonds have a strong absorption system starting near 3000 Å. Custers and Raal (46)

have used very thin specimens to show that the absorption coefficient rises sharply in Type I diamonds at 2220 Å. Photoconductivity in Type I diamond is observed to increase rapidly with decreasing wavelength near 3000 Å, but the increase for Type II appears near 2300 Å (3). Anomolous x-ray diffraction spikes were observed in several diamonds by Raman and Nikalantan and were subsequently established as characteristic of Type I diamonds by Lonsdale and Smith (47). Lonsdale (48) reported that the spikes were not temperature sensitive in contrast to the behavior of the primary reflection found in all diamonds.

Raman presented an explanation of the 7 - 8 μ absorption in Type I diamond based on crystal symmetry. He assumed the Type I diamonds are the most perfect in structure and exhibit tetrahedral symmetry. The Type II diamonds were assumed to have octahedral symmetry (49, 50).

A semiquantitative study of the impurities in diamond was conducted by Chesley (51) in 1942 using spectrographic analysis on 33 diamonds of varied origin and properties. Search was made for 30 elements, of which 13 were found. A rigorous comparison of Type I and II samples was not made, but the one known Type II sample was the purest sample tested. Raal (52) made a more quantitative spectrographic study of the impurities in diamond. He looked for the 13 elements observed by Chesley and also for nickel. Only Si, Ca, Mg, Al, Fe, Ti, Cu, and Cr were detected in this study. The samples used were cleaved or sawed into three sections with the central section having two parallel sides for optical transmission measurements. The two end sections were crushed for spectrographic analysis. No significant difference between the impurities in Type I and Type II diamonds was noted. In

general, the Type II specimens were purer than the Type I, but particular Type II specimens were found which were less pure than some Type I specimens.

In a study of comparative properties of diamond, Sutherland, Blackwell, and Simeral (47) noted excellent correlation between the ultraviolet absorption and infrared absorption intensities, but poor correlation was found between strengths of infrared absorption and x-ray diffraction spikes. From several considerations, they considered Type II to be relatively pure and Type I to be relatively impure. They suggested possible impurity centers in Type I diamonds to be (1) foreign atoms, (2) vacancies, or (3) carbon atoms in an abnormal electronic state. Their study indicated no correlation between variations in the carbon 12 to carbon 13 ratio and Type I characteristics. Also irradiation damage failed to produce Type I absorption bands, indicating that vacancies were not responsible for Type I properties.

Frank (53) explained the diffraction spikes in Type I diamonds assuming segregated (100) planes of impurity atoms. Frank suggested silicon as the possible impurity element. Further calculations by Caticha-Ellis and Cochran (54) agreed well with Frank's work except the number of necessary impurity atoms was found to be a factor of at least 80 higher than the concentration of silicon present in the samples tested.

In 1955, Lax and Burstein (55) reported that the symmetry of the perfect diamond lattice forbids single phonon absorption of irradiation but that this absorption may be allowed when imperfections are present. This proof was further evidence that the basic difference between Type

I and Type II is the presence of certain impurities rather than a difference in crystal structure.

In 1959, twenty-five years after Robertson, Fox, and Martin classified diamonds into Types I and II, Kaiser and Bond (56) reported a correlation between the nitrogen concentration and the absorption at 3065 Å and 7.8 μ. Concentrations of nitrogen as high as 0.2% were found. They assumed that the nitrogen occurred in substitutional positions in diamond and that it produced deep lying donor states. The absorption band at 3155 Å was thought to correspond to ionization of these impurity levels. Correlation of a second infrared absorption band with the absorption peaks in the 4155 Å band also was obtained.

Lightowlers and Dean (57) repeated the studies of Kaiser and Bond, finding agreement with the correlation of nitrogen concentration with 7.8 μ and 3065 Å absorption over a concentration range factor of almost 100. However, no quantitative correlation appeared to exist between the second infrared absorption band and the 4155 Å absorption band. Nonetheless, the second infrared system was more common in diamonds with strong 4155 Å absorption systems. One Type IIa crystal did not show correlation of nitrogen content with absorption properties. Compensation of the donor-electrons by aluminum acceptor levels was suspected, but the concentration of aluminum was found to be completely insufficient. The density of nitrogen was shown to be non-uniform in this sample, and this appeared to be the best explanation for the behavior. Bulk optical absorption measurements would be insensitive to small regions of high absorption surrounded by regions of low absorption.

Calculations by Yoneda (58) on the x-ray diffraction spikes of diamond indicated densities as high as 0.8% were needed to explain the results. However, a subsequent calculation by Frank (59), with slightly different assumptions, indicated that the nitrogen content obtained by Kaiser and Bond was sufficient to produce the observed spikes.

The presence of substitutional nitrogen donors in diamond was confirmed by ESR in 1959 by Smith, Sorokin, Gelles, and Lasher (60). The donor electron occupies an antibonding orbital located on the nitrogen atom and one of its nearest neighbor carbon atoms. For nitrogen, the nuclear spin $I = 1$ gives rise to a splitting of the absorption into three peaks with ratio 1:1:1. However, this structure is observed only when the crystal is oriented with a $\langle 100 \rangle$ axis parallel to the magnetic field. The side peaks may split into as many as four peaks, depending upon the orientation of each of the four $\langle 111 \rangle$ axes with respect to the magnetic field. With a $\langle 100 \rangle$ axis parallel to the magnetic field, all four $\langle 111 \rangle$ axes make angles of 54°40' with the magnetic field, and the side peaks are, therefore, superimposed into one large peak. The g-value was found to be isotropic and equal to 2.0024 ± 0.0005. A weak additional spectrum, roughly 180 times smaller, was detected and attributed to the presence (1.1%) of C^{13} which has nuclear spin $\frac{1}{2}$. The spin concentrations were estimated to be in the range $10^{15} - 10^{17}$/cc. This was several orders of magnitude less than the amount of substitutional nitrogen observed by Kaiser and Bond (56). It was assumed that most of the nitrogen is present in a non-paramagnetic form such as adjacent substitutional pairs.

Further work on the ESR spectrum of substitutional nitrogen in

diamond has been conducted by Loubser and Du Preez (61). Additional weak lines near the main nitrogen lines have been observed. The weak lines were divided into three groups. Group A lines were attributed to interaction with C^{13}. Group B lines were reported to be due to the nitrogen quadrupole moment. Group C lines were attributed to N^{15} nuclei (spin $I = \frac{1}{2}$).

A study of the distribution of the paramagnetic nitrogen in Type I diamond was conducted by Samsonenko (62). In the majority of the specimens a normal spectrum of donor nitrogen ($\Delta H = 0.3$ Oe) was observed. However, in some specimens a broad spectrum was found coinciding with the normal nitrogen resonance. He assumed that the broadening was due to separation of the centers by a distance such that the dipole-dipole interaction of paired electrons was significant. Calculations of the density of these centers gave approximately 10^{20} cm^{-3} for the regions giving rise to the broad part of the spectrum and 3×10^{19} cm^{-3} in the regions of normal nitrogen resonance. This study is important in at least two respects. The overall density of paramagnetic nitrogen centers is two or three orders of magnitude higher than that given by Smith, et al (60), and therefore compares well with observed nitrogen concentrations in Type I diamonds. Also, the concentration of paramagnetic nitrogen was not always uniform. This also agrees well with previous knowledge that Type I diamonds often have regions of stronger and weaker Type I properties (63).

Evans and Phaal (64) observed impurity platelets on (100) planes in Type I diamonds by transmission electron microscopy on very thin specimens. Nitrogen is assumed to be the relevant impurity since the density of the platelets can be explained only by the high concentration

of nitrogen in Type I diamonds. Small dislocation loops lying in (111) planes were observed and ascribed to the condensation of vacancies following formation of the platelets. Neither the platelets nor the dislocation loops are observed in Type II diamonds. The absence of low-angle x-ray scattering was reported to indicate that the nitrogen was in substitutional positions in the platelets.

The Type IIb diamonds have p-type conductivity apparently associated with an acceptor level at 0.35 eV above the valence band (65, 66). Bell and Leivo (67) reported that photoconductivity could be excited in Type IIb diamonds by visible and near infrared light. The major peak occurs at 660 mμ, and a slight peak appears at 890 mμ. Peaks in the infrared absorption observed by Stein (68) and in the low temperature (150° K) photoconductivity observed by Johnson (69), both of this laboratory, give further evidence of the acceptor level at 0.35 eV and also indicate a level at 0.52 eV (70). Krumme and Leivo (71, 72) have recently reported photoconductivity measurements at liquid nitrogen and liquid helium temperatures. The observed photoconductivity spectrum was accounted for in terms of acceptor levels with activation energies at 0.30, 0.37, 0.52, and 0.7 eV and a combination of phonons. The level at 0.52 eV was also reported by Halperin and Nahum (73) in 1961 on the basis of thermoluminescence data.

Electron Spin Resonance in Diamond

Among the first paramagnetic centers in diamond detected by electron spin resonance were lattice defects produced by neutron and electron irradiation (74, 75, 76). The absorption spectrum was first divided into three systems: (a) a single isotropic line with g-value = 2.0028

± 0.0004, whose intensity and line width increase with irradiation dose and decrease with heating; (b) a system of 12 anisotropic lines which are about 100 times smaller than (a) in intensity and are unaffected by heating; (c) additional weak lines not yet analysed in detail.

Baldwin (77) observed three centers labeled A, B, and C, with g-values of 2.00230, 2.00234, and 2.00238 ± 0.00010, respectively. On illumination with ultraviolet light, the A-center increased to completely mask the B-center. Hyperfine interactions were observed in the A-center due to the nearest and second-nearest neighbor C^{13} nuclei which are in 1.1% abundance in diamond. The A-center resonance is excited by photons of energy $\geq$ 2.83 eV and quenched by photons with energy $\geq$1.10 eV. The A-center was identified as an isolated vacancy. The C-center resonance was observed only with the reference phase of the phase detector in quadrature with the modulation field.

Faulkner, Mitchell, and Whippey (78) identified four systems in neutron irradiated diamonds. Systems (a) and (b) coincided with (a) and (b) above. System (c) contained six lines and had <100> symmetry axes. System (d) was a broad anisotropic absorption. Dependence of each center on radiation dose was observed.

Clark, Duncan, Lomer, and Whippey (29) reported a fairly good correlation between the strength of the ESR (a)-system and the optical density at 2.695 eV. Also, fair correlation was found between the strength of the ESR (c)-system and the integrated strength of the GR1 optical absorption band between 1.6 and 2.5 eV. However, although both the GR1 band and the ESR (c)-system decrease with high temperature annealing, the temperature dependence of this decrease is not

the same for both systems.

Dyer and Du Preez (28), whose work was previously discussed, observed a single isotropic ESR line in diamonds irradiated with 0.78 MeV electrons. The line was observed in the Type IIa sample before irradiation, but no ESR absorption was observed in the two Type I samples before irradiation. The strength of the irradiation induced ESR absorption was changed by heating in darkness at 500°C in vacuo. However, in some samples the signal increased, while in others it decreased. The GR1 optical absorption band decreased and the ND1 band increased in all specimens when they were heated. Intense illumination with light from a high-pressure mercury lamp produced an increase in the size of the GR1 band and the uv band and a decrease in the ND1 band and the ESR line in the two Type I samples. Illumination had no effect on the Type IIa sample. Subsequent heating restored the Type I samples to their condition previous to illumination. The heating and illumination effects could be repeated indefinitely.

The detection of substitutional nitrogen donors in natural Type I diamond by ESR has been discussed in an earlier section. Bell, et al (79, 80, 81) of this laboratory has shown a correlation between the density of uncompensated acceptors and the concentration of spins in semiconducting (Type IIb) diamond. They observed a broad, isotropic peak with g-value 2.0030 ± 0.0003. A complex, orientation dependent spectrum was observed in Type I diamonds by Smith, Gelles, and Sorokin (82) and attributed by them to aluminum acceptors, However, the identity of this center is still in question.

Bell, et al (79, 81) investigated the ESR spectrum of a crushed Type

I diamond having no detectable initial signal. Crushing created a signal with g-value 2.0029 ± 0.0003. Subsequent heating at 500° C and 10^{-6} mm Hg caused no effect, but heating at 600° C at 10^{-6} mm Hg for one hour caused a significant decrease in signal size and linewidth. The signal continued to decrease for a short time at 780° C, but then it reached a constant value which was not changed by heat treatment of 4 hours at 1100° C. A broad line appeared after heat treatment of 870° C for one hour. A control specimen was given the same heat treatment as the crushed sample, but no change in the ESR spectrum or infrared spectrum was observed.

CHAPTER II

ELECTRON SPIN RESONANCE

Simple Theory

In most compounds, there is a pairing of electron spins. Organic molecules which are exceptions to this rule are called free radicals and are generally unstable. Perfect solids with covalent or ionic bonds are diamagnetic since they contain no unpaired spins. However, in all natural crystals, there are defects due to impurities and lattice defects which may be paramagnetic.

The simplest system to consider is the case of isolated unpaired electrons. In the absence of a magnetic field, the energy levels are degenerate in spin. Upon application of a magnetic field $\vec{H}$, the degeneracy will be removed, and the levels will split into two levels. The classical interpretation is that the spins orient either parallel or antiparallel to the magnetic field. The spin part of the Hamiltonian operator for this system is

$$[H] = \gamma\hbar\,\vec{S} \cdot \vec{H}. \tag{2.1}$$

where γ is the gyromagnetic ratio, $\hbar$ is Planck's constant divided by 2π, and $\hbar\vec{S}$ is the electron spin operator. For a magnetic field in the z-direction with magnitude H_o, the Hamiltonian is

$$[H] = \gamma\hbar H_o S_z. \tag{2.2}$$

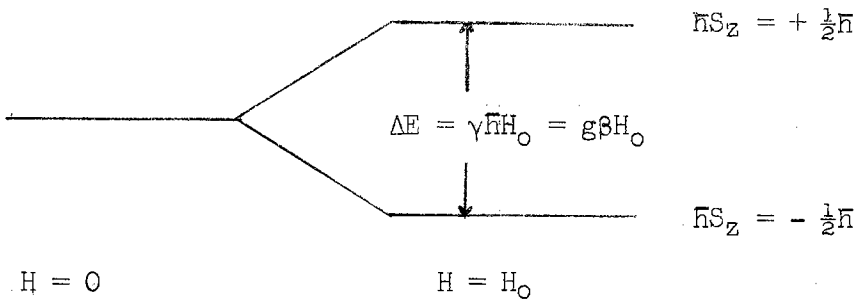

Figure 2-1. Separation of the energy levels of an unpaired electron by a static magnetic field H_o.

The eigenvalues for $\hbar S_z$ are $\pm \frac{1}{2}\hbar$, and the degenerate levels are thus split by $\pm \frac{1}{2}\hbar H_o$ as in Fig. 2-1. The energy separation is therefore

$$\Delta E = \gamma\hbar H_o. \tag{2.3}$$

Often it is of greater advantage to use the expression

$$\Delta E = g\beta H_o \tag{2.4}$$

where β is the Bohr magneton $\frac{e\hbar}{2mc}$, and g = g-factor is defined by the equation.

Photons of energy ΔE can cause transitions between the levels. The induced transition is often called "spin flip" and is the basis of electron spin resonance. The resonance absorption is usually observed at a fixed photon energy by sweeping the magnetic field through the resonance condition.

When the unpaired electron is associated with a nucleus possessing a magnetic moment, it will experience an additional magnetic field due to the nuclear spin I. The levels will be split into 2I + 1 components, and the ESR absorption will have 2I + 1 peaks. Typical splitting of the levels and the resulting ESR spectrum for I = 1 is illustrated in Fig. 2-2. The hyperfine interaction thus provides a possible means

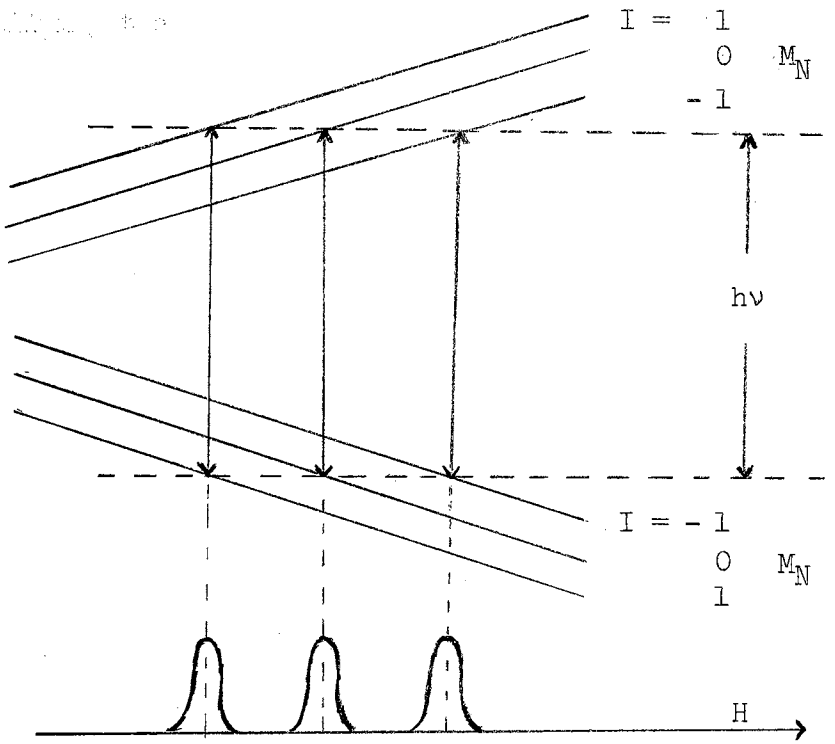

Figure 2-2. Typical electron spin resonance from an electron associated with a nucleus of spin I = 1.

of identifying the paramagnetic center. The hyperfine interaction may be partially or completely masked by broadening factors and further complicated by crystalline field effects.

Classical Treatment of the Effect of Rotating Magnetic Fields

Although the resonance phenomenon is, strictly speaking, a quantum mechanical problem, a classical treatment contributes significantly to one's insight. The electron is considered to be a small magnet with magnetic moment $\vec{\mu}$. In the presence of a magnetic field $\vec{H}$, the electron will experience a torque $\vec{T}$ given by

$$\vec{T} = \vec{\mu} \times \vec{H}. \tag{2.5}$$

But the torque is also equal to the rate of change of angular momentum,

which is $\frac{1}{\gamma}\frac{d\vec{\mu}}{dt}$. Equating the two expressions for the torque gives

$$\frac{1}{\gamma}\frac{d\vec{\mu}}{dt} = \vec{\mu} \times \vec{H} \tag{2.6}$$

and

$$\frac{d\vec{\mu}}{dt} = \gamma\vec{\mu} \times \vec{H}. \tag{2.7}$$

The form of this equation may be changed somewhat by transformation to a rotating coordinate system. The direction of $\vec{H}$ is taken to be the z-axis in the fixed laboratory system. The rotating system is shown in Fig. 2-3(a), where the z'-axis coincides with the z-axis, and the x'- and y'-axes rotate about the common z-axis with an angular frequency $\vec{\omega}$. The time rate of change of the magnetic moment observed in the new system will then be

$$\left(\frac{d\vec{\mu}}{dt}\right)_r = \frac{d\vec{\mu}}{dt} - (\vec{\omega} \times \vec{\mu}). \tag{2.8}$$

Therefore in the rotating system, equation (2.7) transforms to

$$\left(\frac{d\vec{\mu}}{dt}\right)_r = \gamma\vec{\mu} \times (\vec{H} + \frac{\vec{\omega}}{\gamma}). \tag{2.9}$$

The form of equation (2.9) is the same as the form of (2.7) with $\vec{H}$ being replaced by an effective field

$$\vec{H}_e = \vec{H} + \frac{\vec{\omega}}{\gamma}. \tag{2.10}$$

The effective field is observed to be zero when $\vec{\omega}$ corresponds to the "Larmor frequency" $-\gamma\vec{H}$, which illustrates that the magnetic moment is constant in the rotating coordinate system and therefore must be precessing about $\vec{H}$ at the Larmor frequency.

Now consider the case of a static magnetic field with magnitude H_o along the common z-axis and a rotating magnetic field with magnitude H_1 and in the direction of the x'-axis. Equation (2.10) is still valid and may be written as

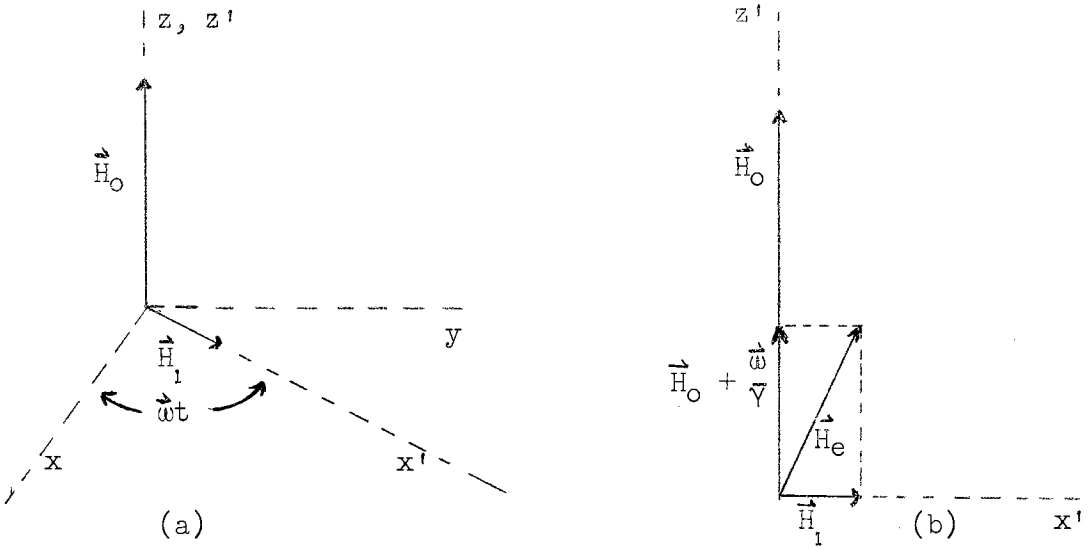

Figure 2-3. (a) Rotating coordinate system. (b) Effective magnetic field in rotating system.

$$\vec{H}_e = H_1\vec{i}' + (H_o + \frac{\omega}{\gamma})\vec{k}'. \tag{2.11}$$

Although $\vec{\mu}$ is now observed to precess about $\vec{H}_e$, whenever the conditions $H_1 \ll H_o$ and $H_1 \ll (H_o + \frac{\omega}{\gamma})$ both hold, the effects of $\vec{H}_1$ are negligible. However, when the frequency $\vec{\omega}$ corresponds closely to the Larmor frequency $-\gamma\vec{H}_o$, it is possible to have $(H_o + \frac{\omega}{\gamma}) < H_1$ with $H_1 \ll H_o$. The direction of $\vec{H}_e$ will differ significantly from the z'-axis, and the precession of $\vec{\mu}$ about $\vec{H}_e$ will introduce periodic changes in the z'-component of $\vec{\mu}$. In the laboratory system, the magnetic moment will precess about $\vec{H}_o$ at varying angles with the z-axis. When the resonance condition

$$\vec{H}_o + \frac{\vec{\omega}}{\gamma} = 0 \tag{2.12}$$

is exactly satisfied, the magnetic moment will precess about $\vec{H}_1$ at an angular frequency of $-\gamma\vec{H}_1$. The motion of $\vec{\mu}$ in the laboratory system will be a combination of the precession about $\vec{H}_1$ as observed in the rotating system and the precession about $\vec{H}_o$ at the Larmor frequency.

The classical magnetic interaction energy expression for the system is

$$E = -\vec{\mu} \cdot \vec{H} \simeq -\mu_z H_o. \tag{2.13}$$

Therefore energy must be absorbed from the rotating magnetic field when the z-component of $\vec{\mu}$ is decreased. However, the motion of the moment is periodic. Therefore, if the resonance condition is maintained for a sufficient time and no relaxation processes occur, there will be no net absorption, but alternate receiving and giving of energy.

Bloch Equations

The preceding description did not include considerations of relaxation effects leading to equilibrium conditions. When a substance is placed into a magnetic field of magnitude H_o in the z-direction, the electrons will align themselves parallel or antiparallel to the magnetic field and, under equilibrium conditions, will assume a Boltzmann distribution. There is a resulting thermal equilibrium magnetization $M_o\vec{k}$, which is given by

$$M_o\vec{k} = \chi_o H_o \vec{k}, \tag{2.14}$$

where χ_o is the static magnetic susceptibility. Bloch (83) assumed that the system would approach equilibrium conditions governed by the equations

$$\dot{M}_z = -\frac{(M_z - M_o)}{T_1}, \tag{a}$$

$$\dot{M}_x = -\frac{M_x}{T_2}, \tag{b}$$

$$\dot{M}_y = -\frac{M_y}{T_2}, \tag{c}$$

(2.15)

where the "longitudinal" relaxation time T_1 is generally called the "spin-lattice relaxation time", and the "transverse" relaxation time T_2 is generally called the "spin-spin relaxation time". The characteristic decay time of M_z is assumed to be different from that of M_x and M_y, because energy transfer is required for changes in M_z, but the energy of the spin system is not changed with variations of M_x or M_y, which are perpendicular to $\vec{H}_o$.

In the absence of relaxation effects, the equation of motion is

$$\frac{d\vec{M}}{dt} = \gamma\vec{M} \times \vec{H}. \tag{2.16}$$

With the assumption that $H_1 \ll H_o$, so that the equilibrium magnetization would be very nearly $\vec{M}_o$, the equation of motion including relaxation effects is

$$\frac{d\vec{M}}{dt} = \gamma(\vec{M} \times \vec{H}) + \frac{M_o - M_z}{T_1}\vec{k} - \frac{M_x}{T_2}\vec{i} - \frac{M_y}{T_2}\vec{j}. \tag{2.17}$$

This equation may be written in the rotating coordinate system as

$$\left(\frac{d\vec{M}}{dt}\right)_r = \gamma(\vec{M} \times \vec{H}_e) + \frac{M_o - M_{z'}}{T_1}\vec{k}' - \frac{M_{x'}}{T_2}\vec{i}' - \frac{M_{y'}}{T_2}\vec{j}'. \tag{2.18}$$

Since

$$\vec{H}_e = (H_o + \tfrac{\omega}{\gamma})\vec{k}' + H_1\vec{i}', \tag{2.19}$$

it follows that $(\vec{M} \times \vec{H}_e)$ may be written

$$\vec{M} \times \vec{H}_e = M_{y'}(H_o + \tfrac{\omega}{\gamma})\vec{i}' + [M_{z'}H_1 - M_{x'}(H_o + \tfrac{\omega}{\gamma})]\vec{j}' - M_{y'}H_1\vec{k}', \tag{2.20}$$

and equation (2.18) becomes

$$\frac{dM_{x'}}{dt} = \gamma M_{y'}(H_o + \tfrac{\omega}{\gamma}) - \frac{M_{x'}}{T_2}, \tag{a}$$

$$\frac{dM_{y'}}{dt} = \gamma M_{z'}H_1 - M_{x'}(H_o + \tfrac{\omega}{\gamma}) - \frac{M_{y'}}{T_2}, \tag{b} \quad (2.21)$$

$$\frac{dM_{z'}}{dt} = -\gamma M_{y'} H_1 + \frac{M_o - M_{z'}}{T_1} . \qquad (c)$$

Equations (2.21) may be simplified to

$$\frac{dM_{x'}}{dt} = -M_{y'}(\omega_o - \omega) - \frac{M_{x'}}{T_2} , \qquad (a)$$

$$\frac{dM_{y'}}{dt} = -M_{z'}\omega_1 + M_{x'}(\omega_o - \omega) - \frac{M_{y'}}{T_2} , \qquad (b) \quad (2.22)$$

$$\frac{dM_{z'}}{dt} = M_{y'}\omega_1 + \frac{M_o - M_{z'}}{T_1} , \qquad (c)$$

by the substitutions $\omega_o = -\gamma H_o$ and $\omega_1 = -\gamma H_1$.

When the time of passage through the resonance condition is long compared to the relaxation times, the magnetization can be considered to have its equilibrium value. To a first approximation, this can be expressed by $\dot{M}_{x'} = \dot{M}_{y'} = \dot{M}_{z'} = 0$. Equations (2.22) may then easily be solved for $M_{x'}$, $M_{y'}$, and $M_{z'}$, and give

$$M_{x'} = \frac{M_o T_2^2 \omega_1 (\omega_o - \omega)}{[1 + T_1 T_2 \omega_1^2 + T_2^2(\omega_o - \omega)^2]} , \qquad (a)$$

$$M_{y'} = -\frac{M_o T_2 \omega_1}{[1 + T_1 T_2 \omega_1^2 + T_2^2(\omega_o - \omega)^2]} , \qquad (b) \quad (2.23)$$

$$M_{z'} = \frac{M_o[1 + (\omega_o - \omega)^2 T_2^2]}{[1 + T_1 T_2 \omega_1^2 + T_2^2(\omega_o - \omega)^2]} . \qquad (c)$$

Equations (2.23) may be further simplified when H_1 is very small, so that $T_1 T_2 \omega_1^2 \ll 1$. Then they have the simple form

$$M_{x'} = \frac{M_o T_2^2 \omega_1 (\omega_o - \omega)}{1 + T_2^2(\omega_o - \omega)^2} , \qquad (a)$$

$$M_{y'} = -\frac{M_o T_2 \omega_1}{1 + T_2^2(\omega_o - \omega)^2} , \qquad (b) \quad (2.24)$$

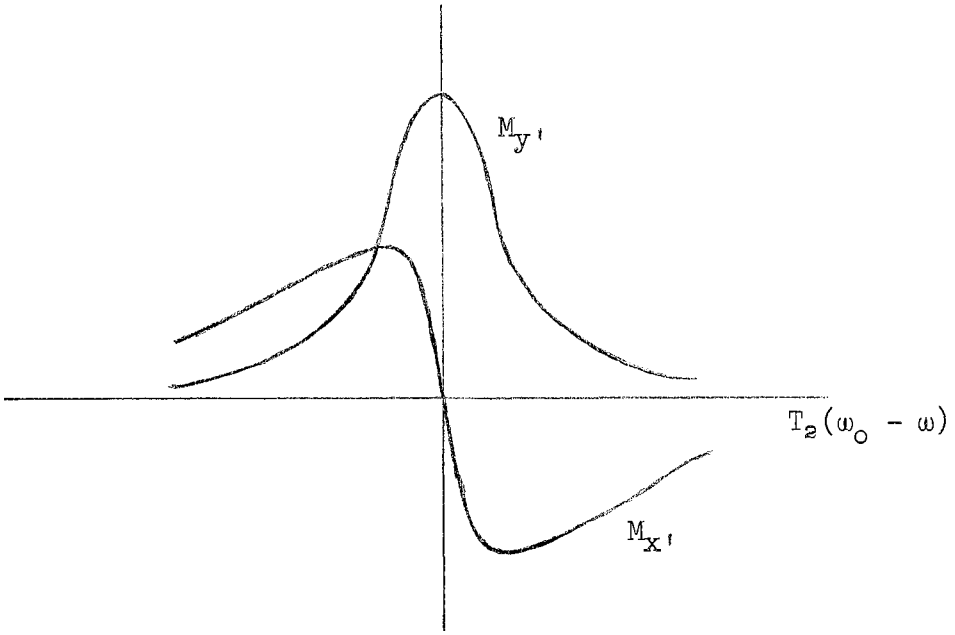

Figure 2-4. Transverse magnetization.

$$M_{z'} = M_o. \qquad (c)$$

In practice, the method used for obtaining the rotating magnetic field H_1 is the extraction of a component of an alternating field. A field linearly oscillating in the x-direction such that $H_x(t)$ is given by $H_x(t) = H_{xo} \cos \omega t$ may be separated into two rotating components rotating about the z-axis with angular frequencies ω and $-\omega$, respectively. This is demonstrated in Fig. 2-5, where the rotating fields are defined by

$$\vec{H}_R = \tfrac{1}{2}H_{xo}(\vec{i} \cos \omega t + \vec{j} \sin \omega t) \qquad (a) \quad (2.25)$$

$$\vec{H}_L = \tfrac{1}{2}H_{xo}(\vec{i} \cos \omega t - \vec{j} \sin \omega t). \qquad (b)$$

It is clearly seen that the rotating field $\vec{H}_1$ corresponds to $\vec{H}_R$ with $2H_1 = H_{xo}$.

The high frequency susceptibility $\chi = \chi' - \chi''$ is introduced, and M_x is taken to be the real part of the complex quantity $\chi[2H_1 \exp(i\omega t)]$.

Then M_x is given by

$$M_x = \chi' 2H_1 \cos \omega t + \chi'' 2H_1 \sin \omega t. \tag{2.26}$$

From simple considerations of the components of $M_{x'}$ and $M_{y'}$ in the x-direction, M_x may also be written as

$$M_x = M_{x'} \cos \omega t - M_{y'} \sin \omega t. \tag{2.27}$$

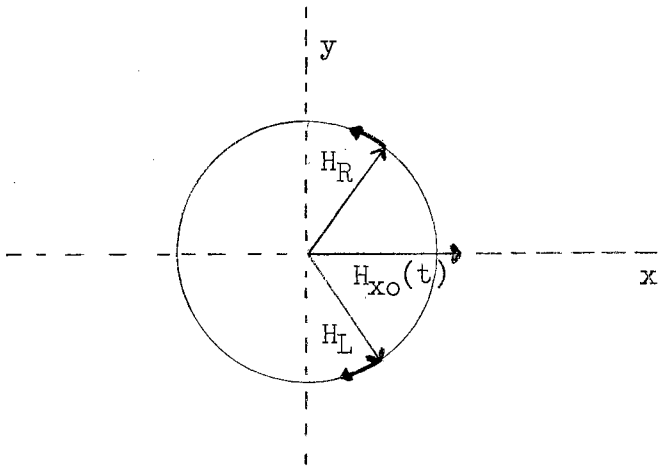

Figure 2-5. Separation of an alternating field into two rotating components.

Comparison of equations (2.26) and (2.27) then yields

$$\chi' = \frac{M_{x'}}{2H_1}, \quad \chi'' = -\frac{M_{y'}}{2H_1}. \tag{2.28}$$

When a coil of inductance L_o is filled with a substance with susceptibility $\chi(\omega)$, the inductance is increased to $L_o[1 + 4\pi\chi(\omega)]$, where $\chi(\omega) = \chi'(\omega) - i\chi''(\omega)$. For a coil with resistance R_o in the absence of the filling substance, the impedence with the filling substance will be

$$\begin{aligned} Z &= iL_o\omega(1 + 4\pi\chi' - i4\pi\chi'') + R_o, \\ &= iL_o\omega(1 + 4\pi\chi') + L\, 4\pi\chi'' + R_o. \end{aligned} \tag{2.29}$$

Therefore, χ' is responsible for a change in inductance, and χ'' effect-

ively changes the resistance.

If uniform magnetic fields occupy the volume V and the peak value of the alternating current is i_o, the magnetic energy stored in the coil is

$$\frac{L_o i_o^2}{2} = \frac{H_{xo}^2 V}{8\pi} = \frac{H_1^2 V}{2\pi} . \tag{2.30}$$

The average power absorbed in the spin system contained in the volume V is

$$\bar{P} = \frac{i_o^2 \Delta R}{2} = \frac{i_o^2 (L_p \omega 4\pi \chi'')}{2\pi} . \tag{2.31}$$

The value of i_o^2 obtained from equation (2.30) may be substituted into (2.31). The average power absorbed in the spin system is then given by

$$\bar{P} = 2\omega H_1^2 \chi'' V. \tag{2.32}$$

The power absorbed can be written as a function of ω by substituting for χ'' from preceding equations. This yields

$$\begin{aligned} \bar{P} &= -\omega H_1 V M_y , \\ &= \frac{\omega H_1 V M_o T_2 \omega_1}{1 + T_2^2 (\omega_o - \omega)^2} \\ &= \frac{\omega H_1 V \chi_o H_o T_2 \omega_1}{1 + T_2^2 (\omega_o - \omega)^2} \\ &= \frac{\omega \omega_o \chi_o H_1^2 T_2 V}{1 + T_2^2 (\omega_o - \omega)^2} \\ &= \pi \omega \omega_o \chi_o H_1^2 g(\omega - \omega_o) V , \end{aligned} \tag{2.33}$$

where $g(\omega - \omega_o) = \dfrac{T_2}{\pi[1 + T_2^2 (\omega - \omega_o)^2]}$. (2.34)

The width of the function at half intensity is given by

$$\omega - \omega_o = \frac{1}{T_2}, \tag{2.35}$$

and the maximum value of $g(\omega - \omega_o)$, T_2/π, occurs when $\omega = \omega_o$.

The line shape can be affected by the following interactions: (1) dipolar spin-spin interaction; (2) spin-lattice interaction; and (3) exchange interaction. The resultant line shape may not be Lorentzian, and definitions of T_2 sometimes given in terms of line shape parameters can differ somewhat from the definition previously given for T_2.

The expressions obtained by consideration of an equivalent LC circuit are general and apply to microwave cavities as well.

CHAPTER III

INSTRUMENTATION

General ESR Spectrometer

As has already been discussed, the condition for resonance is

$$E = h\nu = g\beta H. \tag{3.1}$$

Because of the Boltzmann distribution of electrons in the energy levels, highest sensitivity is obtained at the highest possible energy separation or highest frequency ν which can be obtained. However, there are other considerations for determining ν. In practice, the power available decreases rapidly for wavelengths shorter than 3 cm. Also, detecting elements are inferior at higher frequencies. Sample size is also very important for high frequency work. Although spectrometers using wavelengths of 1.25 cm or 8 mm are more sensitive than 3 cm spectrometers for studying very small specimens such as small single crystals, they are approximately of equal sensitivity for studies of larger samples or samples in which concentration of spins is to be determined (84). The most common ESR spectrometers operate in the 3 cm wavelength range which is classified as the x-band region of the microwave spectrum and corresponds to frequencies near 9.5 kMc/sec. For free electrons, g is approximately 2, whence

$$\nu = 2.80\ H \text{ megacycles/gauss sec.} \tag{3.2}$$

A magnetic field of approximately 3400 gauss is therefore required for free electron resonance.

Because of the coupling mechanism for transitions, as described in the general theory of ESR, it is necessary to have the microwave magnetic field $\vec{H}_1$ perpendicular to the large magnetic field $\vec{H}_o$. Also, the rate of precession is proportional to H_1. Hence the sample needs to be placed at a point of strong $\vec{H}_1 \perp \vec{H}_o$. A microwave resonance cavity is used for this purpose since it stores large amounts of energy in the resonant modes, giving rise to large values of microwave magnetic field $\vec{H}_1$. The "Q factor" of the cavity is defined as

$$Q = \frac{\text{Energy Stored in Cavity}}{\text{Energy Lost}} = \frac{\omega \cdot \text{Energy Stored}}{\text{Rate of Energy Loss}} . \qquad (3.3)$$

The "unloaded Q" is determined by considering only the energy dissipated in the cavity walls. The "loaded Q" also includes the energy lost via the cavity coupling holes and is the factor measured. Typical loaded Q values are 3500 for rectangular cavities and 10,000 for cylindrical cavities.

In order to determine the energy absorption due to the ESR signal, either the reflected energy from the cavity or the energy transmitted through the cavity is observed. Spectrometers utilizing the reflection type cavity are more versatile and are used more often. Since the spectrometer used in this study utilizes a reflection cavity, only this type spectrometer will be discussed. The cavity is constructed such that only the desired resonant mode is established. The sample is positioned in the region of highest microwave magnetic field, and the cavity is turned so that the microwave magnetic field in that region

is perpendicular to the static field. Criteria for selecting certain cavity shapes and modes will be discussed in a later section.

Passage through the resonance condition may be accomplished by varying either the frequency ν or the magnetic field H_o. Because of several practical considerations, such as the frequency instability of the klystron and the sharp frequency dependence of high Q cavities, it is much more convenient to stabilize the klystron at a particular frequency (usually the sample cavity resonance frequency) and vary the magnetic field linearly in time, sweeping past the resonance condition expressed by equation (3.1). The resonance signal can be observed as a small dip in the reflected power level. Since the reflected power level is subject to various fluctuations, especially drift in the klystron or cavity frequencies or the klystron power output, modulation coils are usually added to allow a small alternating field to be superimposed onto the slowly sweeping field. Changes in the reflected power are then observed at the modulation field frequency. The signal thus determined is proportional to the first derivative of the resonance signal provided the modulation field amplitude is sufficiently small. A phase detector is usually incorporated into the detection system so that only signals having a particular phase relationship with the modulation field will be detected and other signals will be rejected.

The basic reflection cavity spectrometer has the following components: a microwave sample cavity; microwave circuitry to introduce microwave energy into the cavity and separate the energy reflected from the cavity for detection; an electromagnet with associated power supply including a linear sweep unit; a modulation field unit which

introduces an alternating magnetic field to the linearly swept field; and a signal detection system including a modulation frequency phase-detector and amplifier. An example of a basic reflection cavity spectrometer is the bridge spectrometer using the "magic-T" as the bridge element as shown is Fig. (3-1).

Description of the ESR Spectrometer Used in the Study

Magnet System

An x-band spectrometer operating at 9.5 kMc/sec requires (for $g = 2$) a magnetic field of 3400 gauss with sufficient homogeneity and stability to prevent distortion of narrow signals. When the line widths are not less than 100 milligauss, the homogeneity is not as critical as in nuclear magnetic resonance (NMR) or ESR of solutions. The magnet power supply must be well regulated and also equipped to sweep the field over a large range. The gap must be large enough to accomodate the cavity and all necessary accessories such as cryogenic equipment. Although it would be advantageous to have a very large gap and extremely high homogeneity, the cost of these features must be considered when the magnet is selected.

The magnet used in the investigation is a Varian 6" rotating electromagnet, Model 4007-1, with ring shim pole pieces and a Model V-2200 Varian power supply. The magnet can be turned a full 200° about the vertical axis to allow single crystal orientation studies. The magnet gap of 2.875" is a significant factor in cavity and dewar design. The magnetic field contour is illustrated in Fig. 3-2.

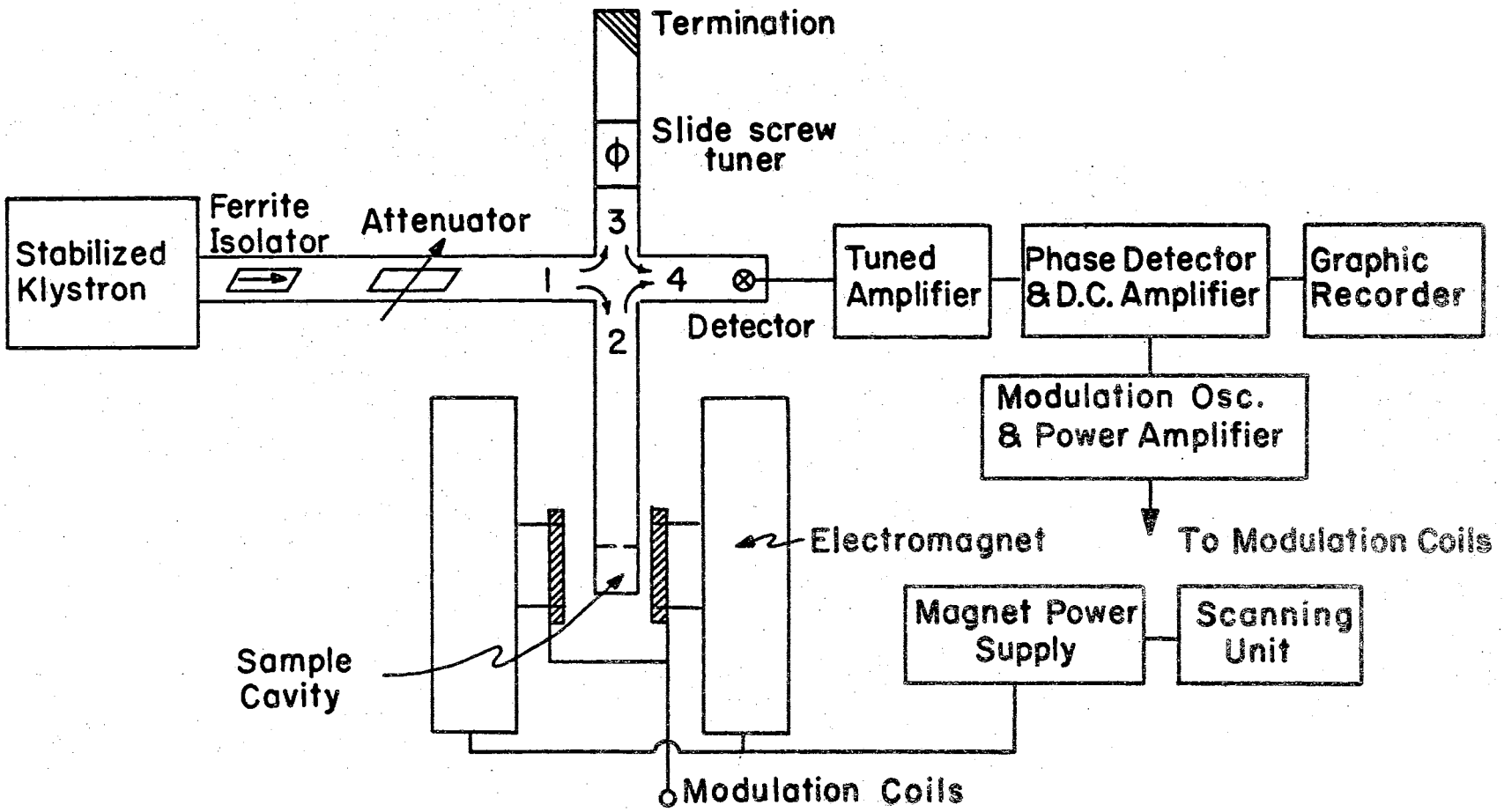

Figure 3-1. Basic components of an ESR bridge spectrometer. (After Bell (79).)

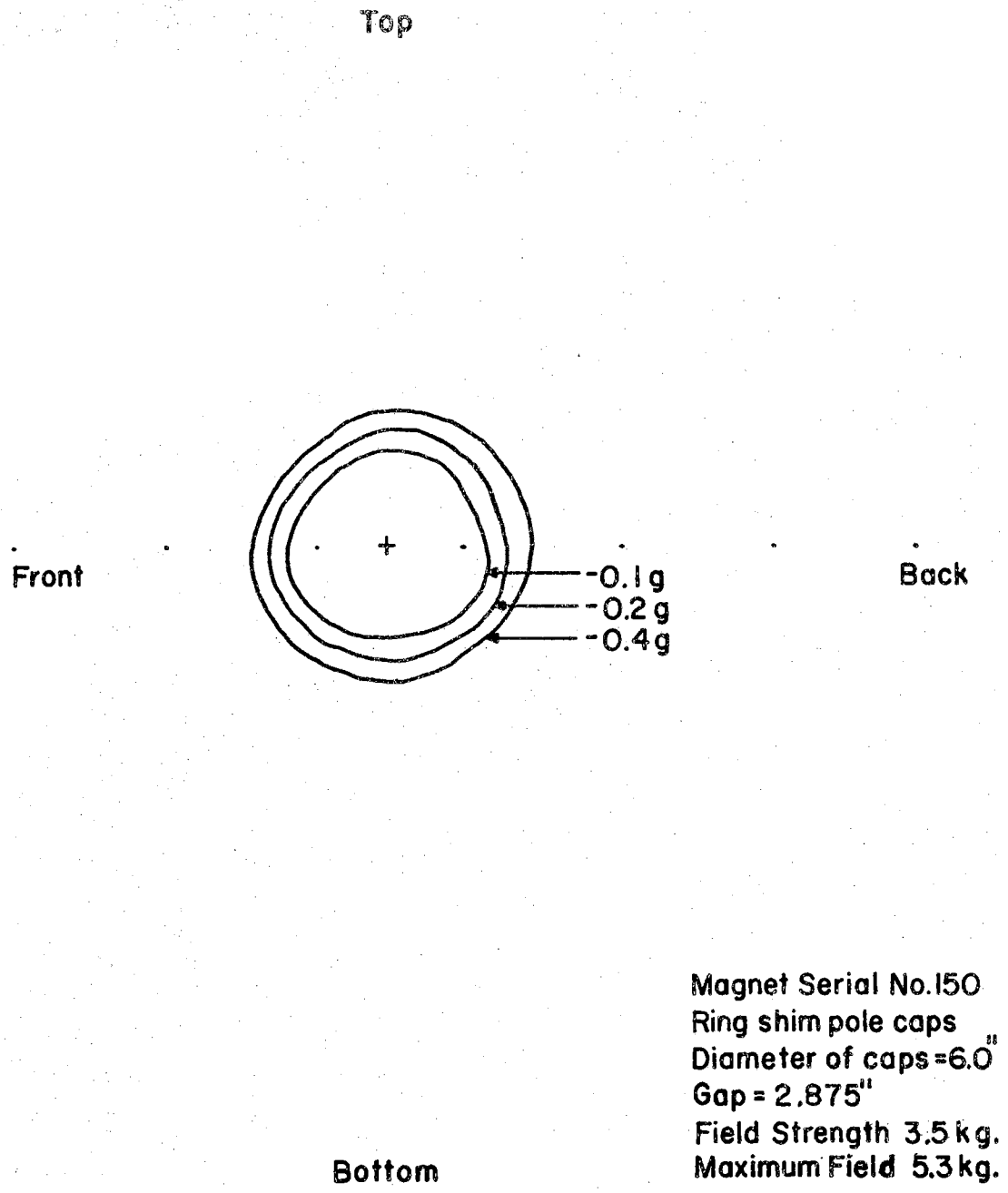

Figure 3-2. Magnetic field plot of Varian Model V4007-1 electromagnet.

The magnetic field strength is determined by use of a NMR detector. The NMR probe is rigidly supported by a clamp around one of the magnet pole pieces. A h/p 524 D electronic counter is used to measure the frequency of the NMR oscillator. The field can be determined from the proton resonance frequency ν by the simple relation

$$H = 2.34868 \times 10^{-4} \nu \text{ gauss sec} \quad (79). \qquad (3.3)$$

Klystron Frequency Stabilization

Although the klystron is selected mainly on the basis of frequency stability, output power, and tuning range, the stability is not sufficient in a sensitive ESR spectrometer unless some stabilizing system is used. A stabilization system which has been used quite successfully for ESR work is the Pound i. f. circuit (85, 86) or its modified form (87).

The stabilization system used in the present study is a modified Pound circuit utilizing a Triconix Model KSL klystron stabilizer with a slightly altered circuit.[2] This arrangement allows the stabilizer to be used essentially according to initial design or in the modified Pound circuit.

In "normal" operation, a small 70 kc/sec modulation signal is introduced onto the klystron reflector. (This is introduced through the exterior modulation connection of the power supply instead of directly as in the unmodified Triconix stabilizer.) The detected output of a cavity is utilized to sense the magnitude and direction of any shift of the klystron frequency with respect to the cavity resonance frequency. The

---

[2]The circuit of the Triconix stabilizer was changed by M. D. Bell while he was a Research Associate at Oklahoma State University.

stabilizer adds a ± dc voltage to the klystron reflector to bring the frequency of the klystron back to the cavity resonance frequency. The cavity used for frequency stabilization may be either the sample cavity or a variable frequency reference cavity tuned to the sample cavity frequency. The circuit changes are shown in Fig. 3-3.

The modified Pound circuit is shown in Fig. 3-4. A small part of the microwave power from the klystron is coupled through the 20 db directional coupler into arm 1 of the magic-T. The power divides into arms 2 and 3 which are adjusted to equal effective lengths. The modulating arm 3 is a matched load so that there is no reflected power in the absence of the 70 kc/sec modulation. However, because of the modulation voltage, side bands 70 kc/sec above and below the klystron frequency are reflected back to the magic-T. When the reference cavity is critically coupled, there is no reflected power from arm 2 when the frequency of the klystron coincides with the cavity resonance frequency. When the frequencies do not coincide, the reflected wave from the cavity has a magnitude dependent upon the frequency difference. The out-of-phase component of the reflected wave has opposite sign on the two sides of the cavity frequency. The two reflected waves from arms 2 and 3 are divided between arms 1 and 4. The reflected waves down arm 1 are dissipated in the ferrite isolator. The waves entering arm 4 are mixed at the detector and give a 70 kc/sec signal with magnitude dependent upon the frequency difference of the klystron and cavity resonance and with phase differing by 180° on either side of the cavity resonance. The 70 kc/sec error signal is amplified and compared with the reference phase signal in the phase detector. The output of the phase detector

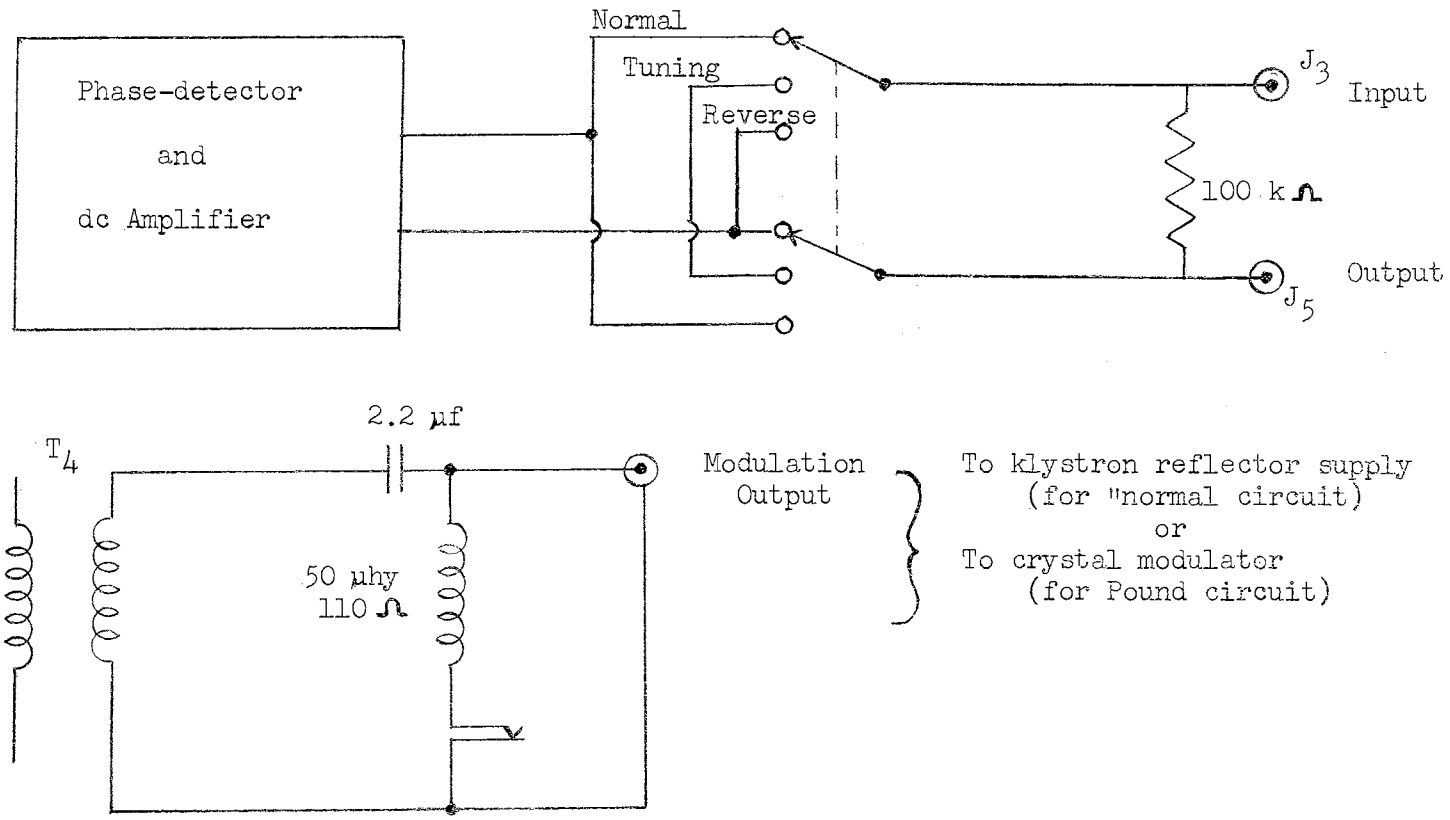

Figure 3-3. Modification of the Triconix stabilizer.

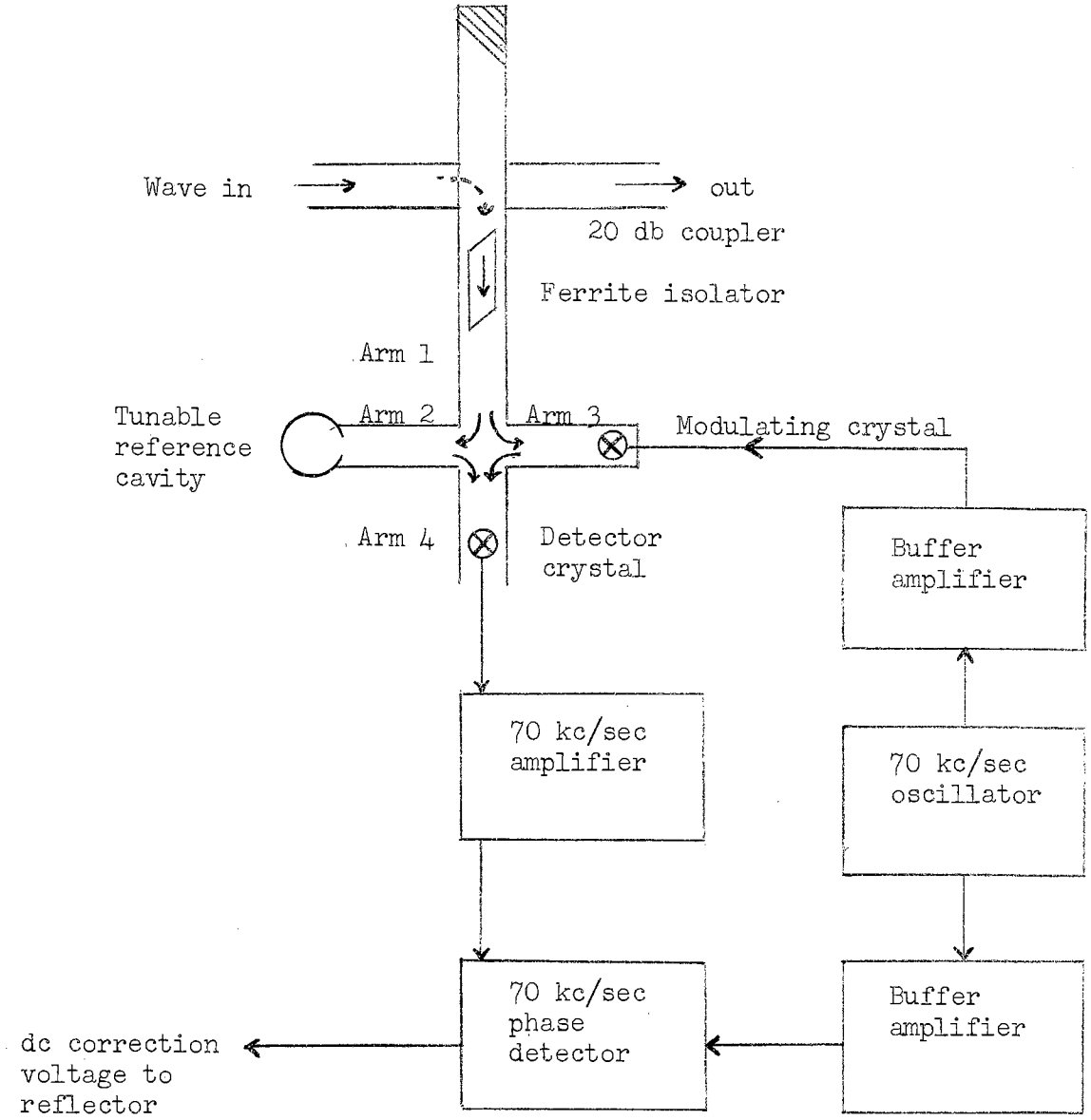

Figure 3-4. Modified Pound frequency stabilizer.

is a ± dc voltage with magnitude determined by the amplitude of the error signal and sign determined by the phase. The dc voltage is applied to the reflector of the klystron to correct the klystron frequency and lock the klystron to the cavity frequency. Since the reflector is at a high negative potential with respect to ground, care must be exercised in isolating the phase detector circuit.

Since the klystron frequency is sensitive to temperature and load, the klystron is mounted in a silicone oil bath surrounded by water cooling coils, and a ferrite isolator is used to isolate the klystron from reflected power from the load. A vibration free support is provided for the microwave components and the other critical parts of the spectrometer. The power supply for the klystron is a well-regulated commercial unit. The filament current is supplied by a transistorized dc supply (79). In order to obtain the fine adjustment of the klystron frequency desired in work with a high Q sample cavity, the battery reflector voltage supply shown in Fig. 3-5 was used. Although capacitors across the batteries would help reduce any noise in the battery voltage, a short circuit in the capacitors could reduce the reflector voltage to zero and jeopardize the klystron.

Reference Cavity

The requirements of a reference cavity are (1) high Q, (2) high frequency stability, (3) frequency tuning range covering all resonant frequencies possessed by the various sample cavities to be used, and (4) a fine frequency adjustment to allow very close matching to the sample cavity. The reference cavity constructed for the study is

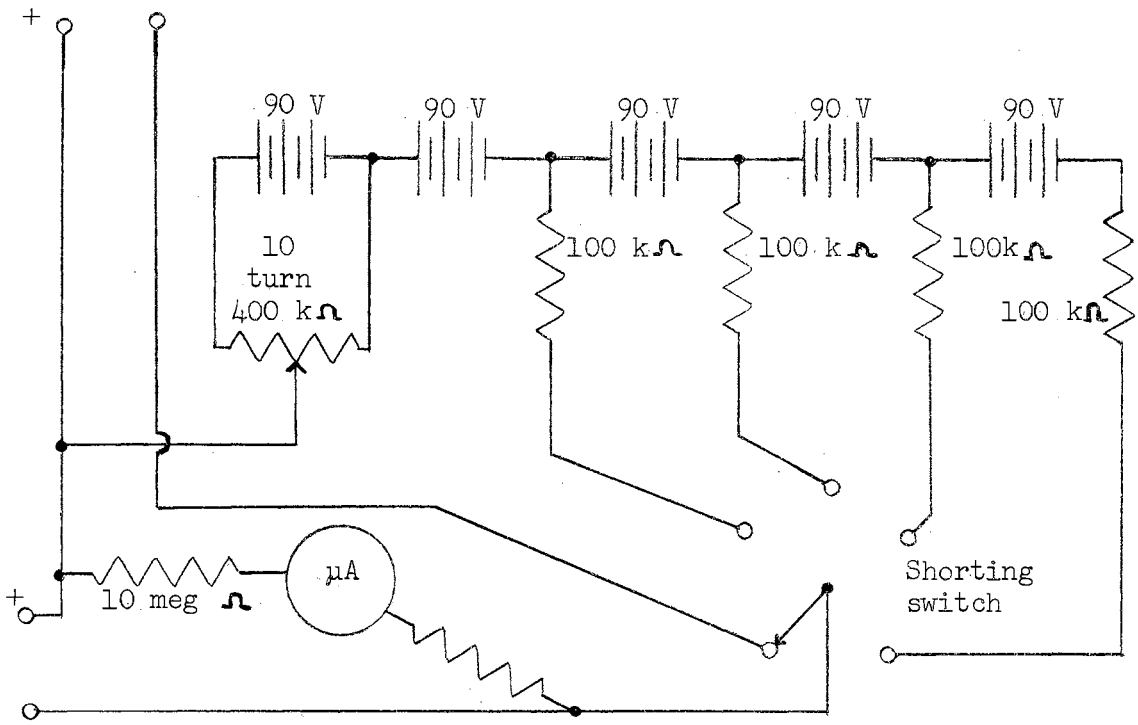

Figure 3-5. Klystron reflector voltage supply.

shown diagramatically in Fig. 3-6. The cylindrical wall of the cavity is made of quartz plated with silver on the inside surface. The top plate is a thin silver disk backed by a heavy brass disk. The coupling is adjusted by a small screw in the brass disk immediately above the coupling iris in the silver disk. The bottom plate is a small silver disk backed by a small brass disk attached to a Model 599-299-100 Brown and Sharp micrometer head. The micrometer head is thermally insulated with plexiglas. The cavity system is then almost totally surrounded by styrofoam insulation for further temperature stabilization. A plug can be removed to allow the micrometer to be read through the transparent plexiglas. The cavity operates in the TE_{011} mode, with no inter-

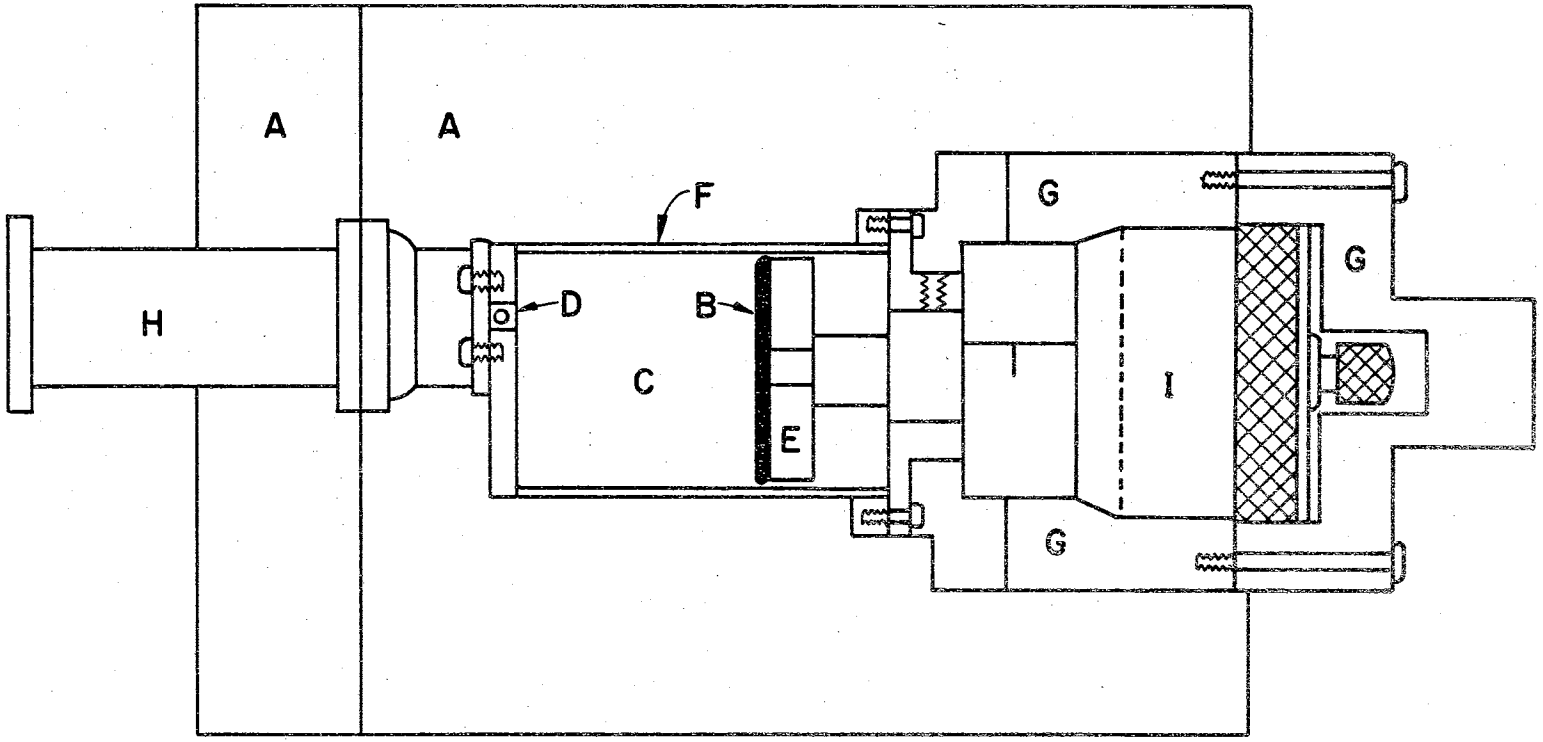

A — Styrofoam Insulation
B — Moveable Cavity Bottom Plate
C — Resonance Cavity
D — Iris and Coupling Screw
E — Eccosorb Epoxy
G — Plexiglas
H — Waveguide
I — Micrometer

F - Silver Plated Quartz Cylinder

Figure 3-6. Cylindrical reference cavity.

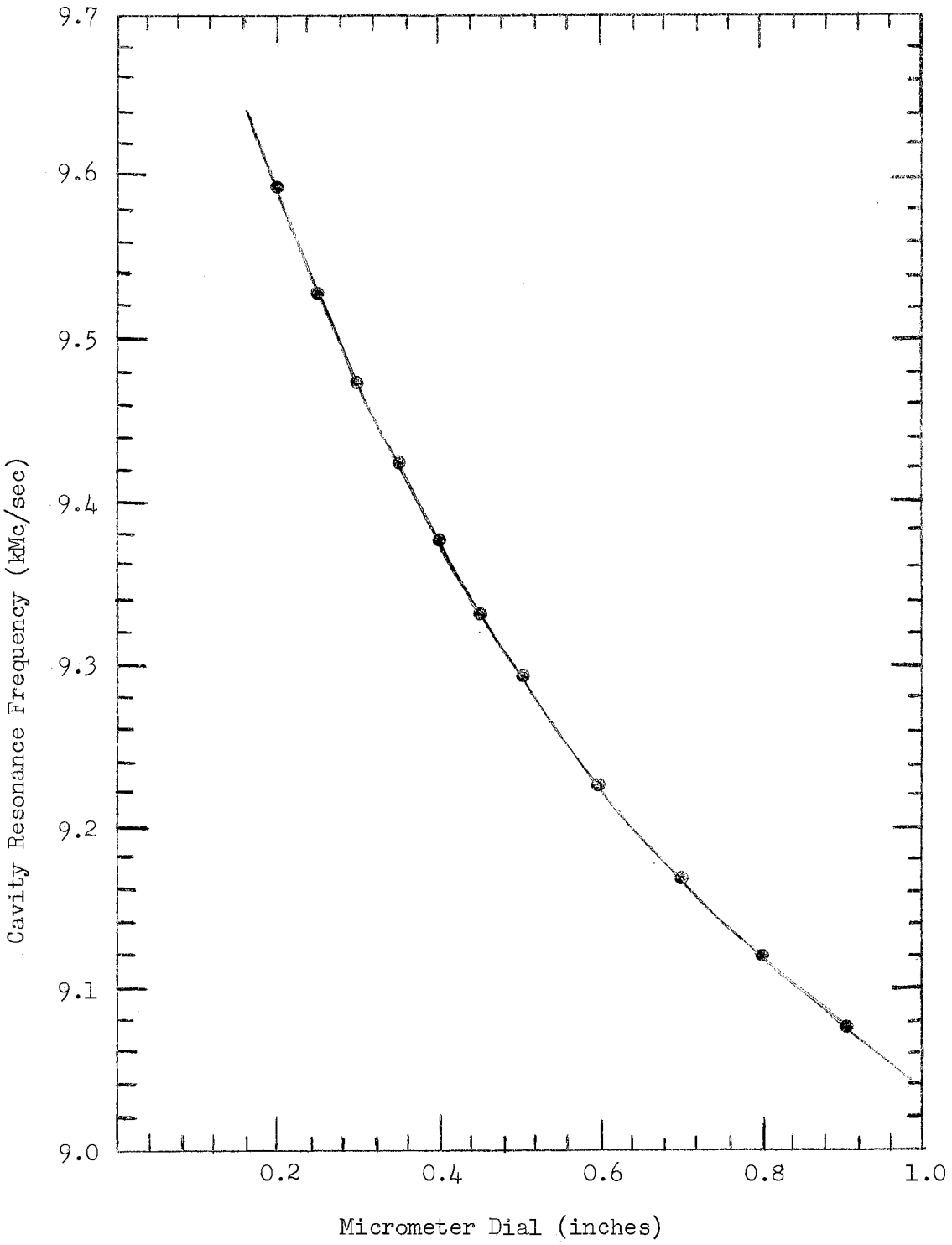

Figure 3-7. Cylindrical reference cavity frequency calibration.

ference from other modes except in the low frequency extremity of its range. The frequency variation with end plate micrometer adjustment was determined by comparison with a calibrated Model 810 Narda wavemeter and is shown in Fig. 3-7.

Microwave Circuit

The spectrometer used in the present study is illustrated in Fig. 3-8. The power from the regulated klystron is divided by the magic Tee T_1, into arms 2 and 3. The power down arm 2 is introduced into arm 1 of the microwave circulator after passing through a precision variable attenuator which controls the power to the sample. The power entering arm 1 of the circulator exits by arm 2 and is coupled into the cavity. The power reflected from the cavity enters the circulator by arm 2 and exits by arm 3. The power is then divided by the magic Tee T_2, and half of the power is detected by the crystal detector in arm 2. The other half of the signal is dissipated (or lost) in arm 3. (An improvement could be made in the system by utilizing matched crystals in arms 2 and 3.) The power from arm 3 of T_1 is used to bias the crystal detector. The variable attenuator in the bias arm is used to adjust the bias voltage to the crystal; the phase shifter is used to adjust the phase for observation of the absorptive (χ'') or dispersive (χ') component of the magnetic susceptibility. The cavity is slightly undercoupled to allow detection of both χ'' and χ'.

A slide screw tuner is incorporated into the sample arm to correct for imperfections in the circulator behavior. A 20 db directional coupler is used to couple a small amount of the incident wave into an arm

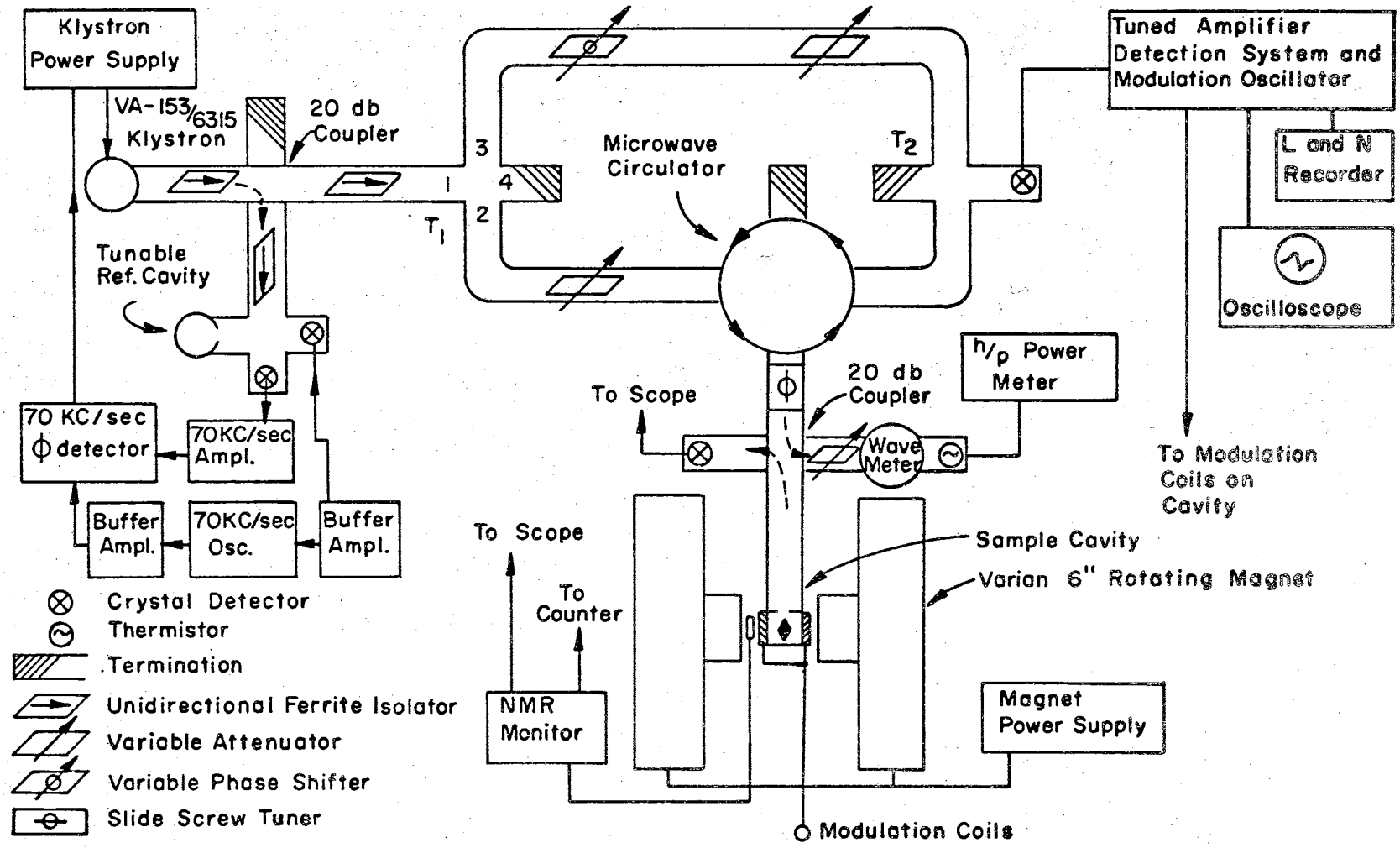

Figure 3-8. Electron spin resonance spectrometer used in the study.

equipped with a wave meter for frequency determination and a power meter for determination of the incident power. A small part of the reflected wave is coupled to a detector for observation on the oscilloscope. The klystron frequency may be measured more accurately by use of a transfer oscillator and electronic counter.

Magnetic Field Modulation

Although a low frequency modulation system with bolometer detection is available for use with the spectrometer (79), a 100 kc/sec modulation system was used exclusively in the present study. The system consists of a pair of modulation coils mounted on the cavity walls so that the modulation field is parallel to the large dc field and a Varian 100 kc/sec modulation control unit containing a tuned amplifier, phase detector, crystal oscillator, and a modulation amplifier. For the greater part of the study, a cylindrical cavity was used. Two 500 turn coils of #40 copper wire were wound and potted in an epoxy cylinder which fits around the cavity. The coils turn with the dc magnet so that the modulation field is always parallel to the dc field. The coils were impedence matched with capacitors to maximize the modulation field inside the cavity. Graphs of the modulation field at the sample position versus the modulation amplifier control dial setting are shown for the cylindrical cavity and for the Varian rectangular cavity in Fig. 3-9.

To a first approximation, the ESR signal intensity is proportional to the modulation amplitude for small modulation field. However, as the modulation amplitude is increased, the curve departs from a true derivative of the resonance signal. The maximum sensitivity is ob-

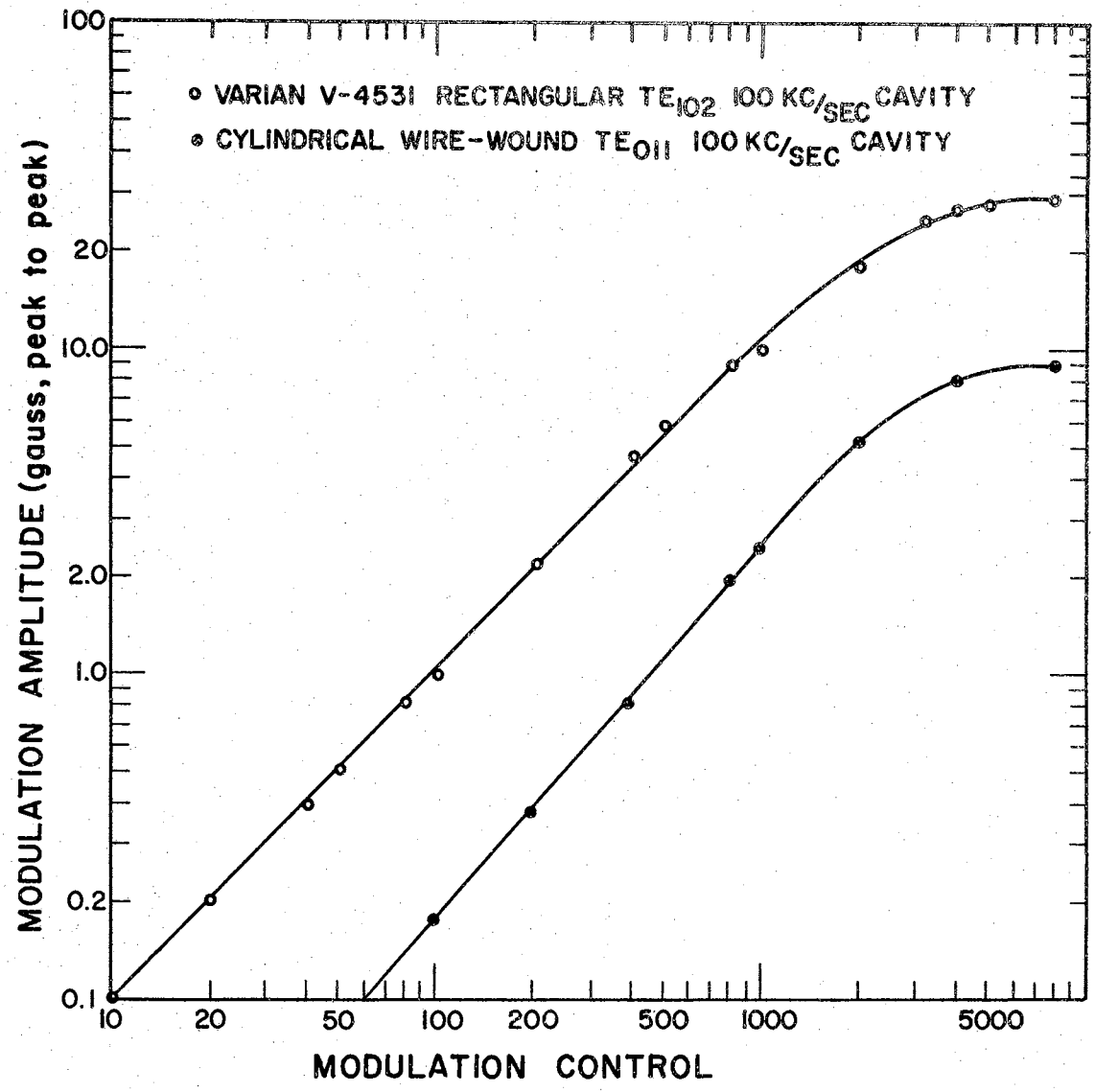

Figure 3-9. 100 kc/sec modulation field calibration.

tained when the peak to peak modulation amplitude is on the order of the line width of the ESR signal, but the signal begins to be quite noticeably distorted when the modulation amplitude is over 1/10 of the linewidth (84).

Microwave Sample Cavity

Since the sample must be placed inside the cavity, special cavity designs are necessary for measurements under particular conditions such as low temperature studies, pressure effect studies, or optical illumination studies. Many cavity designs are described in the literature, and reference will be made later to several in particular.

The two cavity systems used in the present investigation were a Varian V-4531 rectangular ESR cavity operating in the TE_{102} mode and a right circular cylindrical wire-wound cavity operating in the TE_{011} mode. The microwave field configuration for these cavities is shown in Fig. 3-10. The sample is placed in the center of either cavity. The position of maximum microwave magnetic field is also a point of minimum microwave electric field. This is very important in the case of semiconducting diamond samples because a conductor in an area of high microwave electric field will distort the mode configuration and lower the Q.

The Varian cavity is equipped for variable temperature work in the range -185° C to 300° C. The dewar insert of the system is a double wall, high purity quartz cylinder. Horizontal slots are provided in the cavity wall for optical illumination. An optical filter mount was built to fit on the cavity over the slots. Corning colored glass fil-

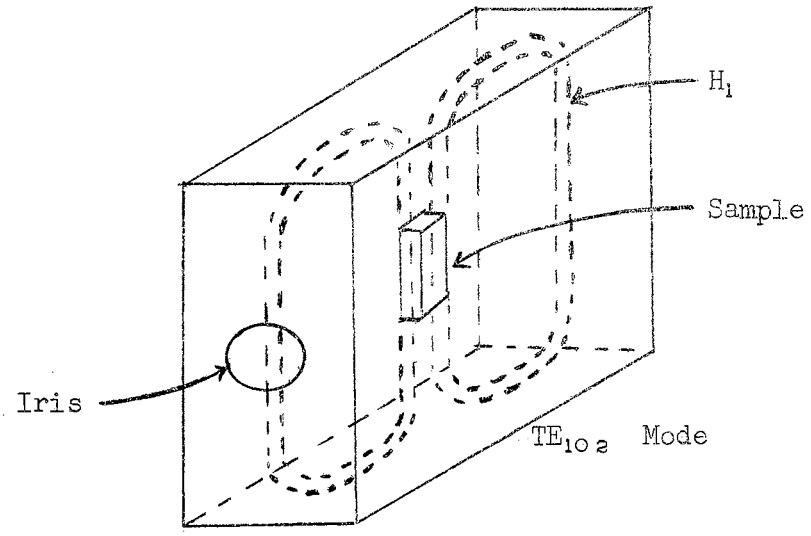

(a)

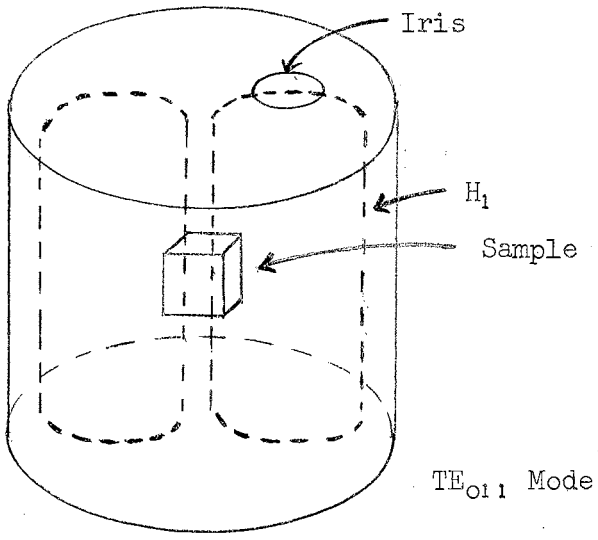

(b)

Figure 3-10. Sample cavities showing microwave magnetic field and location of sample.

ters can be slipped into the mount singly or in groups of two or three. The quartz dewar insert is transparent to light of the wavelengths utilized in this phase of the illumination study.

Several cavities were constructed and tested for use in the illumination study. Since the ESR spectrum of many diamonds is orientation dependent, greatest consideration was given to cylindrical cavities of various types. The first cavities considered were pyrex cylinders plated with thin coats of DuPont "Liquid Bright Gold" or "Liquid Bright Silver" which were painted onto the inside surface and heated to 500° C. Copper or silver end plates were glued to the cylinders. The Q of these cavities was on the order of 7000 when several platings of metal were used. However, the 100 kc/sec modulation is very noticeably attenuated by the metal on the walls. A compromise between the Q and the modulation amplitude must be reached, and a suitable wall thickness with respect to the microwave skin depth and the 100 kc/sec skin depth was selected.

A dielectric cavity was constructed with teflon as the dielectric. The design was patterned after the design specifications of Rosenbaum (88). If a quartz dielectric cavity were used, it would allow illumination of the sample directly through the walls. Another advantage of the dielectric cavity is the freedom from metal walls which attenuate the modulation field. The main advantage in this type of cavity is the ability to observe the ESR spectrum of the dielectric material itself. Optical effects on the ESR spectrum of suitable dielectrics could quite effectively be studied with this type cavity.

The problem of modulation field attenuation has been fairly effectively solved for TE_{011} cylindrical cavities by the use of a helical

groove of small width and pitch around the cylindrical wall (89, 90). The groove attenuates all TM cavity modes but does not seriously effect the TE_{01n} modes when the pitch is small. The same effect is accomplished by wire-wound cavities such as the wavemeter constructed by Barlow, Effemey, and Hargrave (91).

Wire-wound cylindrical cavities for preliminary checks for applicability to the present study were constructed using #28 and #30 enameled copper wire and a shell of Eccobond 45 epoxy. The cavity Q was determined to be on the order of 10,000 for both. Attenuation of the 100 kc/sec modulation field was checked by comparison with a third cavity from which the wire had been removed. There was no noticeable attenuation in either cavity.

The cavity designed and constructed for the present study is a wire-wound right circular cylindrical cavity which resonates in the TE_{011} mode and has a 3.2 cm diameter and 3.2 cm length. The dimensions were selected on the basis of the mode chart and mode shape factor for right circular cylindrical cavities (92). Secon 99.999% pure 0.010" diameter copper wire was wound onto a highly polished solid aluminum mandrel (Fig. 3-11) which had been coated with Devcon mold release agent. The mandrel was placed in a lathe and turned by hand. Clear Hysol XC9-C419 epoxy was brushed onto the mandrel as the wire was wound. The clear epoxy provides an insulation between the successive turns of wire and also makes a smooth, easily cleaned inside surface for the cavity. Since the clear epoxy is not affected by acetone or methyl alcohol, these solvents may be used to clean the cavity walls. The clear epoxy was previously tested for ESR signal, but none was found.

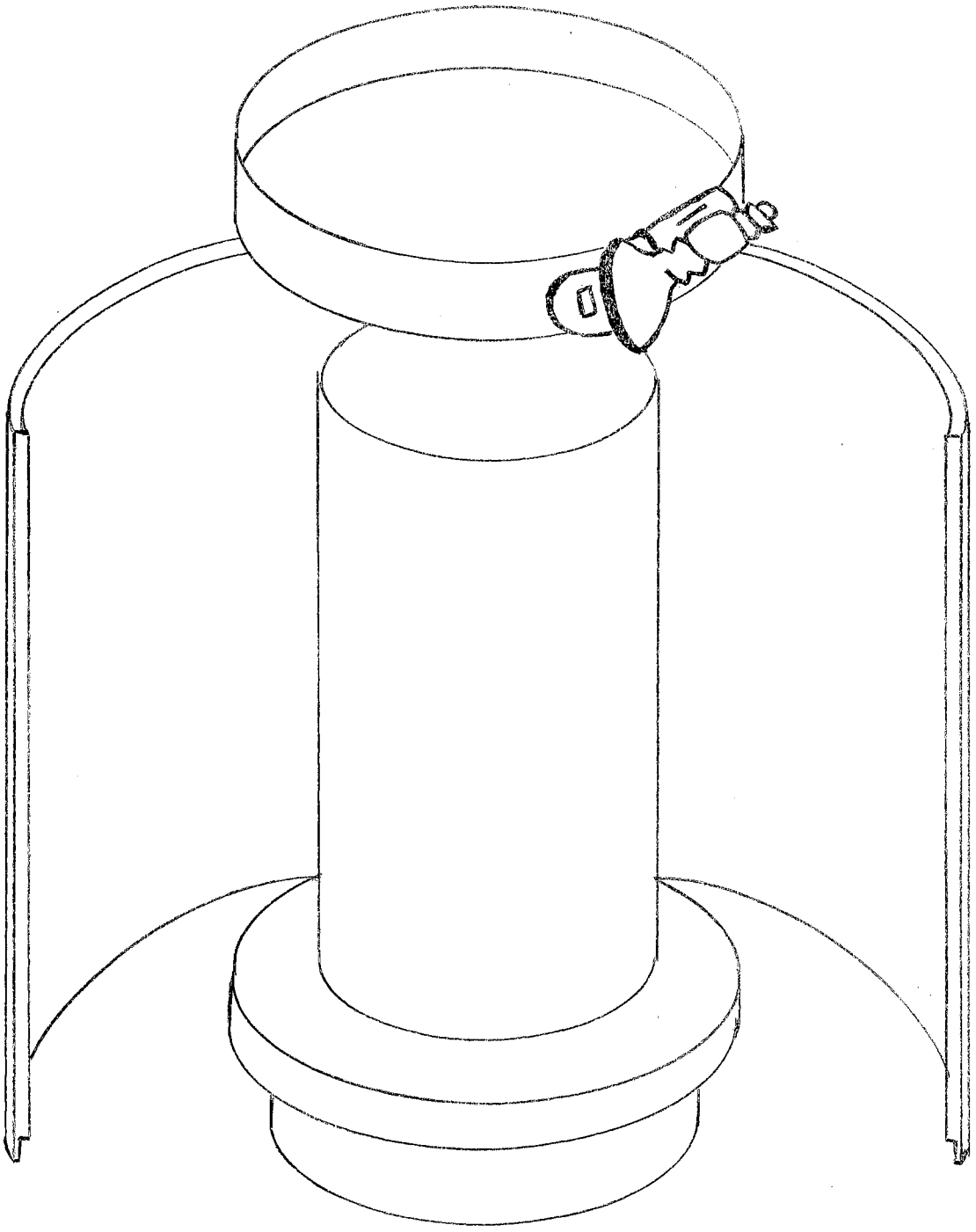

Figure 3-11. Aluminum mandrel and potting shell.

After sufficient wire had been wound on the mandrel, the mandrel was removed from the lathe and heated to hasten the curing of the epoxy. The aluminum shell illustrated in Fig. 3-11 was placed around the mandrel and secured with a circular metal band. The shell was then filled with Emerson and Cumming Stycast 3180M epoxy mixed with lithium aluminum silicate which has a negative coefficient of thermal expansion. The epoxy was cured at an elevated temperature and left for several hours. The shell was then removed, the mandrel was remounted in the lathe, and the wall was turned down to the proper thickness. The wire was then stripped out of the cavity for a very short distance, and the end of the mandrel was thoroughly cleaned to remove any adhering epoxy. A plastic hammer was used to carefully drive the mandrel through the heavy aluminum washer. It was not necessary to taper the aluminum mandrel when a good mold release agent was used. The cavity was shortened in the lathe to the 3.2 cm length desired.

A plastic cylinder of clear Hysol epoxy containing two 500 turn modulation coils was molded and machined to fit between two brass rings glued to each end of the cavity as illustrated in Fig. 3-12. The coil leads were attached to metal binding posts molded into the plastic shell. Coaxial cables were connected to the binding posts. The coaxial cables were connected to a shielded cable, and a capacitor was used for impedence matching.

The top plate is very similar to that described for the reference cavity. The bottom plate is a copper disk fitted into a plexiglas plate. Both end plates are fastened to the respective brass rings with four brass screws. The bottom plate has a small hole in the cen-

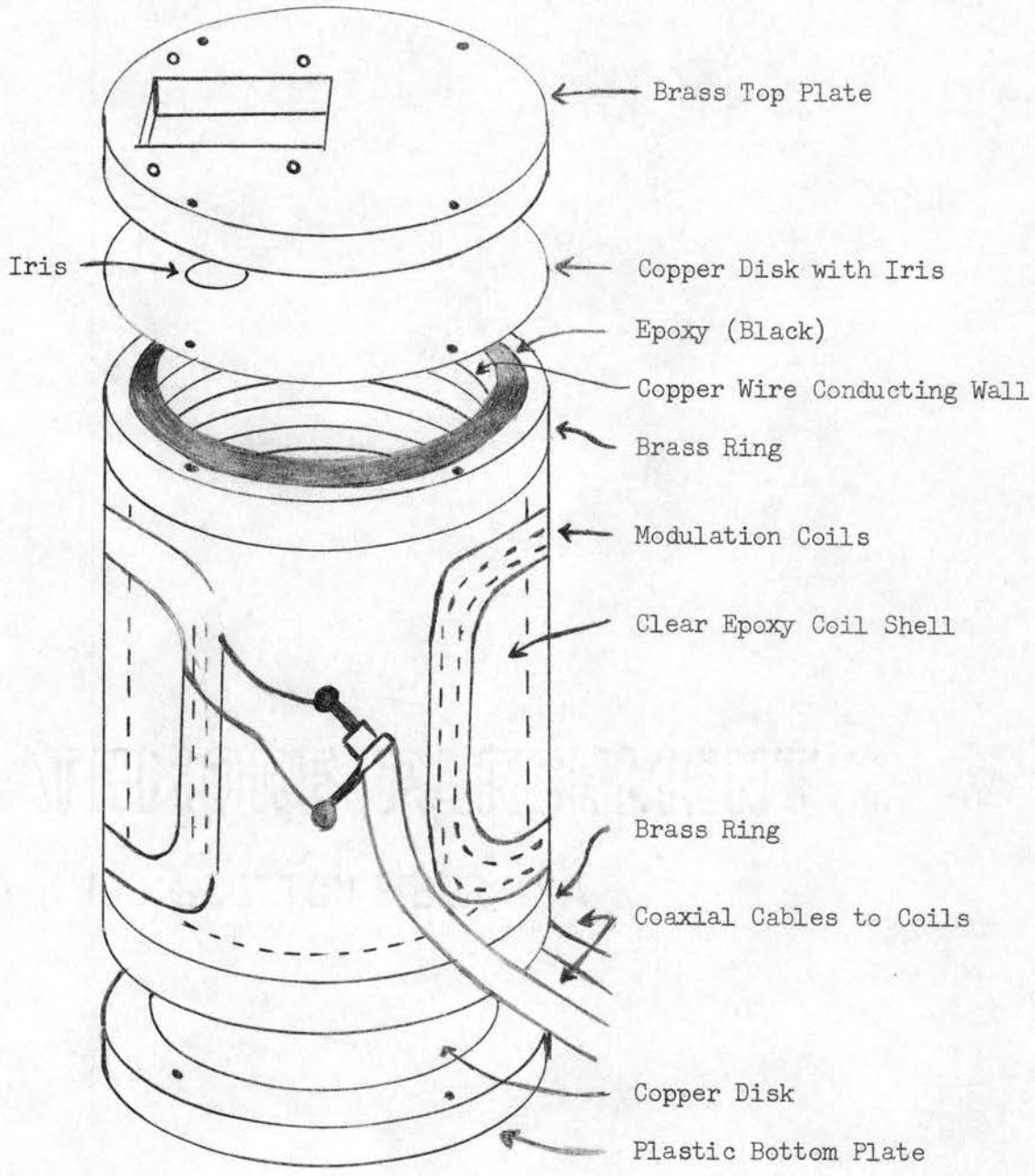

Figure 3-12. Cylindrical sample cavity.

ter for entrance of the light pipe. The loaded Q of the cavity was experimentally determined to be on the order of 10,000.

The sample is mounted as shown in Fig. 3-13. A small plexiglas threaded cylinder is glued to the center of the top plate with Duco cement. Sample mounts made of plexiglas with short Suprasil quartz tubes attached with Duco cement can be screwed into the threaded cylinder after the cavity bottom plate is removed. Diamond samples are temporarily glued to the Suprasil quartz tube. When the samples are oriented using x-ray techniques, a small Suprasil quartz fiber is glued to the diamond in a known crystaline direction for orientation reference. The magnet will rotate in the plane perpendicular to the sample mount axis.

The coupling to the cavity, illustrated in Fig. 3-14, is accomplished with a two vane dielectric coupling system (93). The quartz vanes enter the waveguide through a long slot. They are supported by two teflon blocks riding on a threaded stainless steel rod. The stainless steel rod is threaded on one end with left-handed threads and on the other end with right-handed threads. The teflon blocks move apart or together as the rod is turned. The stainless steel rod is fastened to a long nylon rod. The vanes were made from a quartz microscope slide and several short sections of quartz rod, cemented together with Thermal American quartz cement. Each vane was cut to a length approximately 1/4 the wavequide wavelength at the cavity frequency. The teflon blocks and stainless steel rod are housed in a stainless steel x-band waveguide which is sealed to the regular waveguide. The nylon rod exits through a hole in a teflon seal at the top of the waveguide section. The vanes may be moved closer or farther from the iris, and

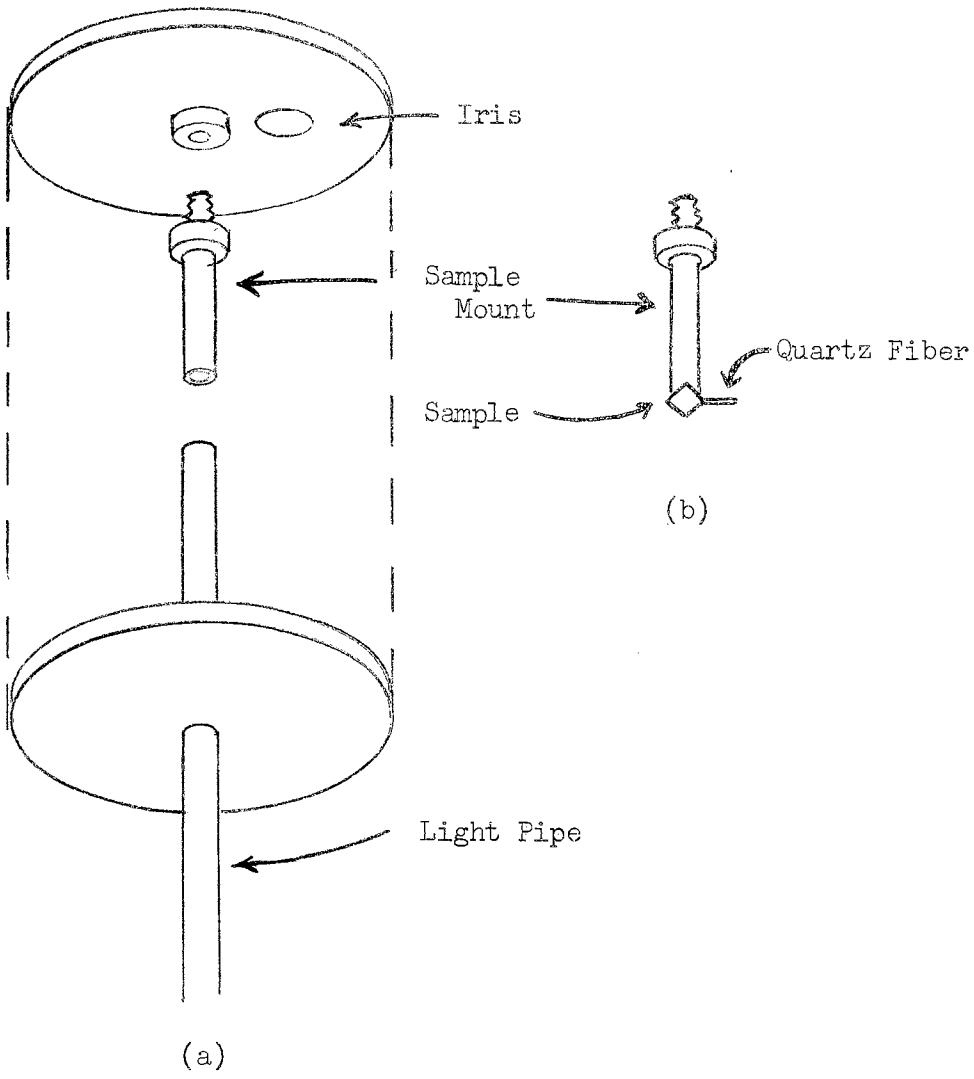

Figure 3-13. (a) Cavity with sample mount. (b) Oriented and mounted sample.

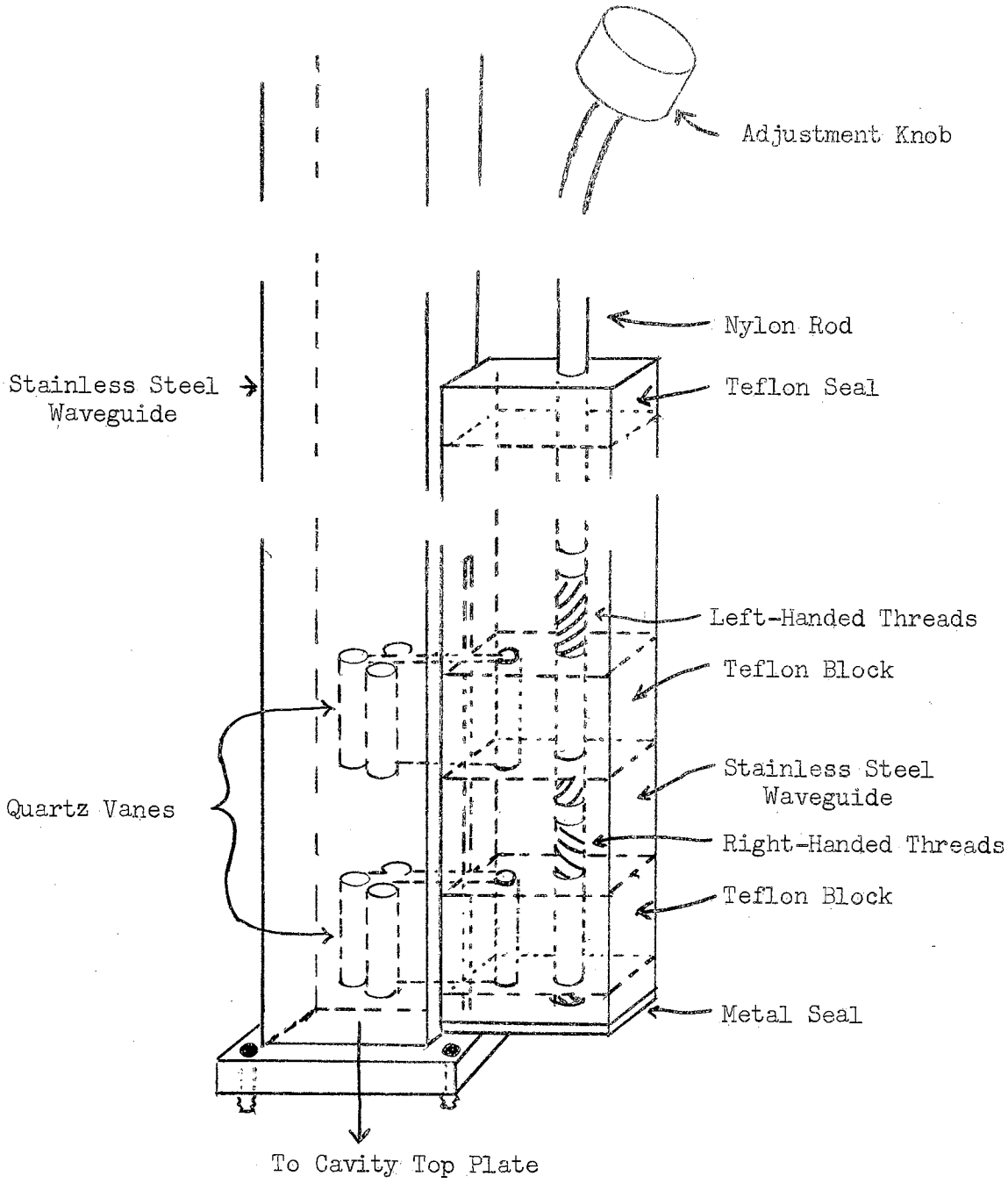

Figure 3-14. Dielectric coupling system.

the vane separation can be varied. The coupling system is adequate in most cases, but for very lossy samples such as the semiconducting diamonds, the cavity can not be critically coupled. The coupling range can be extended considerably by adding a heavy copper wire, cut to the vane length, to each vane.

A styrofoam dewar system was constructed to fit around the cavity and fit snugly between the cavity pole pieces. The dewar was designed to hold liquid nitrogen which would be in contact with the brass cavity top plate. The dewar turns with the rotation of the magnet, and the modulation coils are turned by the dewar. A small copper tube was epoxied to the waveguide about 5" above the iris. Dry nitrogen could be passed through the tube to purge the cavity and waveguides. Four small holes were drilled in the cavity bottom plate to allow the gas to escape. The dewar worked nicely in every way except as a nitrogen reservoir. The dewar had been constructed from two blocks of styrofoam, and the seal between the two sections had many small leaks that were impossible to patch.

The system was converted to a variable temperature arrangement based on the principle of the Varian variable temperature system. The heat exchange coils of the Varian unit were utilized. Dry nitrogen was passed through the coils immersed in a large dewar of liquid nitrogen. The cold gas then passed through a short rubber tube insulated with fiberglass into the copper tube in the side of the stainless steel waveguide. The cold gas was forced to exit out the four small holes in the bottom plate of the cavity. The waveguide system above the cavity was insulated with fiberglass. The temperature could be varied by a

change in the gas flow rate. The temperature could not be measured when a sample was mounted for ESR measurements. However, a thermocouple was placed at the sample position, and the temperature was determined for the two flow rates used in the study. The temperature on successive days using the same flow rate was very nearly the same, as evidenced by the resonant frequency of the sample cavity which is temperature dependent. ESR data was taken at room temperature and at approximately - 50° and - 90° C using this system. One difficulty encountered in the variable temperature system was the inability to rotate the magnet after the sample was cold. The rubber hose providing the cold gas becomes rigid. The liquid nitrogen system was originally designed to allow orientation studies at low temperatures.

Optical Illumination System

The initial work in the study was conducted with Corning colored glass filters mounted on the Varian variable temperature cavity in front of the horizontal slots. Light sources included tungsten filament lamps, a high-pressure mercury arc lamp, and a Westinghouse 250 watt heat lamp. The light from the various light sources was focussed by a 6" diameter aluminum front surface mirror. With this system it was not possible to study the effects of light with wavelength shorter than the fundamental absorption edge of diamond without also including visible wavelengths.

As was previously mentioned, the light pipe for sample illumination in the wire-wound cavity system enters through a small hole in the center of the bottom plate. The light pipe is a 12" Engelhard

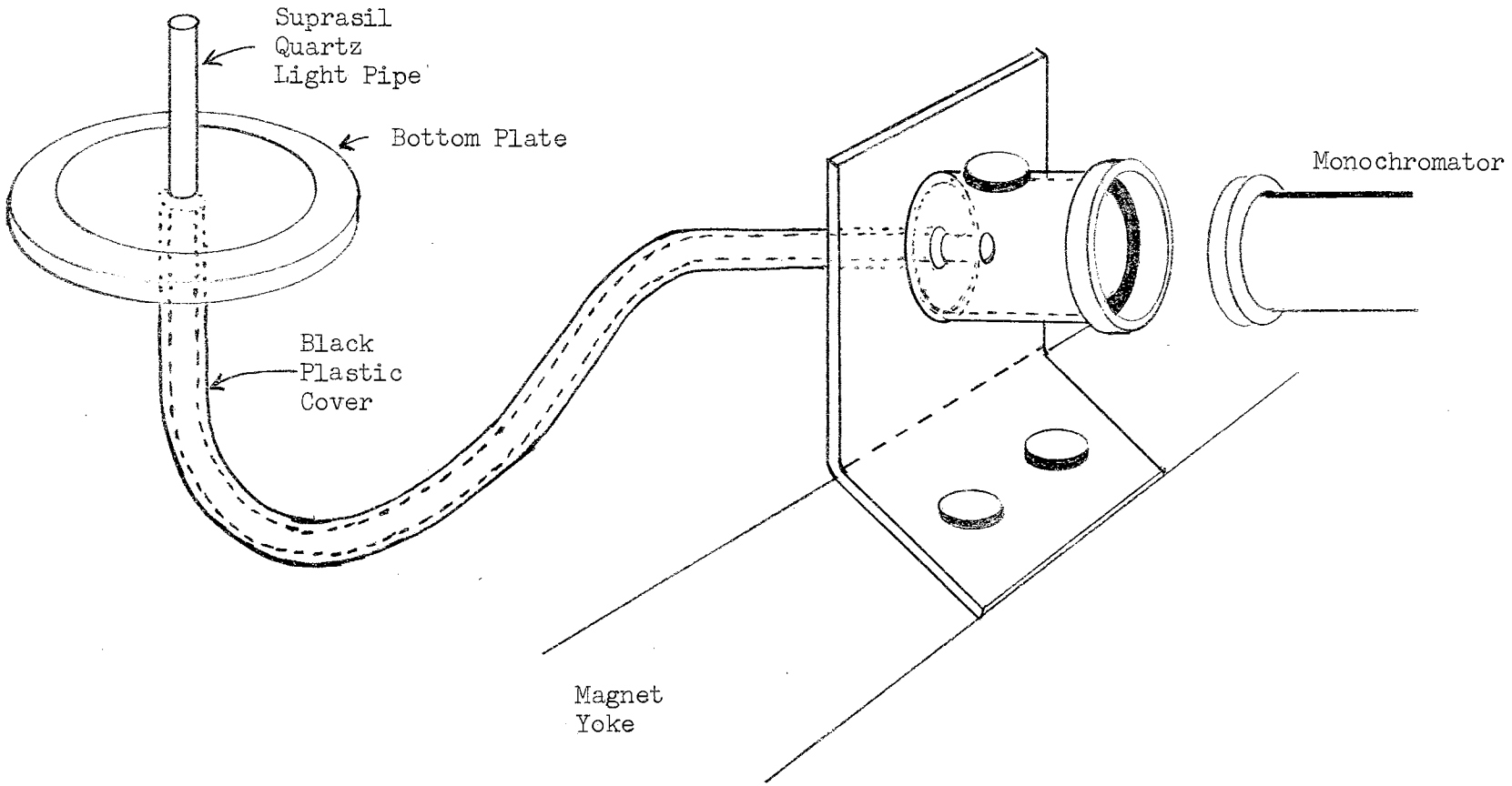

Figure 3-15. Suprasil light pipe mounting arrangement.

Suprasil quartz rod bent into the shape illustrated in Fig. 3.15. A 3 mm diameter rod was first used, but a 4 mm diameter rod worked better and was used in all the later work. A brass mount fastened to the magnet yoke supports the end of the light pipe and receives the extended lens system from the Bausch and Lomb uv monochromator. The monochromatic light beam is roughly positioned by the brass mount. A 1/2 " threaded plug can be removed from the brass mount to allow critical focussing of the light beam on the light pipe. The light pipe is shielded from stray light by a black plastic tube which covers the light pipe from the brass mount to the cavity bottom plate. The short wavelength cut-off for the quartz lenses in the monochromator is approximately 195 mμ, which is well below the fundamental absorption edge for diamond.

Light sources used with the monochromator included a high-pressure mercury arc lamp, a high intensity 6-volt tungsten filament automobile lamp, and a deuterium lamp with a Suprasil window, which was operated at approximately 45 watts.

X-Ray Illumination Mount

A small cylindrical dewar with styrofoam insulation was constructed for irradiation of samples with x-rays at liquid nitrogen temperature. The dewar system, illustrated in Fig. 3-16, will hold liquid nitrogen for approximately 15 minutes if it has been sufficiently pre-cooled. The sample is glued to a quartz sample tube and inserted through the styrofoam lid. The sample rests on the 1/4" copper rod. The x-ray beam is unaffected by the styrofoam walls, and the sample is effectively shielded from

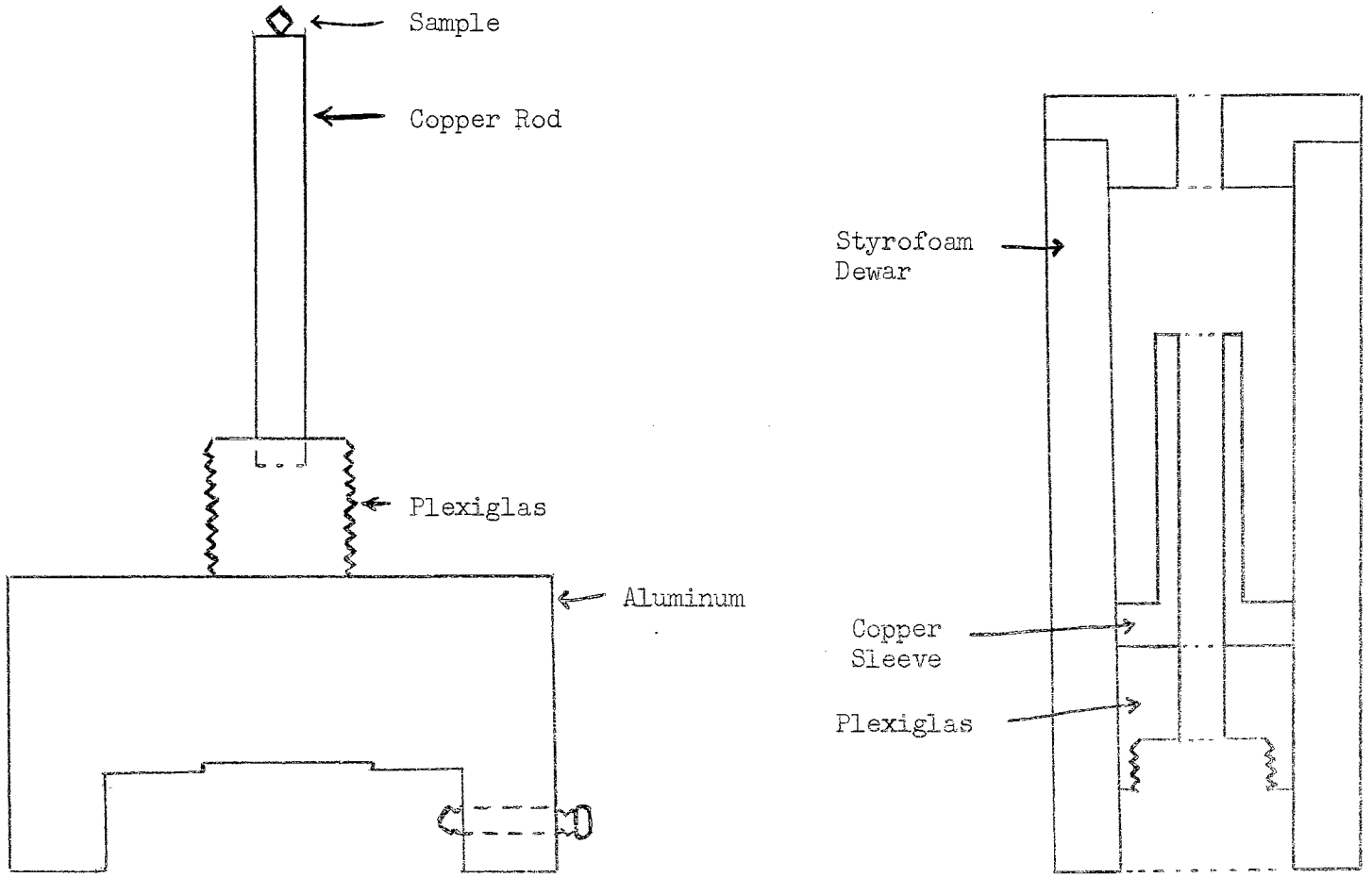

Figure 3-16. X-ray illumination dewar.

room light.

After the sample has been irradiated the desired period of time, it is lifted slightly off the copper rod while the dewar is unscrewed from the aluminum stand. The dewar is then screwed onto the pre-cooled Varian variable temperature cavity, and the sample is slipped into the cavity by way of the hole vacated by the copper rod.

CHAPTER IV

RESULTS AND DISCUSSION OF THE STUDY

General Remarks

The ESR spectra of several diamonds were investigated. Experiments were first conducted with the colored glass filter system with the Varian variable temperature cavity. A significant change was observed in the spectrum of one sample at room temperature. The effect was stronger in this sample at low temperatures, and a low temperature effect was observed in a second sample. The effect of light on the spectra of these two samples was strongly dependent upon the light intensity, even though the spectra returned to the initial conditions very slowly in the absence of light. Therefore, a new system was sought which would provide better light focussing on the sample. The x-ray illumination system was used since a large number of electrons could be excited across the forbidden gap.

The cylindrical cavity with the Suprasil quartz light pipe provides a much more efficient illumination system. The cylindrical cavity system has a higher Q and allows rotation of the magnet and modulation coils for orientation studies. However, the high Q gives rise to increased saturation problems, and the spectra of several samples had to be observed with the reference phase in quadrature with the modulation field (94, 95, 96).

Since the styrofoam dewar completely fills the region between the magnet pole pieces, the magnetic field can not be determined by use of the NMR probe. Therefore the g-value, line width, or hyperfine splitting must be determined from data taken with the Varian cavity.

A brief study of the luminescence of approximately 72 diamond specimens was conducted.[3] All the diamonds were first illuminated by long and short uv light from a filtered mercury arc lamp and were observed through colored filters. Then most of the samples were investigated somewhat more rigorously with the Bausch and Lomb monochromator and colored filters. Monochromatic light was focussed on the sample, and luminescence was observed through the Corning colored glass filters.

Optical Illumination Effects on the ESR Spectra

Group 1

The diamonds investigated in the study are divided into groups having similar behavior. The first group consists of two samples, D-22 and D-37. D-22 is a very very pale green, smooth, triangular diamond; D-37 is a very pale yellow triangular diamond. The optical transmission cut-off wavelengths for D-22 and D-37 are 285 mμ and 277 mμ, respectively.[4] Both specimens are weak photoconductors when illuminated with visible light.[5]

---

[3]Luminescence studies had been previously conducted by other workers in the laboratory.

[4]The ultraviolet transmission cut-off wavelengths for specimens in the study were determined by C. C. Johnson or C. J. Northrup in surveys of specimens at Oklahoma State University.

[5]Photoconductivity measurements were made by C. J. Northrup in a survey of the Oklahoma State collection.

The luminescence behavior of D-22 is typical of the strongly blue luminescing specimens described by Chandrasekharan (14, 15). D-22 exhibits a fairly strong afterglow. A bright blue pulse is easily observed when the sample is illuminated with red light after 313 mμ activation. A slight peak is observed in the luminescence intensity for excitation wavelengths in the region 210-240 mμ.

The luminescence of D-37 is much weaker than that of D-22 but is still strong compared to most blue luminescing samples in the collection. There is a noticeable green luminescence with the stronger blue emission. A slight peak in luminescence intensity occurs for excitation wavelengths between 215 mμ and 225 mμ. The effect of red light after uv activation was not determined.

Room temperature studies of the effects of light on the ESR spectrum of D-22 were made using Corning glass filters. A noticeable increase in the signal was produced by illumination of the sample with long wavelength uv light. Also, the signal could be reduced to the original level by illumination with red and infrared light. These effects were again obtained at various low temperatures down to - 155° C. The effects were stronger at low temperatures.

The sample was irradiated for 10 minutes with x-rays at liquid nitrogen temperature. It was then transferred to the variable temperature cavity which was at approximately - 130° C, and the ESR signal was checked. The sample was at all times shielded from light during this phase of the study. However, no significant change in the signal was obtained.

After construction of the new cavity and light pipe system, the

effects of monochromatic light were checked at room temperature and at approximately - 60° and - 90° C. The effects at room temperature were observable but weaker than the effects at the lower temperatures. Therefore, the most complete study was made at approximately - 90° C. The signal increased when light of any wavelengths between 310 mμ and 320 mμ was incident on the sample. The increase of the signal depended on the intensity of the light and the time of illumination. The signal increased for more than 15 minutes for high intensity light and for a much longer period with weak light. The enhanced signal decayed slowly in the absence of light, decreasing only slightly after 1½ hours. The signal returned to normal very rapidly when the sample was illuminated with light passing through Corning filter 2-64, which transmits wavelengths longer than 640 mμ.

The ESR signal for D-22 appears to be made up of two superimposed isotropic peaks with apparently the same g-value (2.0027 ± 0.0002). There seems to be a very broad peak which is unaffected by light and a more narrow peak that increases or decreases with light depending on the wavelength.

Studies of the effects of light on the ESR spectrum of D-37 were conducted with Corning glass filters at room temperature and at approximately - 90° and - 130° C. However, the work done at room temperature indicated that the effects were absent or extremely weak at room temperature. The effects were noticeably stronger at - 130° C than at - 90° C. The diamond was also irradiated with x-rays for 10 minutes at liquid nitrogen temperature. The procedure was the same as that used for D-22; no significant change was noted in the signal of D-37 either.

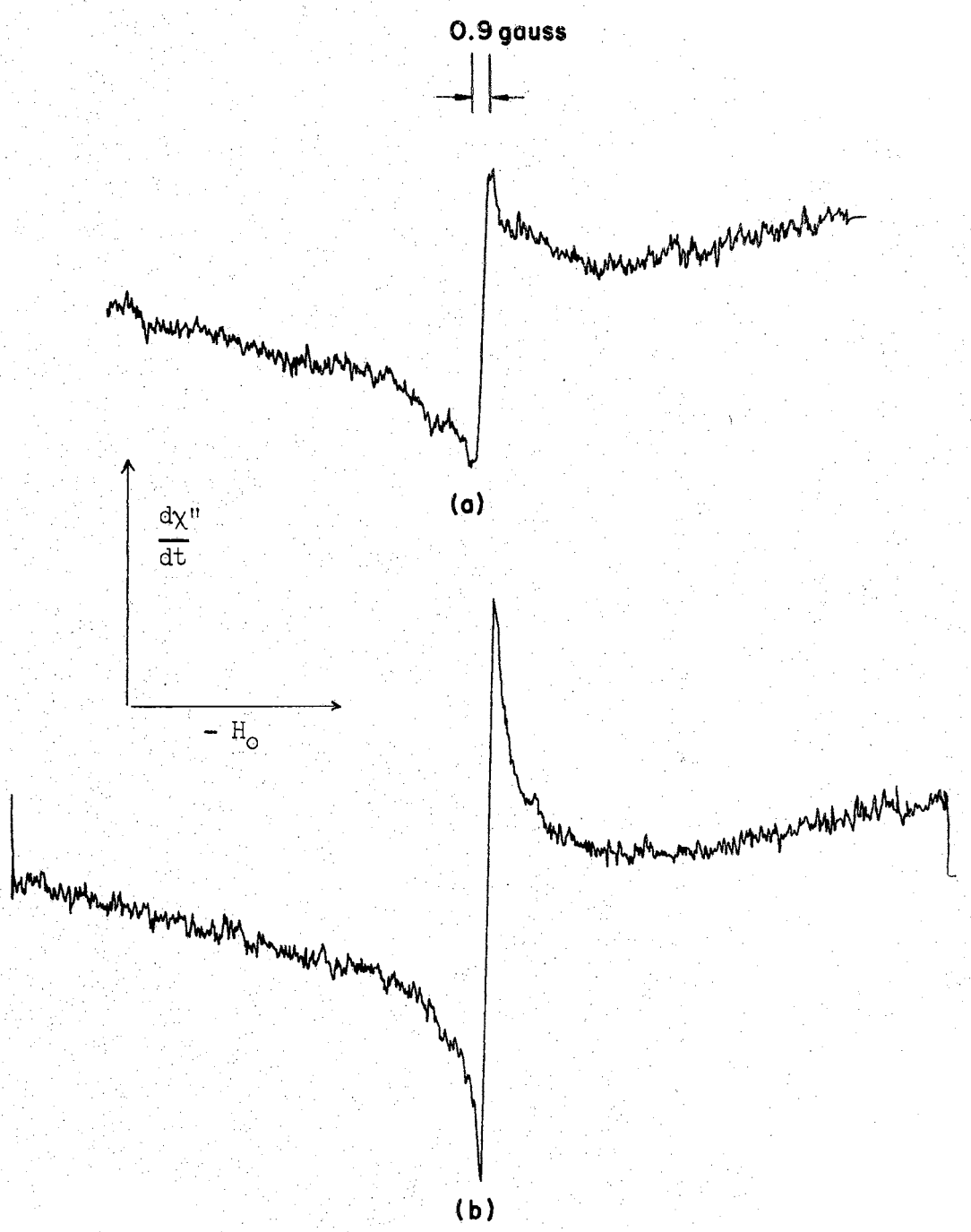

Figure 4-1. Electron spin resonance spectrum of D-22. (a) Normal or deactivated state. (b) Activated state produced by uv excitation.

After construction of the new cavity and light pipe system, the effects of monochromatic light were checked at approximately - 90° C. The signal of D-37 increased for light of wavelengths as short as 254 mμ, and as long as 340 mμ. This is a much broader wavelength region than that observed for D-22. The strongest increase was found near 313 mμ. Also the signal was reduced by wavelengths passed by Corning filter 7-56, which transmits only in the region 0.75 - 4.5 μ. Corning filter 2-64, found effective for D-22, was more effective in reducing the signal of D-37 than filter 7-56. Thus, the deactivating spectrum seems to also be much broader for D-37 but peaks in the same region. The increase or decrease in signal depended on the time of illumination as for D-22. The signal decayed slowly in the absence of light. However, when the deactivating light was used, it was possible to reduce the signal considerably below the normal level. This was in striking contrast to the behavior of D-22, whose signal could never be reduced below the initial level.

The signal of D-37 appears to be only one isotropic peak, which is somewhat broader than the optically affected peak in D-22. The g-values of D-37 and D-22 agree within experimental error, being 2.0028 and 2.0027 ± 0.0002, respectively.[6]

---

[6]The g-values were determined by comparison with diphenyl-picryl-hydrazl (DPPH), a free radical (79).

D - 37
T = - 133° C
g = 2.0028 ± 0.0002

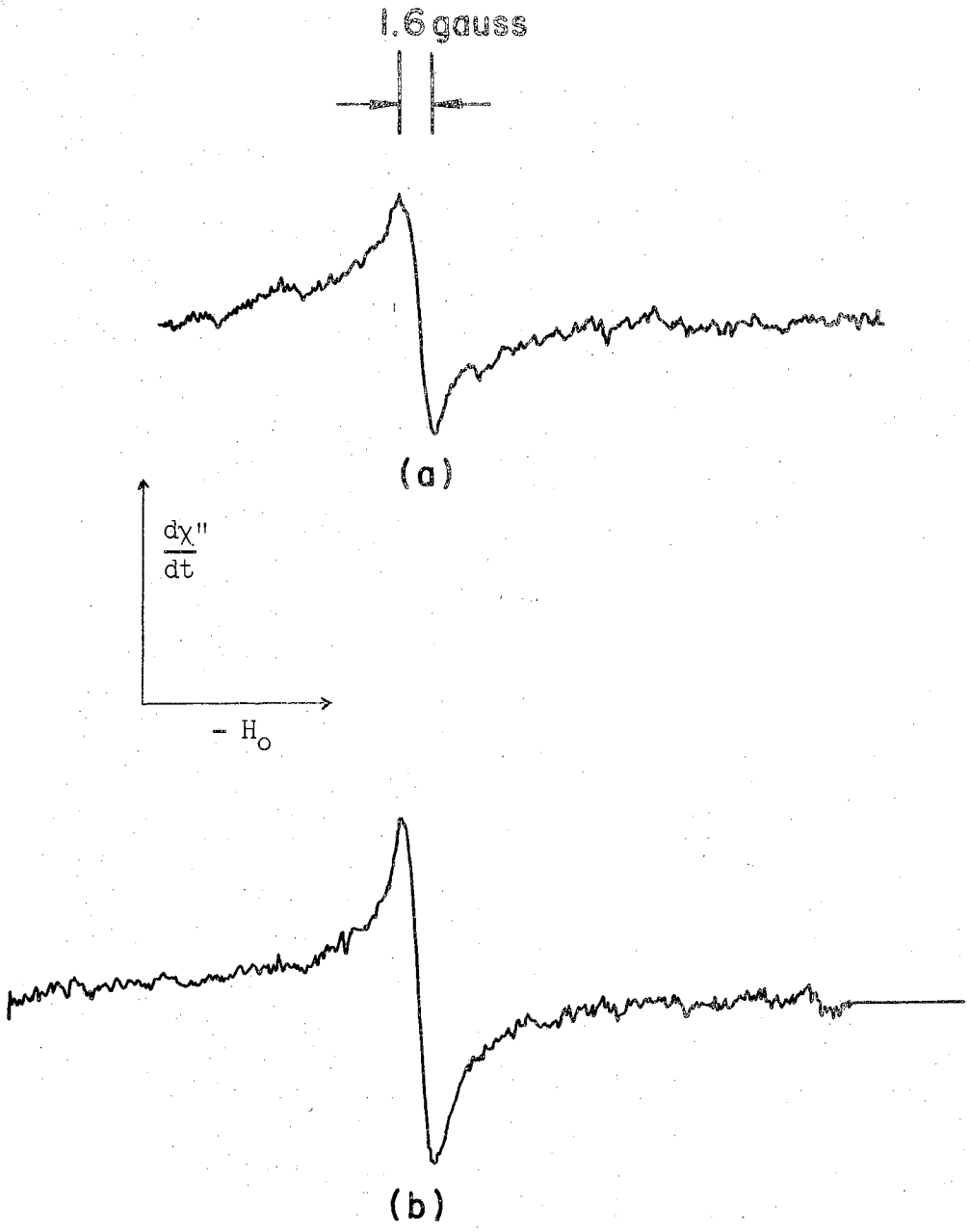

Figure 4-2. Electron spin resonance spectrum of D-37.
(a) Normal or deactivated state.
(b) Activated state produced by uv excitation.

Group 2

A brief summary of optical properties of the Group 2 diamonds is given in Table I. All the samples in this group are single crystals with the exception of D-2 and D-13, which are macles (64). D-2 and D-13 are flat plates with {111} faces and a {111} twin plane parallel to the faces. Diamond D-2 is triangular, D-13 is somewhat irregularly shaped but probably was triangular at one time. Because of the {111} twin plane, there are three common ⟨110⟩ axes but no common ⟨100⟩ axes. Therefore, these crystals were oriented with common ⟨110⟩ axes parallel to the magnetic field $\vec{H}_o$ for ESR work. The ESR spectra of the macles then corresponded to the spectra of the single crystals oriented with a ⟨110⟩ axis parallel to $\vec{H}_o$.

The ESR spectra for all samples in this group are very similar. The spectrum consists of a normal nitrogen resonance and the complex structure described by Smith, Gelles, and Sorokin (82). A broad structure is also observed in D-13, D-18, D-50B, and D-53B. It is strongest in D-50B. It does not saturate easily and is observed only at high power levels.

The saturation properties of these samples differs considerably among samples, but the nitrogen resonance saturates before the complex structure in all cases, and both resonance structures saturate to such an extent that the best signal to noise was always obtained at high microwave power with the reference phase in quadrature with the modulation field. The bridge was balanced for absorptive mode, and the signal obtained is very similar to the "in-phase" absorption signal at low

TABLE I

SUMMARY OF SOME OPTICAL PROPERTIES OF GROUP 2 DIAMONDS

Sample	Color	Optical Cut-Off[a]	Fluorescence[b] 254 mμ Excitation	313 mμ Excitation	366 mμ Excitation
D-2	Colorless	300 mμ	VWB,WG	WB,WG,VWR	VWB,WG,WR,VWDR
D-3	Colorless	307 mμ	WB,MG,WR	MB,MG,WR,VWDR	VSB,SG,WR,VWDR
D-6	Colorless	291 mμ	WB,MG,WR	MB,WG	VSB,MG,WR,VWDR
D-13	Pale Yellow	289 mμ	VSB,VSG,SR,VWDR	VSB,MG,MR,WDR	VSB,MG,MR,WDR
D-18	Very Pale Green	305 mμ	SB,SG	VSB,MG,WR,VWDR	VSB,MG,MR,WDR
D-50B	Medium Yellow	305 mμ	WB,SY,WR	SB,SYG,MR,WDR	VSB,SG,MR,WDR
D-52B	Colorless	307 mμ	WB,WG	WB,MY,WR,VWDR	VSB,MG,MR,WDR
D-53B	Bright Yellow	310 mμ	SB,VSG,SR	SB,MG,MR,MDR	VSB,MG,MR,MDR
D-57	Medium Green	300 mμ	WB,MG	SB,WG	VSB,MG,VWR
D-59	Dark Yellow	280 mμ	SB,VSYG,SR,MDR	SB,VSY,SR,SDR	SB,VSY,SR,SDR
D-67	Pale Yellow	295 mμ	SB,VSG,SR,WDR	SB, VSYG,SR,SDR	VSB,SYG,SR,SDR

S=Strong, M=Medium, W=Weak, V=Very, N=Not Detected, B=Blue, G=Green, Y=Yellow, R=Red, DR=Deep Red.

[a]The ultraviolet transmission cut-off wavelengths for specimens in the study were determined by C. C. Johnson or C. J. Northrup in surveys of specimens at Oklahoma State University.

[b]The blue fluorescence was observed through Corning filter 5-60, the yellow and green were observed through Corning filter 3-71, and the red was observed through Corning filter 2-73 (or 2-61 for DR).

power. A comparison of the in-phase, low power signal and the 90° out-of-phase, high power signal is given for D-3 in Fig. 4-3. For the majority of the samples of Group 2, the in-phase signal broadens, distorts, and gradually disappears as the power is increased. It is difficult to observe the signal at high powers in-phase because the dispersive mode signal is very large and a slight drift of the bridge balance will introduce a quite noticeable component of the dispersive signal. In a few samples there is a broad in-phase signal at high power. This signal is shown in Fig. 4-4(a) and compared with the low power in-phase signal shown in Fig. 4-4(b).

In all diamonds of this group, the magnitude of the nitrogen resonance was affected by light of the proper wavelengths. A decrease in the nitrogen signal due to illumination with 313 mμ mercury light at room temperature was first observed in D-3. It was subsequently observed in D-6 and other samples. In the absence of light the signal returns very slowly to the initial state, changing only very slightly after several hours. However, the signal returned to normal very rapidly when the sample was illuminated with 546 mμ mercury light. Red light with photon energy of 1.6 eV and slightly greater was not noticeably effective. White light from a tungsten filament lamp was very effective in bringing the signal to normal. However, the nitrogen resonance was not noticeably increased above the normal magnitude by any wavelength light utilized. The complex structure did not appear to be affected by the light. Examples of the optically induced changes are given in Fig. 4-5, 4-6, and 4-7. The effects of light at - 90° C were observed to be considerably weaker than the room temperature effects for this group.

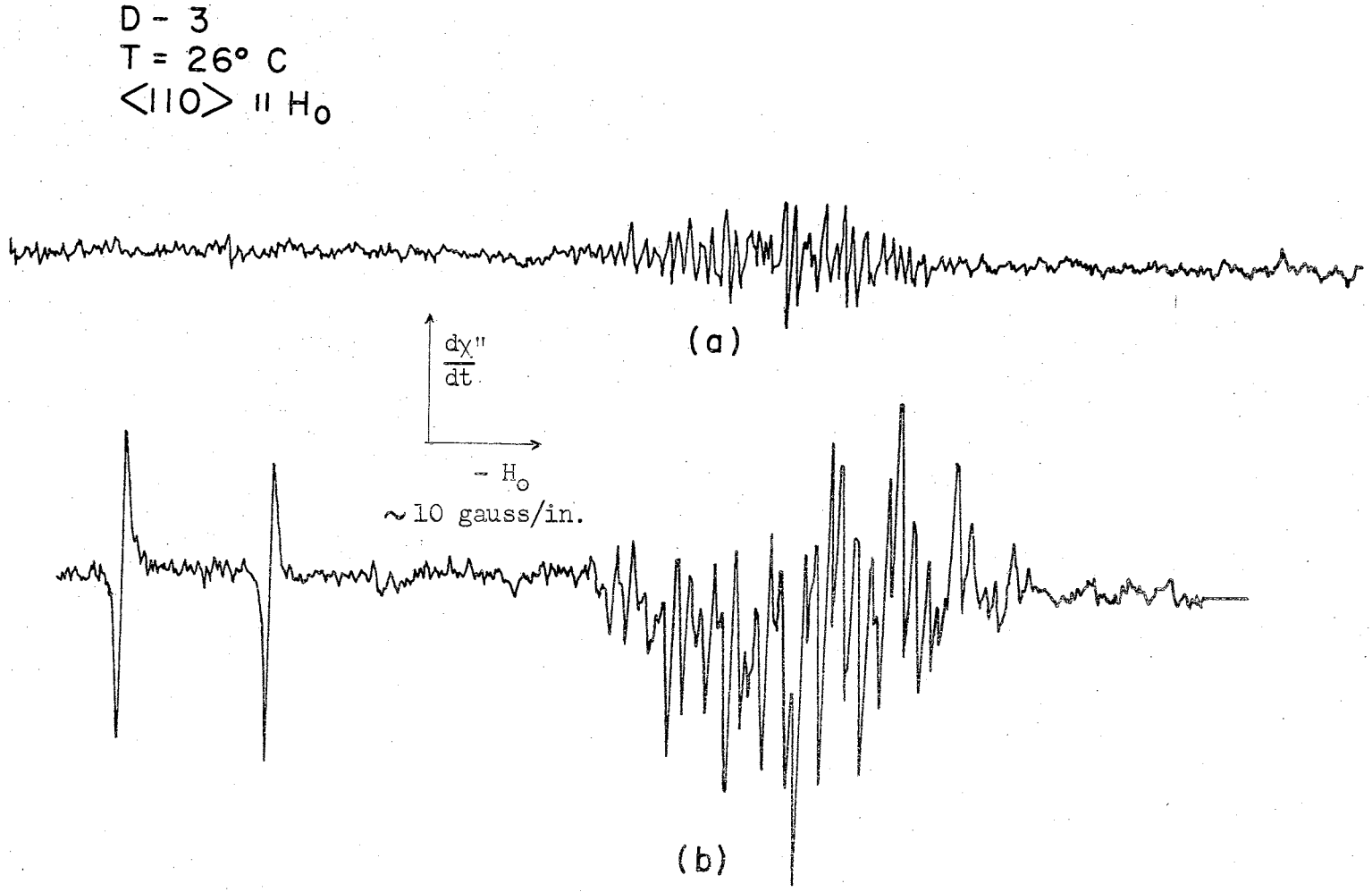

Figure 4-3. ESR absorption spectrum of D-3. (a) Reference phase in-phase, power level - 50 db. (b) Reference phase 90° out-of-phase, power level - 17 db.

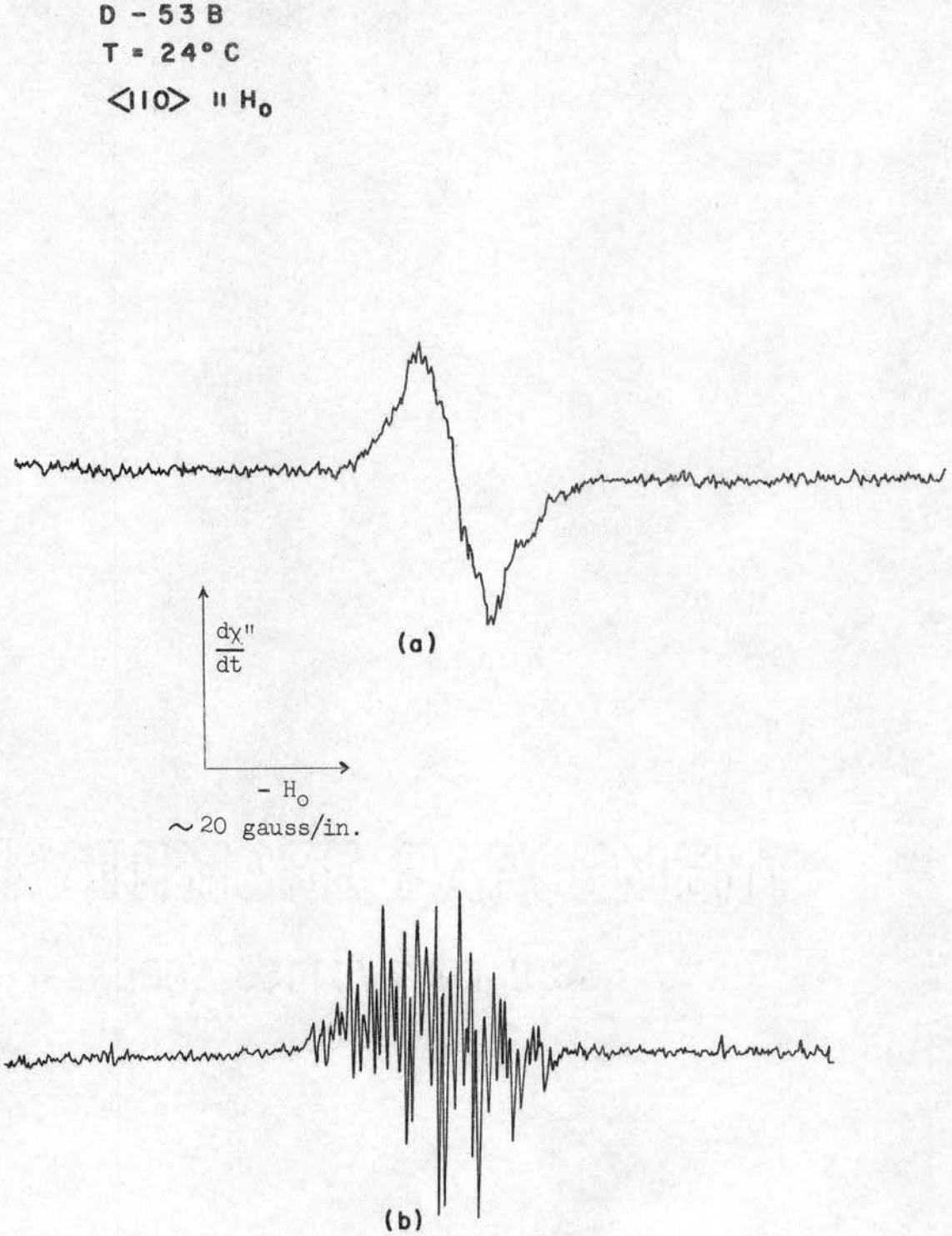

Figure 4-4. ESR absorption spectrum of D-53B. (a) Reference phase in-phase, - 12 db power level. (b) Reference phase in-phase, - 40 db power level.

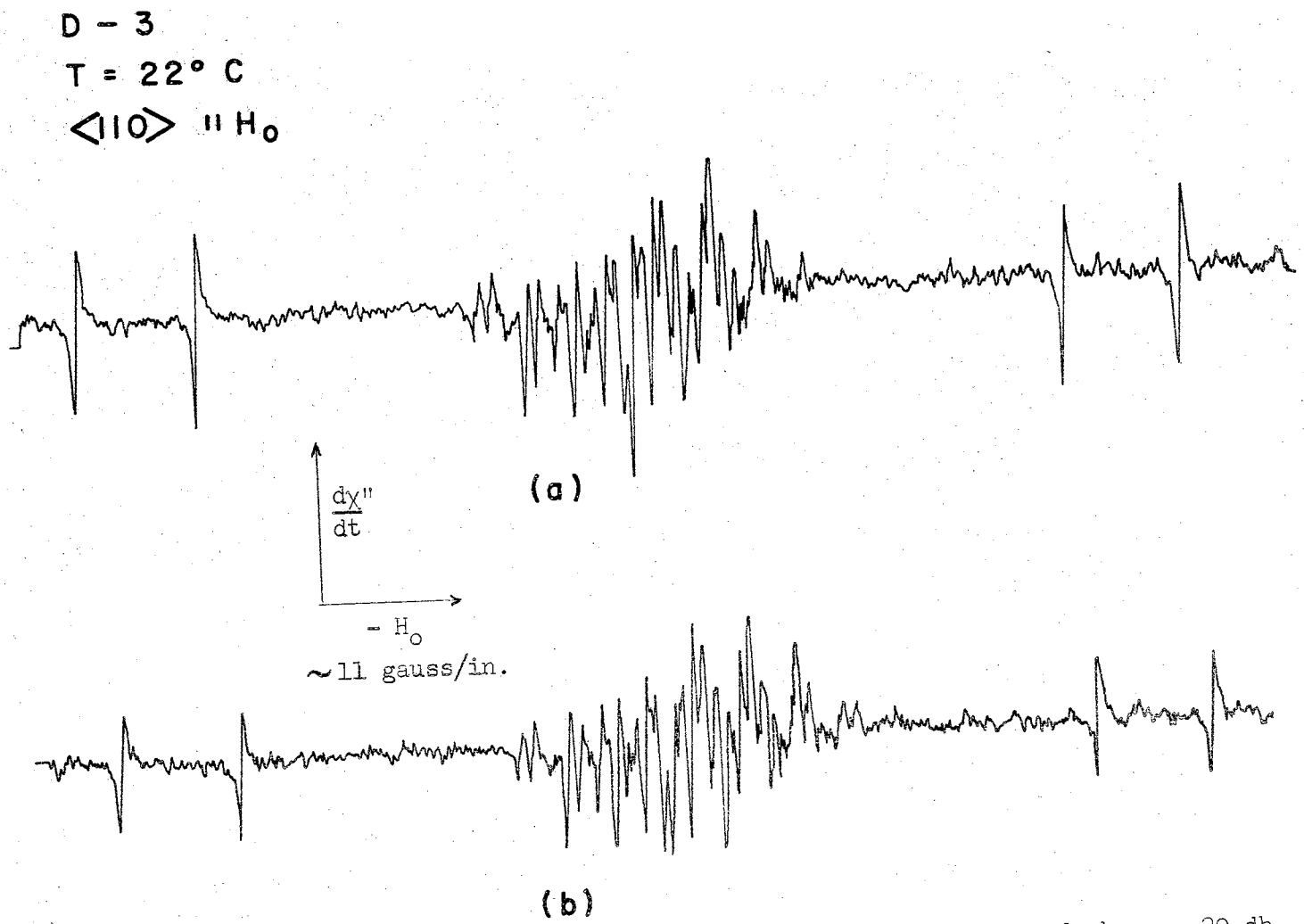

Figure 4-5. ESR absorption spectrum of D-3. Reference phase 90° out-of-phase, -20 db power level. (a) Normal signal. (b) Signal obtained during illumination with 313 mμ light.

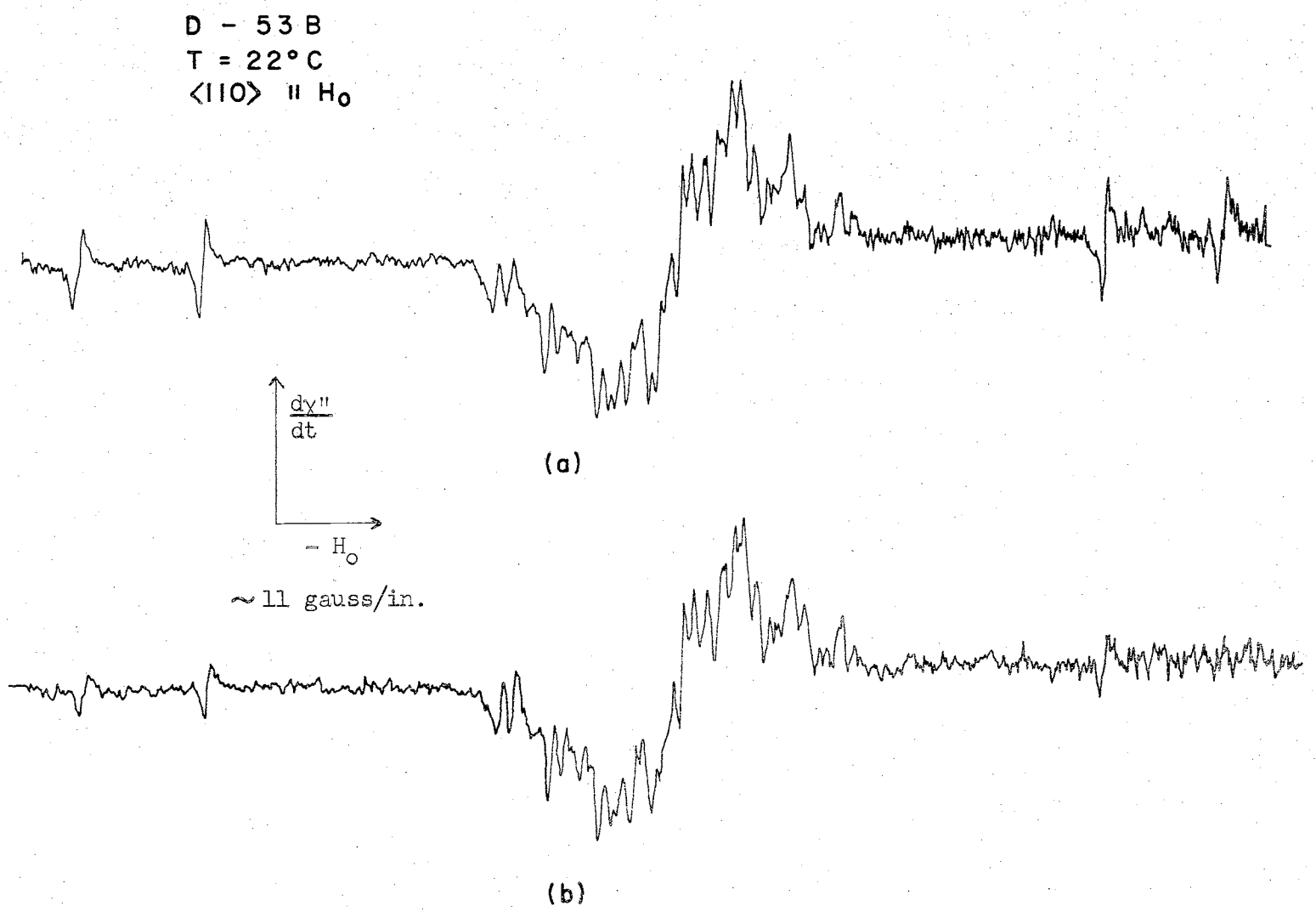

Figure 4-6. ESR absorption spectrum of D-53B. Reference phase 90° out-of-phase, -12 db power level. (a) Normal signal. (b) Signal during 313 mμ illumination.

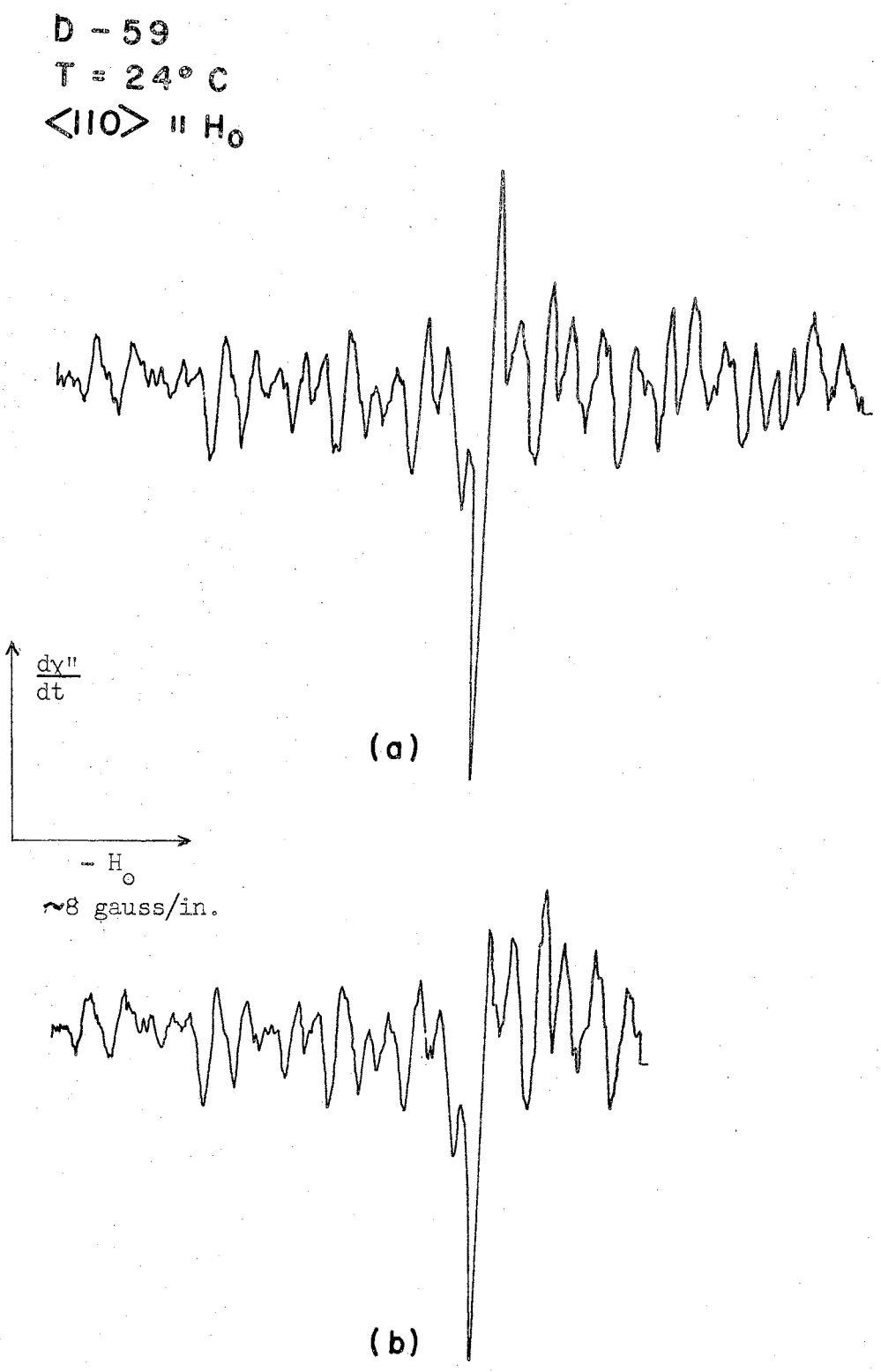

Figure 4-7. ESR absorption spectrum of D-59. Reference phase 90° out-of-phase, -12.5 db power level. (a) Normal signal. (b) Signal obtained during illumination with 313 mμ light.

For all samples in the group, with the exception of D-2, the decrease in signal is greatest for illumination wavelengths near 313 mμ. The effective wavelength band differs among the samples, and 366 mμ mercury light is slightly effective for several samples. However, D-2 shows almost no change in signal due to illumination with 313 mμ mercury light, but a quite noticeable decrease in the nitrogen resonance occurs due to illumination with 366 mμ light.

As the optical effects of this group were first observed, it was quite noticeable that all samples showing the nitrogen resonance and the complex structure were effected by 313 mμ mercury light. There appeared to be a relationship between the optical effect and the complex structure even though no change was observed in the complex structure. However, this apparent relationship was inconsistent with the observations on D-2. It is quite obvious from Table I that D-2 exhibits very weak blue fluorescence, but all other diamonds in the group exhibit strong blue fluorescence when illuminated with 313 mμ or 366 mμ light.

Smith, Gelles, and Sorokin (82) indicated a ⟨100⟩ symmetry axis for the complex spectrum and counted 14 peaks. However, a close examination of Fig. 4-8 reveals that the peaks are not uniform or uniformly spaced in a ⟨100⟩ $\parallel \vec{H}_o$ orientation. This raises some question about the true number of peaks and the symmetry direction. A brief orientation study was conducted, but a more extensive study is anticipated by other workers in this laboratory.

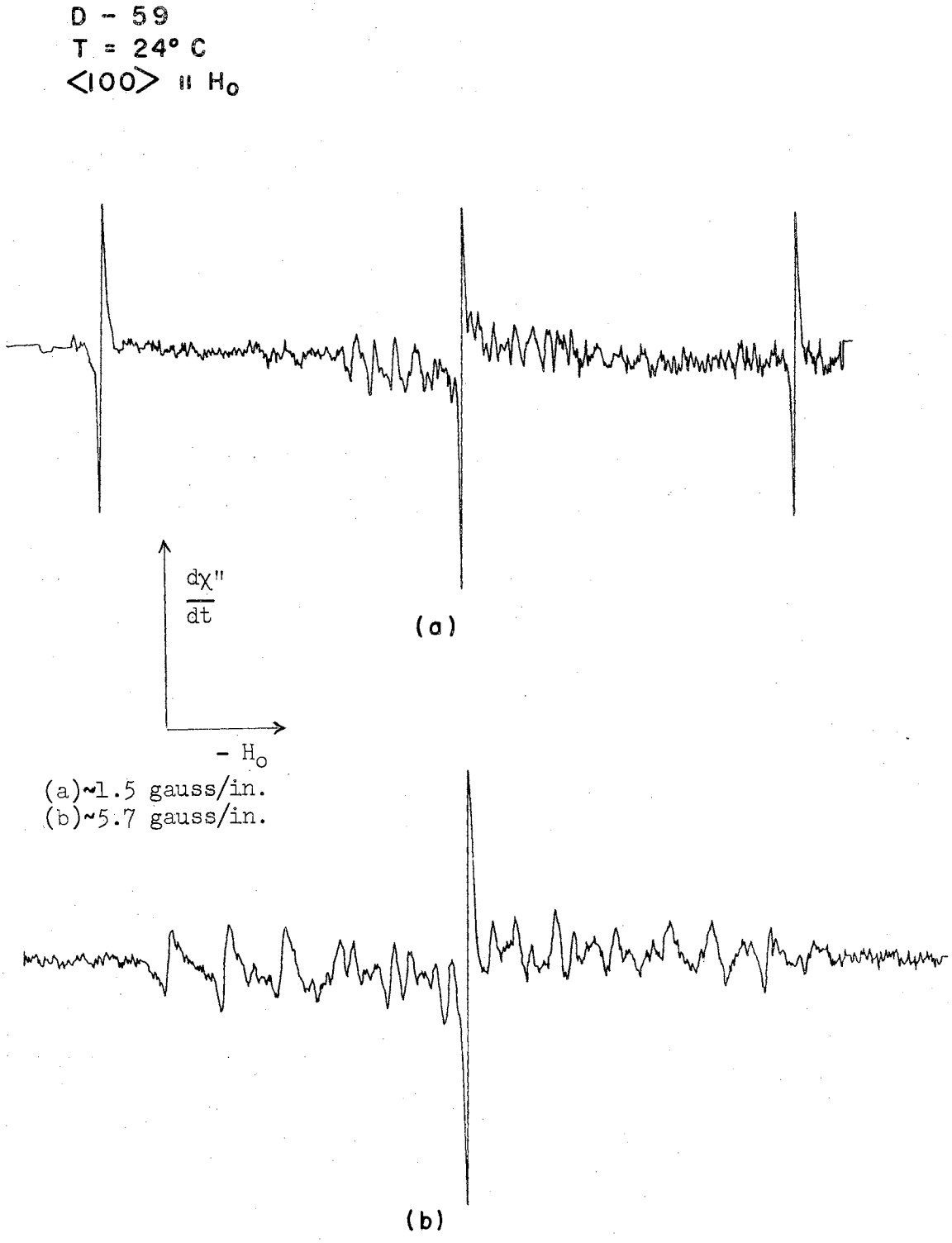

Figure 4-8. Electron spin resonance spectrum of D-59. Reference phase 90° out-of-phase, - 12.5 db power level.
(a) Fast scan. (b) Slow scan of complex central structure.

Group 3

The two diamonds in Group 3, D-60 and D-61, are closely related to the Group 2 specimens. The normal nitrogen resonance and the complex structure are both present. However, the additional structure in the ESR spectra of these samples merits special consideration.

Unusual side peaks were observed in addition to the normal nitrogen resonance side peaks. The in-phase ESR spectrum at high power contains only the two unusual side peaks, one on each side of the central structure. At high power the normal nitrogen resonance must be observed with the reference phase in quadrature with the modulation field. The two unusual side peaks are weakly present under these conditions also. The distance between the peaks appears to be independent of the sample orientation with a constant value of approximately 70 gauss. The peaks are observed readily with a $\langle 100 \rangle \parallel \vec{H}_o$ orientation. As the magnetic field is rotated about a crystaline $\langle 100 \rangle$ axis, the side peaks broaden considerably and disappear in at least one $\langle 110 \rangle \parallel \vec{H}_o$ orientation. The $\langle 111 \rangle \parallel \vec{H}_o$ orientations are not equivalent, as illustrated in Fig. 4-9 (a) and (c). An extensive study of the orientation behavior of these specimens is currently being pursued in this laboratory. The orientation can be checked very readily by the normal nitrogen resonance which is very sharp in these specimens.

Since the effects of light on the ESR spectrum were stronger in D-61 than in D-60, a more complete study was conducted on D-61. Effects of light were observed at room temperature and at - 90° C. At - 90° C the optically induced changes were very weak but similar to the room

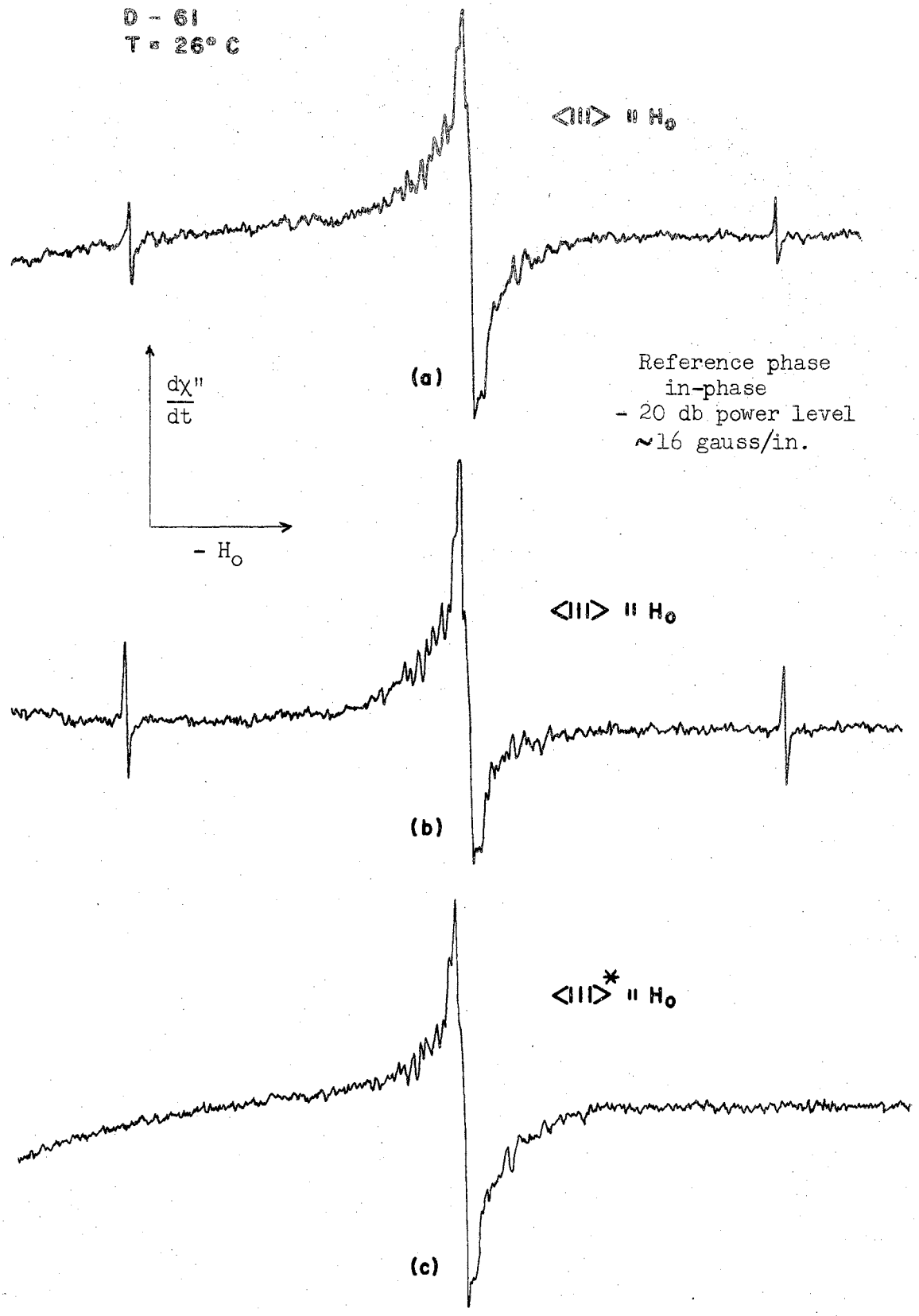

Figure 4-9. ESR spectrum of D-61. (a) Normal spectrum. (b) After 366 mu illumination. (c) Inequivalent ⟨111⟩ ∥ H_o orientation.

temperature effects.

The unusual side peaks are enhanced by illumination of the sample with 313 mμ or 366 mμ mercury light. The increase due to 366 mμ light is considerably stronger than the increase due to 313 mμ light. The effect of 366 mμ light on the unusual side peaks is illustrated in Fig. 4-9 (a) and (b) and in Fig. 4-10. Sample illumination with 366 mμ or 313 mμ mercury light causes a decrease in the normal nitrogen resonance similar to the effects in Group 2. Deactivation is greatest due to 313 mμ illumination. Effects of 366 mμ mercury light illumination on the normal nitrogen resonance are shown in Fig. 4-10. The lifetime of the induced signal change is at least several hours in the absence of light. White light from a tungsten lamp reduces the signal to normal in a few minutes. However, 546 mμ mercury light is not as effective for this group as for Group 2 specimens. Observations of the in-phase central structure at high power before and after sample illumination with 366 mμ light indicates that there is a sharp central peak associated with the unusual side peaks. The unusual resonance might be associated with nitrogen in a state not normally observed and having g-value identical to the normal nitrogen resonance. A brief summary of optical properties of Group 3 is given in Table II.

Group 4

Group 4 consists of two strongly fluorescing samples, D-51B and D-58. A brief summary of their optical properties is given in Table II. D-51B and D-58 are probably the brightest fluorescing specimens in the study.

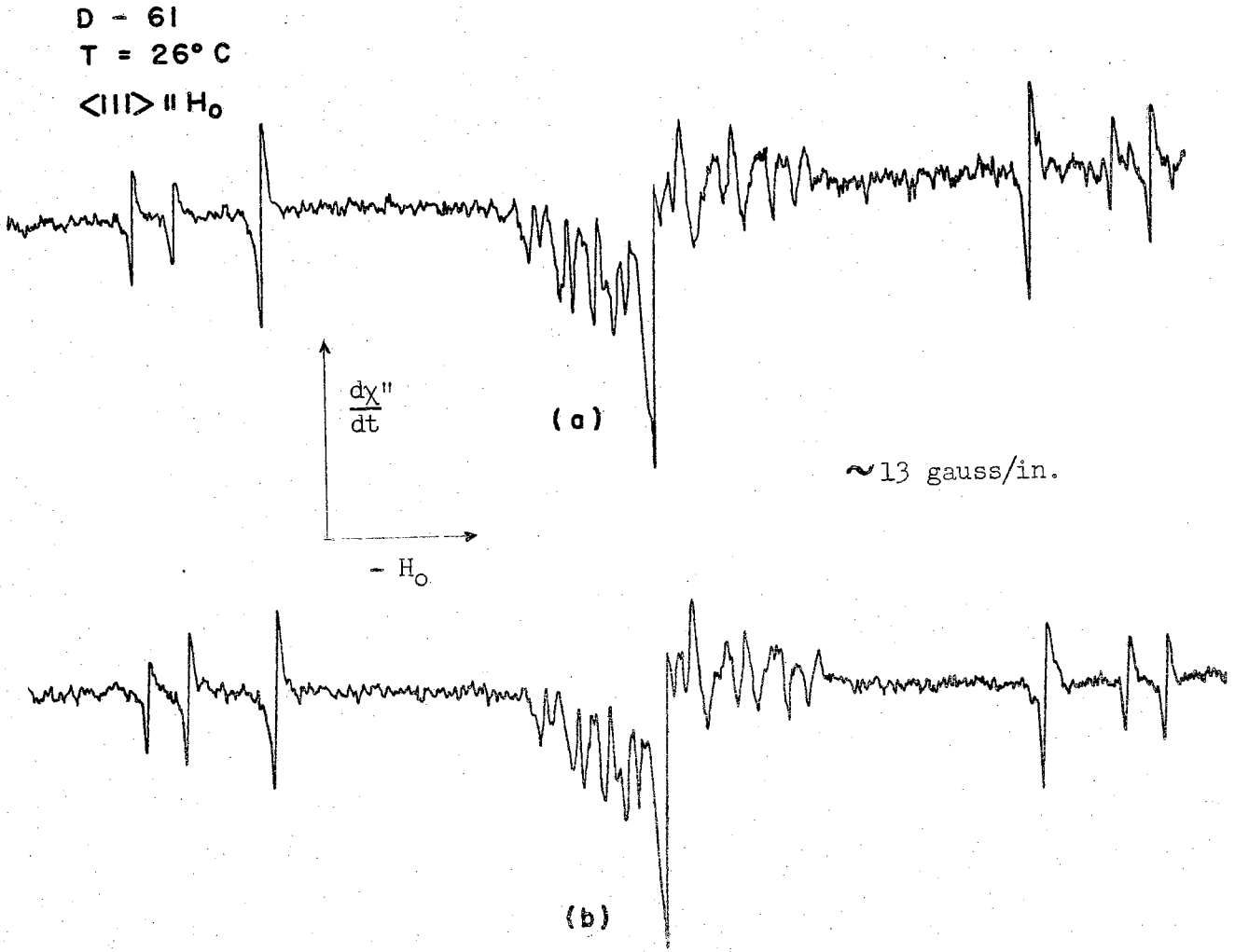

Figure 4-10. ESR absorption spectrum of D-61. Reference phase 90° out-of-phase, - 15 db microwave power level. (a) Normal spectrum. (b) Spectrum during 366 mμ illumination.

TABLE II

SUMMARY OF SOME OPTICAL PROPERTIES OF GROUP 3 AND GROUP 4 DIAMONDS

Sample	Color	Optical Cut-Off[a]	Fluorescence[b] 254 mμ Excitation	313 mμ Excitation	366 mμ Excitation
D-60	Dark Brown	290 mμ	N	VWB,VWG	MB,MYG,WR,WDR
D-61	Dark Brown	290 mμ	N	SB,VWG	VSB,MG,WR,WDR
D-51B	Pale Yellow	280 mμ	WB,VSY,SR,WDR	WB,VSY,SR,SDR	MB,VSY,SR,SDR
D-58	Dark Yellow Green	290 mμ	VWB,MG,VWR	SB,VSY,SR,SDR	MB,VSY,SR,SDR

S=Strong, M=Medium, W=Weak, V=Very, N=Not Detected, B=Blue, G=Green, Y=Yellow, R=Red, DR=Deep Red.

[a]The ultraviolet transmission cut-off wavelengths for specimens in the study were determined by C. C. Johnson or C. J Northrup in surveys of specimens at Oklahoma State University.

[b]The blue fluorescence was observed through Corning filter 5-60, the yellow and green were observed through Corning filter 3-71, and the red was observed through Corning filter 2-73 (or 2-61 for DR).

The ESR spectrum of D-51B is illustrated in Fig. 4-11. The ESR spectrum of D-58 is very similar and is shown in Fig. 4-12. It is obvious from a comparison of the two figures that the ratio of the side peak to central peak height is not the same for the two specimens. However, a study of the ESR spectra at different microwave power levels gives strong evidence that the central peak is the normal nitrogen center plus another sharp peak from a center with almost identical g-value. The orientation behavior of the side peaks is essentially the same as that reported by Smith, Sorokin, Gelles, and Lasher (60). The additional central structure appears to be due to at least two centers and most likely three.

No change occurred in the ESR spectrum upon illumination of either specimen with light. The signal was not significantly reduced by either 313 mμ or 366 mμ mercury light.

Group 5

The previous groups contained diamonds having similar properties, but this group contains samples with widely differing properties. Samples in Group 5 were investigated because of some particular property exhibited by each diamond. The effects of light on the ESR spectra of these diamonds are weak or absent. A short summary of optical properties for Group 5 is given in Table III.

Diamond sample D-8 exhibits a very weak normal nitrogen resonance. The room temperature signal was slightly increased by illumination with red light through Corning filter 2-73 or by white light from a glass envelope tungsten filament lamp. No illumination effects were detected at - 90° C.

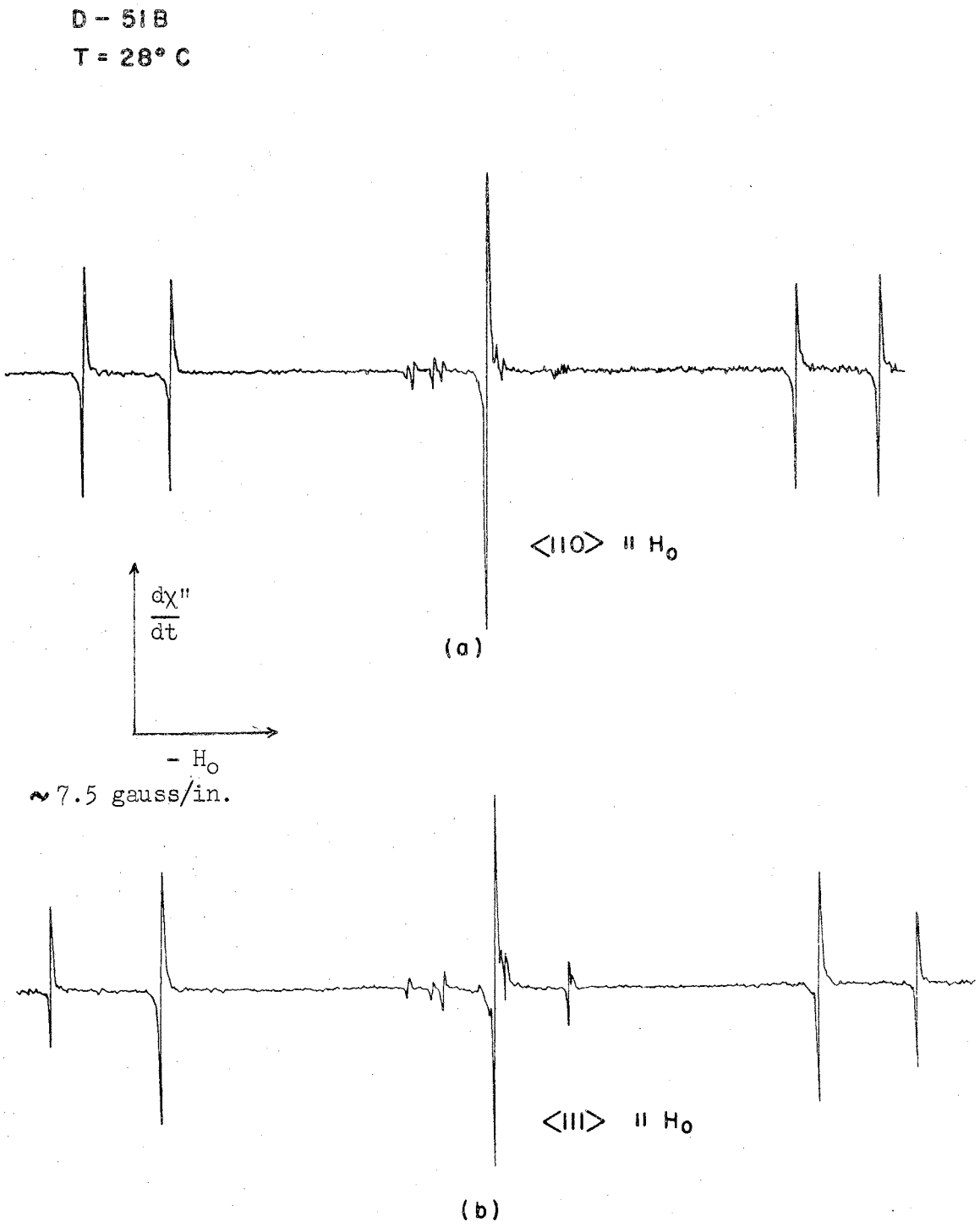

Figure 4-11. Electron spin resonance in D-51B. Reference phase 90° out-of-phase, - 17 db microwave power level.

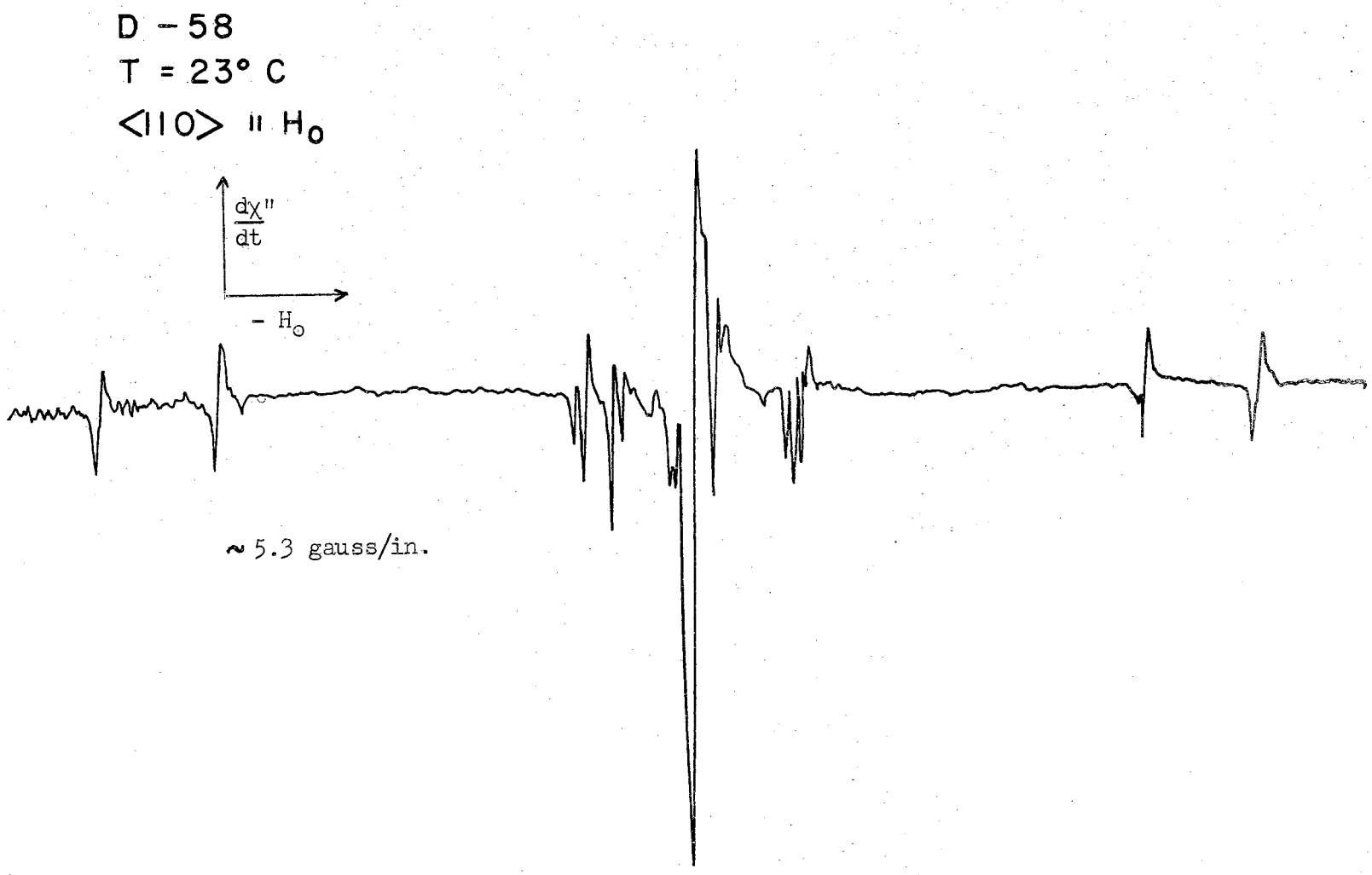

Figure 4-12. Electron spin resonance in D-58. Reference phase 90° out-of-phase, - 17 db microwave power level.

TABLE III

SUMMARY OF SOME OPTICAL PROPERTIES OF GROUP 5 DIAMONDS

Sample	Color	Optical Cut-Off[a]	Fluorescence[b] 254 mμ Excitation	313 mμ Excitation	366 mμ Excitation
D-8	Very Pale Yellow Green	289 mμ	WB,MG	SB,SG,VWR	SB,SG,MR,VWDR
D-24	Very Pale Yellow	300 mμ	WB,WG,VWR	MB,SG,MR,VWDR	SB,MG,WR,VWDR
D-26	Very Pale Gray	301 mμ	VWB,VWG	WB,WG,VWR	SB,MG,VWR
D-36	Very Pale Gray	308 mμ	VWB,VWG	WB,MY,VWR	WB,MY,MR,VWDR
D-43	Colorless	293 mμ	MB,MG,VWR	VSB,MG,WR,VWDR	VSB,SG,MR,WDR
D-46	Very Pale Yellow	290 mμ	MB,VSG,MR	VSB,SG,MR,WDR	VSB,SG,MR,WDR
D-65	Dark Yellow Brown	350 mμ	WY,VWR	VWY	VWB,MY,WR,VWDR

S=Strong, M=Medium, W=Weak, V=Very, N=Not Detected, B=Blue, G=Green, Y=Yellow, R=Red, DR=Deep Red.

[a]The ultraviolet transmission cut-off wavelengths for specimens in the study were determined by C. C. Johnson or C. J. Northrup in surveys of specimens at Oklahoma State University.

[b]The blue fluorescence was observed through Corning filter 5-60, the yellow and green were observed through Corning filter 3-71, and the red was observed through Corning filter 2-73 (or 2-61 for DR).

A small sharp resonance peak was observed in D-24 with the reference phase in quadrature with the modulation field. The signal does not appear to be a nitrogen resonance, but it is so weak that the side peaks might not be observed above the noise for a random orientation of the sample. The resonance line increased very slightly and changed shape when the diamond was illuminated with uv light around 300 mμ.

Diamond D-26 has a very weak easily saturated resonance peak which might be a normal nitrogen resonance central peak. The peak was slightly increased by weak deep red and infrared light through Corning filter 7-69. The peak was slightly decreased by 313 mμ mercury light.

The resonance of D-36 is a fairly strong sharp nitrogen resonance with a very weak complex structure possibly the same as the Group 2 complex structure. Illumination of the sample with 313 mμ mercury light has no effect on the ESR signal. The resonance decreases very slightly when 366 mμ mercury light is used. White light or 546 mμ mercury increases the resonance very slightly above normal.

D-43 has a sharp easily saturated resonance which is too weak to identify. Illumination caused no large effects, and the signal to noise ratio was so poor that the results were inconsistent.

The in-phase spectrum of D-46 at high microwave power is a broad peak plus a complex structure very similar to the signal for D-50 of Group 2. The complex structure itself does not appear to be of the same form as the complex structure of Group 2. Also, the ESR spectrum at high power with the reference phase in quadrature with the modulation field is extremely weak, which gives strong evidence that the complex structure is from a different center than that giving the complex struc-

ture for Group 2. The nitrogen resonance is not detected. There were no detectable effects from illumination with any wavelength light utilized. All of the diamonds in Group 5 are weak or very weak photoconductors when illuminated with visible light with the exception of D-46 which is a very strong photoconductor.[5]

The available diamond collection contains five small cubes which range from bright yellow to dark yellow-brown. The uv cut-off is 340 - 350 mμ for all five cubes.[4] All have extremely strong 7.8 μ infrared absorption and have a very strong broad nitrogen ESR signal with line widths as high as 2.8 gauss.[7] Bell (79) discussed these cubic diamonds, including a consideration of the unusual peaks in the infrared absorption. Optical studies on the ESR spectra were made on several of the specimens using the Varian system, but no positive effects were observed. Further investigations were conducted on D-65, a good representative of the diamond cubes. However, no optically induced changes in the ESR spectrum were detected. A reference phase and microwave power study indicated that the nitrogen resonance behaves very similarly to the saturation behavior of the nitrogen resonance in Group 2 diamonds.

---

[7]The infrared absorption measurements were made by previous workers in the laboratory.

Discussion

The changes produced in the ESR spectra of diamonds by illumination with monochromatic light provide valuable information concerning the energy levels for electron states in the energy gap. Models have been selected to explain the ESR results and relate them to the optical properties of the diamonds.

The model proposed for Group 1 diamonds D-22 and D-37 is shown in Fig. 4-13. As a result of the ESR data, a paramagnetic donor level A is placed 1.6 eV below the conduction band. The 4156 Å blue luminescence band is believed to be produced by electron transitions from the conduction band to level B which is 2.98 eV below the conduction band. The 5032 Å green luminescence band arises from hole transitions to level C which is placed 2.46 eV above the valence band. Electrons are excited

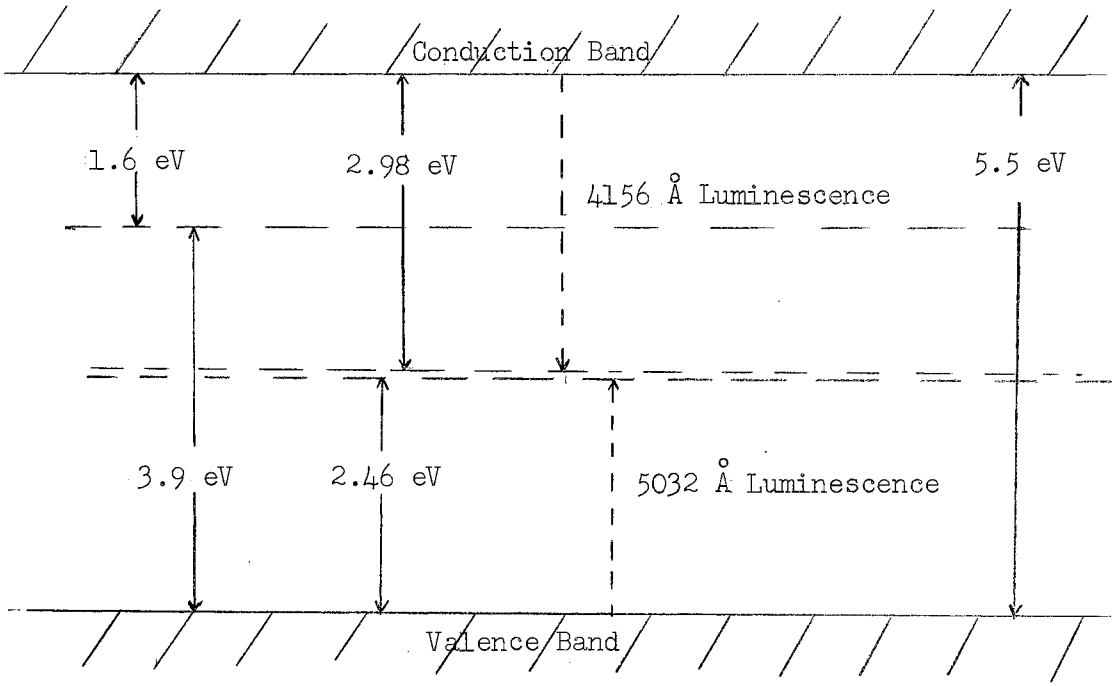

Figure 4-13. Energy level diagram for diamonds D-22 and D-37.

to level A by uv light of wavelengths near 315 mμ (3.9 eV). Red light ($h\nu \geq 1.6$ eV) excites the electrons from level A to the conduction band, and many of the electrons make transitions to level B, producing the blue luminescence pulse easily observed in D-22 and previously discussed by Chandrasekharan (15). It is further assumed that transitions from level B to level C are allowed but that the transition probability is low, as would be expected of different centers (22, 23) which are at different locations in the diamond. Holes then make transitions to level C producing a green afterglow. Green and blue luminescence would both be excited by transitions across the band gap according to this model.

The work of Male (20) gives some justification for this model. Green and blue luminescence both increase sharply as the photon energy of the exciting light approaches the band gap energy. Observations by Mani (9) that the 4156 Å ($h\nu \geq 2.98$ eV) absorption system gives rise to blue luminescence but not green and the 5032 Å ($h\nu \geq 2.46$ eV) absorption system gives rise to green but not blue luminescence also agree with the model. Electrons excited from level B could return, but afterwards there would be no change in the population of states in level C. On the basis of the results on D-22 and D-37 or the work by Male or Mani, there is no reason to select the proposed model over a model with the levels inverted. However, a model with both transitions occurring from the conduction band to the levels or from the valence band to the levels is not consistent with observations. In order to observe both the absorption associated with a center and luminescence from the center due to illumination with light having wavelengths not of the system, it is necessary that the level be only partly filled. Electrons (or holes) excited from one level could return to the other level by that model

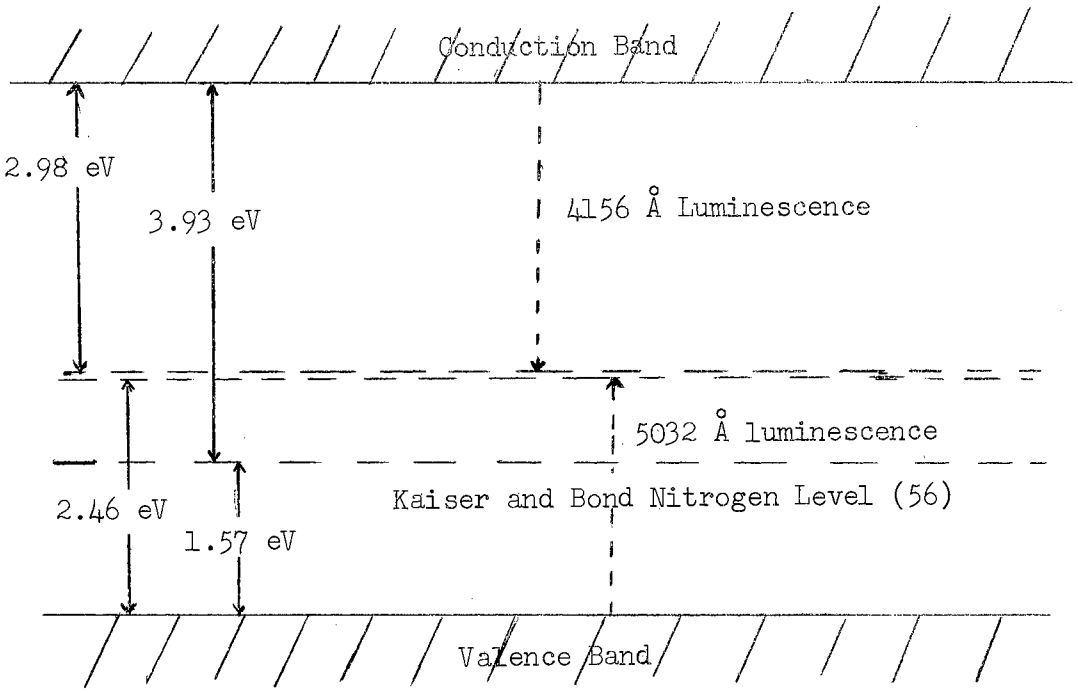

Figure 4-14. Energy level diagram for blue luminescing Type I diamonds.

contrary to the observations of Mani. The following discussion of the work involving the nitrogen resonance will give further justification to the model selected for D-22 and D-37 in preference to the inverted model.

The optically induced changes in the substitutional nitrogen donor ESR spectrum are perhaps the most important results of the study. An energy level model to explain the changes in the nitrogen resonance is illustrated in Fig. 4-14. The donor level is placed 3.93 eV below the conduction band, corresponding to the level attributed to substitutional nitrogen by Kaiser and Bond (56). There appeared to be a correlation of the 3155 Å (3.93 eV) absorption and the nitrogen concentration as well as the correlation between the absorption at 3065 Å (4.04 eV) and the nitrogen concentration (56). Smith, et al (60) suggested that most

nitrogen in diamond is in a non-paramagnetic form, now generally considered to be a substitutional platelet form with pairing of electrons (57, 64).

The paramagnetic nitrogen level is ionized by 313 mμ (3.93 eV) mercury light, but the electrons can return to the level unless they are temporarily trapped at other centers. Therefore there is not always a change in the nitrogen resonance with 313 mμ light. In the case of diamonds with a strong blue luminescence and weak green luminescence, the electrons are temporarily trapped, and the nitrogen resonance is decreased. Although electrons can be excited to the nitrogen level from the valence band with red light ($h\nu \geq 1.57$ eV) according to this model, apparently the liberated holes can readily make transitions to the level so that no significant increase in the nitrogen resonance is observed. Intense 546 mμ (2.3 eV) mercury light is effective in liberating the trapped electrons. White light is more effective than green light alone, and no sharp dependence on wavelength was found.

Since the electrons must be trapped temporarily for reduction of the nitrogen resonance according to the above scheme, it would not be expected that changes would occur when the green luminescence was much stronger than the blue. Group 4 diamonds D-51B and D-58 both exhibit blue luminescence but much stronger yellow luminescence. No change in the nitrogen resonance could be produced by light illumination. However, diamonds D-59 and D-67 of Group 2 have strong yellow luminescence, and a decrease in nitrogen resonance is still produced by 313 mμ (3.93 eV) light.

Diamond D-2 of Group 2 exhibits weak blue and green luminescence. No change in the nitrogen resonance is produced by illumination with

313 mμ (3.93 eV) light which is in agreement with the previous arguments. However, 366 mμ (3.4 eV) mercury light decreases the nitrogen resonance significantly. It is assumed that electrons are excited from the valence band to a long lifetime state leaving free holes to make transitions to the nitrogen level.

In addition to the changes observed in the normal nitrogen resonance, there is also a change in additional structure in diamonds D-60 and D-61 of Group 3. From the results of the ESR work in these diamonds, it is believed that they have uncommon nitrogen centers producing a donor level approximately 3.4 eV above the valence band. The centers are usually ionized because of compensation by lower lying acceptor states. The level is filled with electrons excited from the valence band by 366 mμ (3.4 eV) mercury light. The optically induced effects on the normal nitrogen resonance were apparently due to a combination of the mechanism proposed for D-2 and that proposed for other Group 2 diamonds. Intense 546 mμ (2.3 eV) mercury light was ineffective in reducing the unusual side peaks, but white light reduced the spectrum to normal. Although diamond D-2 mentioned above was affected by 366 mμ light, no unusual side peaks were observed in that specimen.

Summary

Significant changes in the ESR spectra of several diamonds were produced by simultaneously illuminating the specimens with monochromatic light. From an analysis of these effects in conjunction with other optical properties, energy levels for electronic states in the energy gap of diamond have been proposed for several important defect

centers. Evidence is given for the following levels:

(a) The paramagnetic substitutional nitrogen donor level is 3.93 eV below the conduction band and is responsible for the 3155 Å absorption observed by Robertson, Fox, and Martin (3).

(b) The 4156 Å luminescence is associated with electron transitions from the conduction band to an energy level 2.98 eV below the conduction band.

(c) The 5032 Å luminescence is associated with hole transitions from the valence band to an electron energy level 2.46 eV above the valence band.

(d) A donor level 1.6 eV below the conduction band is associated with a paramagnetic center. This level is filled by electrons excited by 315 mu uv light and is responsible for the blue luminescence pulse produced by red light in activated strongly blue luminescing diamonds such as those described by Chandrasekharan (15).

(e) An unusual nitrogen center has an associated donor level 3.4 eV above the valence band.

Studies of the effects of light on the ESR of solids offer tremendous possibilities. Electron spin resonance provides a possible means of identifying centers within a solid but gives no information concerning the position of the energy levels within the energy gap. Changes in the ESR spectrum due to light not only demonstrate a relation between the light wavelengths and the paramagnetic center but also indicates whether the center is populated or depopulated by the light. Thus the optical effects study relates the ESR data to many optical properties of the solid.

SELECTED BIBLIOGRAPHY

(1) A. Mani, "The Fluorescence and Absorption Spectra of Diamond in the Visible Region," Proc. Indian Acad. Sci. A19, 231 (1944).

(2) W. J. Leivo, et al, "Investigation of Semiconducting Properties of Type IIb Diamond," Report No. AFOSR-2642, (May, 1962).

(3) R. Robertson, J. J. Fox, and A. E. Martin, "Two Types of Diamond," Phil. Trans. Roy. Soc. London A232, 463 (1934).

(4) R. Robertson, J. J. Fox, and A. E. Martin, "Further Work on Two Types of Diamond," Proc. Roy. Soc. (London) A157, 579 (1936).

(5) J. F. H. Custers, "Unusual Phosphorescence of a Diamond," Physica 18, 489 (1952).

(6) W. J. Leivo and R. Smoluchowski, "A Semiconducting Diamond," Phys. Rev. 98, 1532 (1955).

(7) P. G. N. Nayer, "Luminescence, Absorption and Scattering of Light in Diamonds," Proc. Indian Acad. Sci. A13, 483 (1941).

(8) P. G. N. Nayer, "The Lattice and Electronic Spectrum of Diamond," Proc. Indian Acad. Sci. A15, 293 (1942).

(9) A. Mani, "Excitation Curves of Luminescence in Diamond," Proc. Indian Acad. Sci. A21, 280 (1945).

(10) C. D. Clark, R. W. Ditchburn, and H. B. Dyer, "The Absorption Spectra of Natural and Irradiated Diamonds," Proc. Roy. Soc. (London) A234, 363 (1956).

(11) F. A. Raal, "A Strong Absorption System in Type I Diamonds," Proc. Phys. Soc. (London) 74, 647 (1959).

(12) H. B. Dyer and I. G. Matthews, "The Fluorescence of Diamond," Proc. Roy. Soc. (London) A243, 320 (1958).

(13) G. O. Gomon, "The Luminescence Spectra of Diamonds," Opt. Spectry. (USSR) 8, 275 (1960).

(14) V. Chandrasekharan, "Phosphorescence Patterns in Diamond," Proc. Indian Acad. Sci. A24, 187 (1946).

(15) V. Chandrasekharan, "The Phosphorescence of Diamond," Proc. Indian Acad. Sci. A24, 193 (1946).

(16) J. B. Krumme and W. J. Leivo, "Luminescence in Semiconducting Diamond," Bull. Am. Phys. Soc. 5, 187 (1960).

(17) J. B. Krumme, "Luminescence in Semiconducting Diamond," (M. S. thesis, Oklahoma State University, 1960).

(18) J. B. Krumme and W. J. Leivo, "Phosphorescence in Semiconducting Diamond," Proc. Okla. Acad. Sci. 44, 105 (1964).

(19) J. H. Wayland and W. J. Leivo, "Lifetimes and Trapping of Carriers in Semiconducting Diamond," Bull. Am. Phys. Soc. 3, 400 (1958).

(20) J. C. Male, "Luminescence Excitation Spectrum of Diamond Near the Fundamental Absorption Edge," Proc. Phys. Soc. (London) 77, 869 (1961).

(21) P. J. Dean and J. C. Male, "Luminescence Excitation Spectra and Recombination Radiation of Diamond in the Fundamental Absorption Region," Proc. Roy. Soc. (London) 277, 330 (1964).

(22) R. J. Elliott, I. G. Matthews, and E. W. J. Mitchell, "The Polarization of Luminescence in Diamond," Phil. Mag. 3, 360 (1958).

(23) C. D. Clark, G. W. Maycraft, and E. W. J. Mitchell, "Polarization of Luminescence," J. Appl. Phys. 33, 378 (1962).

(24) A. Mani, "Polarization of Raman Scattering and of Fluorescence in Diamond," Proc. Indian Acad. Sci. A20, 117 (1945).

(25) I. G. Matthews, "Fluorescence Spectra of Natural and Irradiated Diamonds," J. Phys. Radium 17, 649 (1956).

(26) C. D. Clark, R. W. Ditchburn, and H. B. Dyer, "The Absorption Spectra of Irradiated Diamonds after Heat Treatment," Proc. Roy. Soc. (London) A237, 75 (1956).

(27) R. W. Ditchburn, E. W. J. Mitchell, E. G. S. Paige, J. F. Custers, H. B. Dyer, and C. D. Clark, "The Optical Effects of Radiation Damage in Diamond and Quartz," Conference on Defects in Crystalline Solids (Physical Society, London, 1955) p. 92.

(28) H. B. Dyer and L. Du Preez, "Irradiation Damage in Type I Diamond," J. Chem. Phys. 42, 1898 (1965).

(29) C. D. Clark, I. Duncan, J. N. Lomer, and P. W. Whippey, "Correlation of Optical and Electron Spin Resonance Centers in Electron-Irradiated Diamond," Proc. British Ceramic Soc. 1, 85 (1965).

(30) J. E. Ralph, "Radiation Induced Changes in the Cathodoluminescence Spectra of Natural Diamonds," Proc. Phys. Soc. (London) 76, 688 (1960).

(31) H. B. Dyer and P. Ferdinando, "The Optical Absorption of Electron-Irradiated Semiconducting Diamond," Brit. J. Appl. Phys. 17, 419 (1966).

(32) P. T. Wedepohl, "Electrical and Optical Properties of Type IIb Diamonds," Proc. Phys. Soc. (London) 70, 177 (1957).

(33) P. J. Kemmey, "Irradiation of Semiconducting Diamond," Diamant 5, 4 (1962).

(34) V. A. Fratzke, a"Study of Diffusion in Diamond," (M. S. thesis, Oklahoma State University, 1962).

(35) V. A. Fratzke and W. J. Leivo, "Diffusion in Diamond," Proc. Okla. Acad. Sci. 45, 125 (1965).

(36) R. H. Wentorf and H. P. Bovenkerk, "Preparation of Semiconducting Diamonds," J. Chem. Phys. 36, 198 (1962).

(37) P. J. Van Heerden, "The Crystal Counter," (Thesis, Utrecht, 1945).

(38) L. F. Curtiss and B. W. Brown, "Diamond as a Gamma-Ray Counter," Phys. Rev. 72, 643 (1947).

(39) H. Friedman, L. S. Birks, and H. P. Gauvin, "Ultraviolet Transmission of 'Counting' Diamonds," Phys. Rev. 73, 186 (1948).

(40) R. K. Willardson and G. C. Danielson, "Optical Properties of Counting Diamonds," J. Opt. Soc. Am. 42, 42 (1952).

(41) F. C. Champion, "Electrical Counting Properties of Diamonds," Proc. Phys. Soc. (London) 65, 21 (1952).

(42) A. G. Chynoweth, "Removal of Space-Charge in Diamond Crystal Counters," Phys. Rev. 76, 310 (1949).

(43) A. G. Chynoweth, "Behavior of Space Charge in Diamond Crystal Counters Under Illumination," Phys. Rev. 83, 254 (1951).

(44) R. R. Urlau, H. J. Logie, and F. R. N. Nabarro, "Energy Levels in the Forbidden Gap of Insulating Diamonds," Proc. Phys. Soc. (London) 78, 256 (1961).

(45) J. A. Elmgren and D. E. Hudson, "Imperfection Photoconductivity in Diamond," Phys. Rev. 128, 1044 (1962).

(46) J. F. H. Custers and F. A. Raal, "Fundamental Absorption Edge of Diamond," Nature 179, 268 (1957).

(47) G. B. B. M. Sutherland, D. E. Blackwell, and W. G. Simeral, "The Problem of the Two Types of Diamond," Nature 174, 901 (1954).

(48) K. Lonsdale, "Extra Reflections From the Two Types of Diamond," Proc. Roy. Soc. (London) 179, 315 (1942).

(49) C. V. Raman, "The Crystal Symmetry and Structure of Diamond," Proc. Indian Acad. Sci. A19, 189 (1944).

(50) C. V. Raman, "The Infrared Absorption by Diamond and Its Signifigance," Proc. Indian Acad. Sci. A55, 1 (1962).

(51) F. G. Chesley, "Investigation of the Minor Elements in Diamond," Am. Mineral. 27, 20 (1942).

(52) F. A Raal, "A Spectrographic Study of the Minor Element Content of Diamond," Am. Mineral. 42, 354 (1957).

(53) F. C. Frank, "On the X-Ray Diffraction Spikes of Diamond," Proc. Phys. Soc. (London) A237, 168 (1956).

(54) S. Caticha-Ellis and W. Cochran, "The X-Ray Diffraction Spikes of Diamond," Acta Cryst. 11, 245 (1958).

(55) M. Lax and E. Burstein, "Infrared Lattice Absorption in Ionic and Homopolar Crystals," Phys. Rev. 97, 39 (1955).

(56) W. Kaiser and W. L. Bond, "Nitrogen, a Major Impurity in Common Type I Diamond," Phys. Rev. 115, 857 (1959).

(57) E. C. Lightowlers and P. J. Dean, "Measurement of Nitrogen Concentration in Diamond by Photon Activation Analysis and Optical Absorption," Diamond Research (1964).

(58) Y. Yoneda, "X-Ray Diffraction Spikes of Diamond," Nature 191, 1187 (1961).

(59) F. C. Frank, "X-Ray Diffraction Spikes of Diamond," Nature 191, 1188 (1961).

(60) W. V. Smith, P. P. Sorokin, I. L. Gelles, and G. J. Lasher, "Electron Spin Resonance of Nitrogen Donors in Diamond," Phys. Rev. 115, 1546 (1959).

(61) J. H. N. Loubser and L. Du Preez, "New Lines in the Electron Spin Resonance Spectrum of Substitutional Nitrogen Donors in Diamond," Brit. J. Appl. Phys. 16, 457 (1965).

(62) N. D. Samsonenko, "Distribution of Paramagnetic Nitrogen Centers in Some Type I Diamonds," Soviet Phys.-Solid State 6, 2460 (1965).

(63) G. R. Rendall, "Ultra-Violet Transparency Patterns in Diamond," Proc. Indian Acad. Sci. A19, 293 (1944).

(64) T. Evans and C. Phaal, "Imperfections in Type I and Type II Diamonds," Proc. Roy. Soc. (London) A270, 538 (1962).

(65) T. Young, "The Hall Effect in Semiconducting Diamond," (M. S. thesis, Oklahoma State University, 1958).

(66) M. D. Bell and W. J. Leivo, "Rectification, Photoconductivity, and Photovoltaic Effect in Semiconducting Diamond," Phys. Rev. 111, 1227 (1958).

(67) M. D. Bell and W. J. Leivo, "Photoconductivity in Type IIb Diamond," Bull. Am. Phys. Soc. 1, 382 (1956).

(68) H. J. Stein, "Determination of Energy Levels in Semiconducting Diamond by Optical Transmission Methods," (M. S. thesis, Oklahoma State University, 1957).

(69) C. C. Johnson, "Photoconductivity in Semiconducting Diamond," (M. S. thesis, Oklahoma State University, 1958).

(70) C. Johnson, H. Stein, T. Young, J. Wayland, and W. Leivo, "Photo-effects and Related Properties of Semiconducting Diamonds," J. Phys. Chem. Solids 25, 827 (1964).

(71) J. B. Krumme and W. J. Leivo, "Photoconductivity in Semiconducting Diamond," Bull. Am. Phys. Soc. 10, 162 (1965).

(72) J. B. Krumme, "Photoconductivity in Semiconducting Diamonds at Low Temperatures," (Ph. D. thesis, Oklahoma State University, (1965).

(73) A. Halperin and J. Nahum, "Some Optical and Electrical Properties of Semiconducting Diamonds," J. Phys. Chem. Solids 18, 297 (1961).

(74) J. H. E. Griffiths, J. Owen, and I. M. Ward, "Paramagnetic Resonance in Neutron-Irradiated Diamond and Smoky Quartz," Nature 173, 439 (1954).

(75) J. H. E. Griffiths, J. Owen, and I. M. Ward, "Magnetic Resonance in Irradiated Diamond and Quartz," Conference on Defects in Crystalline Solids, (Physical Society, London, 1955) p. 81.

(76) M. C. M. O'Brien and M. H. L Pryce, "Paramagnetic Resonance in Irradiated Diamond and Quartz: Interpretation," Conference on Defects in Crystalline Solids, (Physical Society, London, 1955) p. 88.

(77) J. A. Baldwin, "Electron Paramagnetic Resonance Investigation of the Vacancy in Diamond," Phys. Rev. Letters 10, 220 (1963).

(78) E. A. Faulkner, E. W. J. Mitchell, and P. W. Whippey, "Electron Spin Resonance in Neutron-Irradiated Diamond," Nature 198, 981 (1963).

(79) M. D. Bell, "Electron Spin Resonance in Diamond," (Ph. D. thesis, Oklahoma State University, 1964).

(80) M. D. Bell and W. J. Leivo, "Electron Spin Resonance in Semiconducting Diamond," Bull. Am. Phys. Soc. 6, 142 (1961).

(81) M. D. Bell and W. J. Leivo, "Electron Spin Resonance in Diamond," Bull. Am. Phys. Soc. 10, 358 (1965).

(82) W. V. Smith, I. L. Gelles, and P. P. Sorokin, "Electron Spin Resonance of Acceptor States in Diamond," Phys. Rev. Letters 2, 39 (1959).

(83) F. Bloch, "Nuclear Induction," Phys. Rev. 70, 460 (1946).

(84) D. J. E. Ingram, Free Radicals as Studied by Electron Spin Resonance, (Butterworths Scientific Publications, London, 1958).

(85) C. G. Montgomery, Techniques of Microwave Measurements, MIT Radiation Lab. Series, Vol. 11, (McGraw-Hill, New York, 1947).

(86) R. V. Pound, "Electronic Frequency Stabilization of Microwave Oscillators," Rev. Sci. Instr. 17, 490 (1946).

(87) M. W. P. Stranberg, M. Tinkham, I. H. Solt, Jr., and C. F. Davis, "Recording Magnetic-Resonance Spectrometer," Rev. Sci. Instr. 27, 596 (1956).

(88) F. J. Rosenbaum, "Dielectric Cavity Resonator for ESR Experiments," Rev. Sci. Instr. 35, 1550 (1964).

(89) A. J. Estin, "High Mode Tunable Cavity for Microwave-Gas Interactions," Rev. Sci. Instr. 33, 369 (1962).

(90) A. R. Cook, L. M. Matarrese, and J. S. Wells, "New Method for Constructing EPR Cavities," Rev. Sci. Instr. 35, 114 (1964).

(91) H. E. M. Barlow, H. G. Effemey, and P. H. Hargrave, "The Use of a Wire-Wound Helix to Form a Circular H_{01} Wavemeter Cavity," Proc. Inst. Elec. Engrs. (London) 107, 66 (1960).

(92) I. G Wilson, C. W. Schramm, and J. P. Kinzer, "High Q Resonant Cavities for Microwave Testing," Bell System Tech. J. 25, 408 (1946).

(93) G. L. Ragan, Microwave Transmission Circuits, MIT Radiation Lab. Series, Vol. 9, (McGraw-Hill, New York, 1948) p. 494.

(94) A. M. Portis, "Rapid Passage Effects in Electron Spin Resonance," Phys. Rev. 100, 1219 (1955).

(95) J. S Hyde, "Magnetic Resonance and Rapid Passage in Irradiated LiF," Phys. Rev. 119, 1483 (1960).

(96) A. A. Bugai, "Passage Effects in EPR Lines with Inhomogeneous Broadening When Using High Frequency Modulation of the Magnetic Field," Soviet Phys.-Solid State 4, 2218 (1963).

VITA

John Paul King

Candidate for the Degree of

Doctor of Philosophy

Thesis: EFFECTS OF LIGHT ON THE ELECTRON SPIN RESONANCE OF DIAMOND

Major Field: Physics

Biographical:

Personal Data: Born near Zena, Oklahoma, November 23, 1938, the son of John F. and Opal R. King.

Education: Attended grade school in Edmond, Oklahoma; was graduated from Edmond High School in 1957; received the Bachelor of Science degree from the Central State College, with majors in physics and mathematics, in May, 1961; completed requirements for the Doctor of Philosophy degree in July, 1966.

Professional Experience: Student trainee, Oak Ridge Institute of Nuclear Studies, in summer 1960; student instructor of general physics for one year (1960-61).

Organization: Member of Sigma Pi Sigma, Junior member of American Physical Society.